METHODS TO ASSESS THE BIODISTRIBUTION OF RADIOLABELLED SOMATOSTATIN ANALOGUES AND TREATMENT RESPONSE OF NEUROENDOCRINE TUMOURS

DR. GOPINATH GNANASEGARAN

A thesis for the examination of

MD

of the

University of London

2004

UMI Number: U602495

UMI U602495

ABSTRACT

Introduction

During the past decade, proof of the principle that somatostatin receptors can be successfully used for in vivo targeting of neuroendocrine tumours (NETs) has been provided. These tumours are imaged with ^{111}Indium-pentetreotide and treated with ^{90}Yttrium labelled somatostatin analogues. The aim of this study was to assess (a) the biodistribution and residency of ^{90}Y labelled agents using the brehmsstrahlung imaging technique (b) the tumour response to various treatment modalities using a simplified scintigraphic method [Functional SPECT tumour volume (STV)].

Material and methods

1) 19 patients with NETs were imaged with ^{111}In-pentetreotide and 14 of them underwent treatment with ^{90}Y-lanreotide. The rest underwent treatment with ^{90}Y-SMT. All the patients were imaged 24 hours post-therapy. Brehmsstrahlung images obtained post therapies were used to assess the ^{90}Y-lanreotide biodistribution in 14 patients and the 5 patients treated with ^{90}Y-SMT, comparing them with ^{111}In-pentetreotide.

2) In 42 patients with NETs a retrospective analysis was performed of the ^{111}In-pentetreotide imaging and CT scan in patients treated with different therapies. A simplified scintigraphic method using ^{111}In-pentetreotide SPECT liver imaging was used to monitor changes in tumour response and to determine how this correlates with CT scan and clinical response.

Results

1) ^{90}Y-lanreotide and ^{90}Y-SMT (with amino acids) have much lower uptake in the kidney ($p < 0.000$ and < 0.041 respectively) than ^{111}In-pentetreotide.

2) 22/42 patients had a good clinical response. A mean fall in total functional STV of 37% was seen in patients with symptomatic relief and a mean increase of 72 % was seen in patients with no symptomatic relief. STV predicted the clinical outcome in 34 patients (81%) and CT predicted the outcome in 21 (50%) patients.

Conclusion

There was a difference in biodistribution between ^{111}In-pentetreotide and ^{90}Y-lanreotide/ ^{90}Y-SMT, especially in the kidneys, which may explain why there is minimal renal toxicity reported with [90] Y-lanreotide/ ^{90}Y-SMT therapies.

Finally, the assessment of functional STV is more useful in monitoring the tumour response after treatment than CT. The changes in functional volumes after therapy correlate well with clinical response.

CONTENTS

Chapter 6 ^{111}In-pentetreotide and brehmsstrahlung imaging in the assessment of biodistribution and bone marrow toxicity of somatostatin analogues 131

DEDICATION

Parents
Mr V Gnanasegaran & Mrs Saroja Gnanasegaran for their love and support.

Teachers
Dr J R Buscombe & Dr A J W Hilson for their leadership in Nuclear Medicine & personally for their guidance, love and support.

Friend
Dr Kalpesh Gandhi for his constant encouragement

ACKNOWLEDGEMENTS

CLAIMS TO ORIGINALITY

The work in this thesis describes the first use of (a) ^{90}Yttrium imaging (brehmsstrahlung) to assess the biodistribution of somatostatin analogues and (b) a new technique to assess the tumour response in patients with neuroendocrine tumours. This work was planned and executed by myself and advised by Dr. J. R. Buscombe and Dr. A. J. W. Hilson, Dept of Nuclear Medicine, Royal Free Hospital, London. A more detailed description of the work is given below.

Chapter 2, 3 and 4 gives a clinical review of current concepts in diagnosis and treatment of neuroendocrine tumours with conventional and nuclear medicine techniques.

Chapter 5 describes brehmsstrahlung imaging experiments conducted. This work was carried out with the supervision of Dr. John C Dickson, Physicist and Ms Laura Gandon, Trainee Physicist at the Department of Nuclear Medicine, Royal Free Hospital, London.

Chapter 6 describes for the first time, the use of ^{111}In-pentetreotide and ^{90}Yttrium labelled somatostatin analogues (brehmsstrahlung) imaging to

(a) Assess the biodistribution of somatostatin analogues (pentetreotide and lanreotide). This work formed part of my MSc in Nuclear Medicine (University of London, 2001).

(b) Use of ^{111}In-pentetreotide and ^{90}Yttrium labelled somatostatin analogues (brehmsstrahlung) imaging to assess the biodistribution of ^{111}In-pentetreotide and ^{90}Y-SMT.

(c) ^{90}Yttrium labelled somatostatin analogues (brehmsstrahlung) imaging to assess the biodistribution of SMT at 4 and 24 hours.

(d) Assess the role of Brehmsstrahlung imaging in the prediction of bone marrow toxicity in patients with neuroendocrine tumours after targeted therapy with ^{90}Y-lanreotide. All the above mentioned work was designed and worked by myself.

Chapter 7 describes for the first time a method - Functional SPECT tumour volume (STV) to assess tumour response using ^{111}In-pentetreotide SPECT imaging in patients treated for neuroendocrine tumours. This work was designed and executed by myself.

LIST OF EXPERIMENTS

LIST OF FIGURES

LIST OF EQUATIONS

Chaper 5

LIST OF FORMULAE

Chapter 6

Chapter 1

Introduction

The practice of oncology is undergoing significant advances. There has been significant growth in our understanding of cancer at the molecular level. Better diagnostic modalities and newer therapeutic agents have improved the management of cancer patients. Nuclear medicine imaging has been exciting and rewarding in the diagnosis, staging, assessment of treatment response and finally in the detection of relapse or residual disease. Nuclear medicine therapy uses unsealed radioactive sources for the selective delivery of radiation to tumours or target organs (Chatal *et al*, 1999). The determining factor in the choice of any therapy is the balance of prolonged survival and symptom relief versus adverse side effects.

The increasing importance of radionuclide therapy with new radiopharmaceuticals labelled with beta- and alpha-emitters, targeted to specific cells, has created the need for a thorough dosimetric analysis (Thierens *et al*, 2001). Presently radioactive dose-response data available for targeted radionuclide therapy is limited. The assessment of biodistribution of the radiopharmaceutical is important because absorbed radiation dose is measured in tumour that are large enough to accumulate and retain a quantifiable amount of the radioactivity administered. But in reality a patient will have cancer at different sites ranging from few cells to a large tumour. Many researchers have shown that as the tumour size decreases the dose delivered to the tumour also decreases, because the electrons carry their energy outside the tumour limits.

Carcinoid tumours develop in the Kulchitsky enterochromaffin cells in the crypts of Lieberkuhn and are characterized by the presence of neurosecretory granules. About

85% of carcinoid tumours are found in the gastrointestinal tract, 10% in the lung mostly as bronchial carcinoids, and the rest in various organs such as the larynx, thymus, kidney, ovary, prostate, and skin (Wallace *et al*, 1996). Carcinoid tumours express somatostatin receptors (87%) (Reubi *et al*, 1993), which are also found in other tumours (endocrine pancreatic tumours, paragangliomas, meningiomas, pituitary tumours, neuroblastomas, and medullary carcinomas including their metastases) (Lamberts *et al*, 1990; Reubi *et al*, 1990). Because somatostatin analogs bind to these receptors on many endocrine tumours, it was a logical step to try to detect these tumours by scintigraphy using radiolabeled somatostatin analogs. It has been shown that somatostatin receptor positive tumours can detected by this method (Krenning *et al*, 1989), and various radiolabelled somatostatin analogues are used in the diagnosis and treatment of neuroendocrine tumours.

In the last few years newer exciting radiolabelled compounds have been used in the treatment of various cancers including neuroendocrine tumours. Presently many more radiopharmaceuticals are in various phases of clinical trials. But the knowledge and understanding of the biodistribution of the radiopharmaceutical in different organs in the body is vital for evaluation of risk and benefits of any therapeutic method. This can serve as a basis to predict therapy effectiveness, optimise drug selection, and select the appropriate drug dose, in order to provide the safest, most effective treatment for each patient.

Once treatment begins, we also need a simple, realistic and valuable method to monitor the treatment response. Tradionally, tumour markers and conventional radiological imaging have been used for this purpose, but currently there is no single method, which is accurate and reliable to assess the treatment response. With the advent of PET and PET-CT the assessment of biological tumour response is quite

close to reality. But how many departments will be lucky enough to have the "state of the art" imaging modality is a serious question.

Finally, the combination of new imaging methods, hopefully, will provide expected levels of resolution and quantitative accuracy, which will increase the impact of the treatment planning scenario in radionuclide therapy. The main aim of this study is (a) to determine a method of demonstrating the biodistribution of beta-emitting targeted radionuclide therapy and to establish their use in diagnosis, treatment and follow up of patients with neuroendocrine tumours, and (b) to develop a method to assess the tumour volume (treatment response) after various treatments.

Neuroendocrine system and tumours

2.1 History: Neuroendocrine tumour concept

Friedich Feyter (1938), using classical histological staining methods, reported the presence of variety of a population of rather pale cells (Helle Zellen) distributed widely throughout the body, particularly in the intestine (Langley, 1994) (Table 2.1). With the increasing application of histochemistry and electron microscopy in the late 1950s and 1960s, Everson Pearse was led to conclude that a number of cells, with the common function of producing polypeptide hormones, shared a variety of ultra structural and cytochemical characteristics. He formulated the "neuroendocrine concept" by grouping these cells together under the acronym APUD, Amine–Precursor Uptake Decarboxylase (Langley, 1994). He went a step further and considered that these cells constituted a novel third branch of the nervous system, which complement the autonomic and somatic nervous system. He also showed that these cells could act together with the autonomic nervous system to control the function of internal organs. When the peptidergic nerves were included in the novel concept of the diffuse neuroendocrine system by Polak in 1979 (Langley, 1994), Pearse extrapolated this idea by suggesting that all cells constituting this system shared a common embryonic origin, namely the neural crest. However, in spite of this phenomenal and remarkable vision, the neuroendocrine concept did not get wide and unanimous approval, as it had to face a rival idea, the paraneuron concept by Fujita in 1977 (Langley, 1994).

Progress in electron microscopic techniques permitted a number of ultra-structural features common to these cells to be defined (Table 2.2).

The number of cell types in the APUD series was only 14 in 1968, but the number has now risen to 40 (Pearse, 1980). A neural origin has been confirmed in only seven members of these 40 (Langley, 1994).

Year	History
1869	Neuroendocrine cells first described in pancreas by Paul Langerhans
1870	Neuroendocrine cells were described in the gut mucosa of several species by Heidenhain
1897	Neuroendocrine cells were described again by Kultschitsky
1902	Secretin, the first gastrointestinal hormone described by Bayliss and Starling
1907	The term Carcinoid introduced by Oberndorfer
1914	Silver staining granules in chromaffin cells by Gosset and Masson Origin of carcinoids from argentaffin cells was proposed by Masson
1930	31 yr old patient with a phenomenal flush of the face was presented by Cassidy
1938	Number of gut cells were brought together under the system-"Helle Zellen" by Friedrich Feyrter
1952	5-hydroxytryptamine was identified in the extracts of the mucosa of the gastrointestinal tract by Erspamer and Asero
1952 to 1954	Association of clinical symptoms with carcinoid tumours was recognised
1953	Occurrence of 5-hydroxytryptamine in a carcinoid of appendix was described by Lembeck
1969	APUD concept by Pearse
1973	Discovery of somatostatin
1977	Paraneuron concept by Fujita,
1980	WHO classification of endocrine tumours applied the term carcinoid to all tumours of the diffuse neuroendocrine system

Table 2.1 Important years in the history of neuroendocine concept (Kloppel *et al*, 1994)

The apparent differences in the concept of APUD cell series, in particular the absence of certain cell types, led Fujita to present a rival concept called the paraneuron concept, less than ten years after the publication of Pearse's novel idea (Table 2.3). Fujita considered that specific cytochemical properties such as the APUD criteria, that is, the presence or absence of specific enzymes involved in amine metabolism, were not crucial and proposed a list of broader but more functional properties to define these cells (Langley, 1994). Because of their more general nature, these were accepted at the time. The major weakness, however was that there was no clear-cut distinction between paraneurons and the genuine neurons. Because of its lack of precision in distinguishing between neurons and paraneurons, this concept has not been widely accepted.

- **High levels of smooth endoplasmic reticulum in the form of vesicles.**

- **Low levels of rough endoplasmic reticulum**

- **Electron dense, fixation-labile mitochondria**

- **High content of free ribosome's**

- **Prominent microtubules, centrosomes**

- **Tendency to produce fine protein micro fibrils**

- **Membrane-bound secretion vesicles**

Table 2.2 APUD Cells – Ultra structural Features as described by Pearse (Langley, 1994)

A Para-neuron is

- A cell that is able to produce-substances identical with, or related to, neurotransmitters or suspected neurotransmitters

- A cell that is able to produce protein/polypeptide substances that may possess hormonal actions

- A cell that possesses synaptic vesicle-like and/or neurosecretion like granules.

- A cell that is recepto-secretory in function. It releases secretions in response to adequate stimuli acting upon its receptor site on the cell membrane

- A cell whose origin is common with neurons, that is, neuroectoderm.

Table 2.3 Fujita's Para-neuron criteria (Langley, 1994)

2.2 Neuroendocrine tumours (carcinoid tumours)

There has been some confusion in the terminology of these tumours. Some authors restrict the term carcinoid to intestinal endocrine tumours, where as others include a variety of neuroendocrine tumours. According to the WHO classification of 1980, carcinoids were defined as tumours of the diffuse neuroendocrine system that are either benign or else neoplasm's with a more favoured prognosis than carcinomas. In the revised classification (Capella *et al*, 1994) of "neuroendocrine tumours of lung, pancreas and gut" the term carcinoid was replaced by the term "neuroendocrine tumour" to designate the totality of neoplasm with neuroendocrine features (Capella *et al*, 1994; Creutzfeldt, 1996). In this chapter term neuroendocrine tumours and carcinoid tumours are used synonymously.

Neuroendocrine tumours are a rare type of cancer that can arise in different parts of the body. These are malignant tumours derived from neoplastic proliferation of cells of the diffuse neuroendocrine system (Gilligan et al, 1995). The exact incidence of carcinoid tumours is unknown since it differs considerably in different populations and with different study types. Overall, the estimated incidence is 1.5 per 100,000 of the population (Newton et al, 1994). They are well known for producing various hormonal syndromes and for their indolent clinical course in most patients; although some of these tumours do not produce hormones of clinical significance. These slow-growing tumours produce non-specific symptoms making diagnosis a challenge.

Carcinoid tumours are the most common neuroendocrine tumours in the gastrointestinal tract and between 10% and 30% of these tumours are gastric in origin (Sjoblom et al, 1988). Carcinoids may be classified according to their embryological origins as foregut, midgut, or hindgut (Solicia et al, 1981). Typically, carcinoids arise from Kulchitsky or enterochromaffin cells. They often present as diagnostic dilemmas due to obscure or non-specific symptomatology. The ability of carcinoid tumours to cause clinical symptoms by secretion of hormones or biogenic amines is best recognised in the form of the carcinoid syndrome. Although generally slow-growing, a significant proportion demonstrates aggressive tumour growth and may be difficult to manage (McStay et al, 2002). In spite of many diagnostic and therapeutic options available, careful selection and multidisciplinary approach of patients is perhaps the most important factor in prolonging survival (Caplin et al, 1998 [1,2]).

2.3 Epidemiology

Neuroendocrine tumours constitute approximately 2% of all malignant tumours of the gastrointestinal system (Moertel, 1987). These tumours are particularly rare in paediatric patients. The exact incidence of carcinoid tumours is unknown since it differs considerably in different populations and with different study types. Overall, the estimated incidence is 1.5 per 100,000 of the population (Newton *et al*, 1994).

2.4 Aetiology

The precise aetiology of neuroendocrine tumours is not well understood. Insight into the molecular biology of these tumours can be gained by studying a subset of tumours that occurs as part of the multiple endocrine neoplasia type I (MEN I) syndrome. In 1954, Wermer recognized that a neoplastic disorder involving the anterior pituitary gland, parathyroid, and pancreatic islet cells was familial and transmitted in an autosomal dominant fashion (Larsson *et al*, 1994). Larsson and his group have reported linkage of the MEN I gene to the muscle phosphorylase locus on chromosome 11q13 (Larsson *et al*, 1988). Using another gene known to be localized to 11q13 (INT2), Bale et al found similar linkage of the MEN I gene with this gene locus (Bale *et al*, 1989). Radford et al investigated DNA isolated from tumours and somatic tissues in 12 patients with MEN I and found loss of heterozygosity markers mapped to chromosome band 11q13 in 9 (82%) of 11 informative tumours. There was no allelic loss from other chromosomes. Such a high incidence of chromosomal deletion involving 11q13 suggests that this region is important in the oncogenesis of neuroendocrine tumours.

2.5 Tumour biology

Carcinoid tumours are derived from so-called APUD-cells (Amine Precursor Uptake and Decarboxylation). These specialized cells accumulate amine precursors (DOPA, 5-hydroxytryptophan) and decarboxylate them to produce biogenic amines (catecholamine or serotonin). They also produce peptides stored with the amines in secretory granules (Wilander *et al*, 1989; Solcia *et al*, 1989). The APUD-concept is currently abandoned, but it continues to provide a convenient framework for explaining the multi-potential capacity of these cells to produce various hormones and amines (Oberg, 1998 $_2$).

The exact aetiology of carcinoid tumourigenesis is unknown, although experimental studies indicate that the nuclear oncogenes N-myc and c-jun are involved (Sagara *et al*, 1995). The HER-2/neu proto-oncogene is reported to be over expressed in a proportion of carcinoid tumours (Wiedenmann *et al*, 1994). Putative tumour suppressor genes have been mapped to chromosome 9 and 16 in mice (Dietrich *et al*, 1994), but p53 gene mutations, or over expression of p53 protein, has not been implicated in the development of carcinoid tumours in humans (Lohmann *et al*, 1993; Wang *et al*, 1995; O'Dowd *et al*, 1995). Malignancy of carcinoid tumours is only clearly determined by the documentation of lymph node or liver metastases. Routine histopathology is unable to reliably predict tumour aggressiveness. Malignancy is suggested by a size greater than 2 cm in most locations except the ileum where nearly all tumours metastasise. Moyana et al examined a series of gastrointestinal carcinoid tumour to evaluate the prognostic potential of histological grade plus immunohistochemistry for MIB-1, p53, and bcl-2 expression (Moyana *et al*, 2000; Ganim *et al*, 2000). MIB-1 antibody reacts with the Ki-67 nuclear protein associated with cell proliferation. The mutated form of the transcription factor for p53 is unable

to stop cell replication, and bcl-2 blocks apoptosis. They also found an independent correlation between increased levels of MIB-1 and p53 and metastatic spread, but not for bcl-2.

2.6 Neuroendocrine markers

2.6.1 Cytoplasmic Constituents

Neuron-specific enolase, a glycolytic enzyme found in the cytosol, is the best known marker of cells with neuroendocrine differentiation. However, this marker is non-specific, as it stains positive on fibroadenomas of the breast, renal-cell carcinoma, and certain malignant lymphomas. Its positivity is therefore not considered to be diagnostic, and consequently, this reagent is also known as non-specific esterase (Klöppel et al, 1994).

2.6.2 Secretory Vesicle Membrane Constituents

Synaptophysin is an integral membrane glycoprotein that is involved in calcium binding and occurs in presynaptic vesicles of neurons and small vesicles of normal and neoplastic neuroendocrine cells (Wiedenmann et al, 1989).

2.6.3 Granule Contents:

Chromogranins A, B, and C are acidic proteins that serve as powerful universal markers for neuroendocrine tissues and tumours. Chromogranins are a family of soluble proteins located in large (dense-core) secretory granules. The most frequently used marker for neuroendocrine tumour is chromogranin A (Klöppel, 1990).

2.6.4 Plasma membrane constituents

These include receptors for peptides or neurotransmitters (somatostatin, glutamate, and gamma-amino butyric acid), and neural cell adhesion molecules (NCAMs), the most important of which appear to be NCAM and L-1 (Langley, 1994). Somatostatin receptors are present in 82% of carcinoid tumours and in 67% to 100% of islet-cell tumours (Reubi et al, 1994). Moreover, most metastases of primary somatostatin receptor–positive tumours are also positive for this peptide. Somatostatin inhibits peptide hormone secretion of most neuroendocrine cells by a mechanism that involves the suppression of secretory pathways that are dependent on cyclic adenosine monophosphate and the disruption of the second messenger function of intracellular calcium (Scherubl et al, 1993). Somatostatin receptor status correlates highly with the ability of long-acting somatostatin analogs, such as octreotide, to inhibit in vivo hormone secretion (Reubi et al, 1990). The presence of these receptors enables in vivo imaging of tumours using [111]Indium-labeled octreotide. Somatostatin analogs are thus used in both imaging and treatment of neuroendocrine tumours.

2.6.5 Growth factors and antigens

The expression of growth factors and the presence of nuclear antigens, although not unique to neuroendocrine tumours, are of particular interest. Ki-67 is a monoclonal antibody against a nuclear antigen present in proliferating cells (Gerdes et al, 1983). Patients who have tumours with a high index for Ki-67 were found to have a significantly shorter survival than those whose tumours are low in Ki-67 content (Chaudhry, 1992 [2]). Various growth factors have been studied, including platelet-derived growth factors, transforming growth factors-alpha and -beta (TGF-alpha and -beta), fibroblast growth factors, and epidermal growth factors, and the data suggest that platelet-derived growth factors may be involved in the autocrine stimulation of

neuroendocrine tumour cells and stimulation of stromal cell growth through paracrine or autocrine mechanisms (Chaudhry, 1992 [1,2]; Chaudhry, 1993). Different types of neuroendocrine cells share many specific properties and express several proteins in common, but the expression of any one-marker protein is not an absolute criterion. Thus, there is no "universal" marker.

2.7 Pathology

Macroscopically, the carcinoid tumours appear as solid and yellow-tan, reflecting their high lipid content. On histology, the tumours are glandular, trabecular, or form rosettes in their pattern of growth. The tumour cells are all quite similar, with a faint pink granular cytoplasm and round nuclei with few mitoses. These cells have been termed as chromaffin cells because they stain with potassium chromate. They are also termed argentaffin cells as they take up and reduce silver. Some tumour cells take up silver but are unable to reduce the silver and are termed agryrophilic (DeLellis *et al*, 1984). Argyrophilic and argentaffin cells have the ability to take up and decarboxylase amine precursors; originally, these cells are thought to be derived from neural-crest cells, but this is not the case. The confusion arose as both neural-crest cells and neuroendocrine-tumour cells were able to synthesise closely related amine products and peptides. Electron microscopy is quite helpful but not diagnostic in the assessment of carcinoid cells, since granules may vary in their size, shape, and density (Black *et al*, 1968). The hormonal content of these granules, which can be measured by immunohistochemistry, confirms the diagnosis of carcinoid tumours. The ability of carcinoid cells to synthesise 5-hydroxytryptamine from dietary tryptophan is pathognomonic of this tumour (Norheim *et al*, 1986). The breakdown product, 5-hydroxyindoleacetic acid, is classically associated with carcinoid tumours, but there are many hormone products that may be present within cells and released into the

circulation. These peptides include prostaglandins, substance P, kinins, somatostatin, corticotropin, gastrin, and neuron-specific enolase. In some instances, more than one hormone may be found within a single cell. Tumour cells not only make various peptides, but also express many types of peptide receptors on the cell membrane. The membrane receptors enable the tumour cells to respond to several growth factors, and, combined with genetic instability, probably contribute to the multifocal nature of carcinoid tumours (Caplin et al, 1998 [1, 2]). Neuroendocrine cells differ from neurons in that axons and specialized nerve terminals are absent in the former, and consequently, their mode of transmission is endocrine or paracrine rather than synaptic. The neuroendocrine cells normally form either small organs, distinct cell clusters within other tissues, or a network of cells dispersed in the lung and gut mucosa (Langley, 1994; Kloppel et al, 1994).

Carcinoid tumours are associated with multiple endocrine neoplasia type 1 (MEN-1) in about 10% of cases (Lehy et al, 1989). MEN-1 candidate genes have been mapped to the long arm of chromosome 11, (Larsson et al, 1988) and the MEN-1 gene was identified by positional cloning (Chandrasekharappa et al, 1997).

2.8 Characterisation of somatostatin and receptor subtypes

Somatostatin (SS) is a cyclic 14-amino acid peptide, which is widely distributed in the body (brain, pituitary, endocrine and exocrine pancreas, gut, kidney and lymphoid tissue) (Table 2.4) and has multiple sites of action (Reubi et al, 1994). Somatostatin is thought to regulate endocrine and exocrine secretion. Somatostatin also possesses antiproliferative properties and acts as a neurotransmitter or a neuromodulator in the central nervous system (Bruns et al, 1996). These effects are mediated by G protein-coupled receptors, of which at least five types have been cloned ($sstr_{1-5}$) (Table 2.5).

All receptors identified so far bind somatostatin-14 and somatostatin-28 with high affinity (Bruns et al, 1996).

All five receptors mediate inhibition of adenyl cyclase. The sstr2 receptor is apparently the predominant subtype expressed in somatostatin receptor-positive tumours (Bruns et al, 1996). The SS-receptors (SSR) are also found in non-neuroendocrine primary tumours and metastases, such as colon carcinomas and lymphomas. They are also found in non-tumoural pathologies such as inflammatory bowel disease (Reubi et al, 1994). These SS-receptors sub-serve two functions, first to recognise the ligand and bind to it with high affinity and specificity, and second to generate a transmembrane signal that evokes a biological response. Large numbers of SSR are found on most tumours with amine precursor uptake and decarboxylation characteristics and neuroendocrine properties, such as carcinoids, paragangliomas, phaeochromocytomas, medullary thyroid cancers and endocrine pancreatic tumours. In addition, large numbers of binding sites with high affinity for SS are also found on breast and brain tumours, as well as on various cells of the immune system (Reubi et al, 1988 and 1990; Lamberts et al, 1991; Papotti et al, 1989; Hofland et al, 1999). Octreotide binds with high affinity to somatostatin receptor subtype 2 (sst_2) and 5 (sst_5), to a lesser degree sst_3, while no binding to sst_1 and sst_4 occurs. Other SS analogues that are in clinical use, such as lanreotide and vapreotide, as well as the hexapeptide MK678, bind to three of the five SS-R subtypes, also displaying high affinity for sst_2 and sst_5 and moderate affinity for sst_3 (Patel et al, 1997).

Anterior pituitary gland Adenomas (GH, TSH)	*Adrenal medulla* Pheochromocytoma, neuroblastoma, ganglioneuromas	**Activated leukocytes** **Autoimmune disease, granulomas, lymphomas**
Skin Merkel cell carcinomas and melanomas	*Glial cells* Well differentiated glia-derived tumours	*GI endocrine cells* Carcinoid and Differenciated neuroendocrine carcinomas
Pancreatic islet cells Islet cell tumours	*Leptomeninx* Meningiomas	*Thyroid cells* Papillary, follicular, medullary carcinomas
Bronchopulmonary nodules Small cell lung cancer, neuroendocrine and intermediate cell carcinomas	*Paraganglia* Paragangliomas	*Miscellaneous sites* Neuroendocrine tumours of ovary, cervix, endometrium, breast, kidney, paranasal sinuses and salivary glands

Table 2.4 Expression of somatostatin receptors on various neuroendocrine tumour cells (Lamberts *et al*, 1991)

Somatostatin receptor subtypes (sst)	Effects
sst subtype 1	Mediate anti-proliferative effects
sst subtype 2	Mediates both anti-secretory and anti-proliferative action
sst subtype 3	Mediate anti-proliferative and pro-apoptotic effects
sst subtype 4	Not well understood
sst subtype 5	Mediate inhibition of GH and cell proliferation.

Table 2.5 The effects associated with somatostatin receptor subtypes (Patel *et al*, 1999; Froidevaux *et al*, 2002; Lewis *et al*, 2003)

2.9 Classification

Williams and Sandler in the early 1960s proposed a classification system based on the anatomical site of origin of the carcinoid tumour (Williams *et al* 1963; Klo"ppel *et al*, 1996).

The tumours were classified into

1. Foregut: respiratory tract, thymus, pancreas, stomach, duodenum, upper jejunum.

2. Midgut: lower jejunum, ileum, appendix, caecum and right colon.

3. Hindgut: transverse and descending colon, sigmoid, rectum, ovaries and uterus.

The foregut carcinoids are generally argentaffin-negative but argyrophilic, contain low levels of serotonin (5-HT) and small cytoplasmic granules; occasionally they secrete 5-hydroxytryptophan (5-HTP) or adrenocorticotropic hormone (ACTH) and other hormones, and have the potential to metastasise to bone. Foregut carcinoids may also occur in the MEN-1 syndrome (Zeiger *et al,* 1992).

Midgut carcinoids are argentaffin-positive, have a high 5-HT content and larger cytoplasmic granules. They rarely secrete 5-HTP or ACTH, but do release 5-HT and tachykinins and cause metastases of liver and classic carcinoid syndrome. They rarely metastasise to bone (Williams *et al*, 1963).

Hindgut carcinoid tumours are argentaffin-negative, but often argyrophilic; they rarely contain 5-HT and possess round variable density cytoplasmic granules. They rarely ever secrete 5-HTP or ACTH, but can contain numerous gastrointestinal hormones, although they rarely cause the classic carcinoid syndrome. They rarely metastasise to bone.

2.9.1 Carcinoid tumours of the bronchus

These tumours are very similar to intestinal carcinoids, and are not related to smoking. Symptoms may be from mechanical obstruction. They may be a direct source of ectopic-hormone secretion, including corticotrophin, and such patients may present with Cushing's syndrome. Carcinoid tumours of the bronchus may also secrete antidiuretic hormone and, infrequently, growth-hormone releasing hormone. Surgical resection is the treatment of choice for bronchial carcinoids whenever possible (Dusmet *et al*, 1996).

2.9.2 Carcinoid tumours of the stomach

These are predominantly associated with the enterochromaffin-like cells of the stomach (Gilligan *et al*, 1995). Three types of gastric carcinoid are recognised. Type I is associated with chronic atrophic gastritis, type A (Gastric atrophy including atrophy secondary to pernicious anaemia) which results in hypergastrinaemia. Type-II tumours usually develop in patients with MEN-1 and Zollinger-Ellison syndrome (Lehy *et al*, 1989) and although relatively benign, have a slightly greater potential to metastasise than type-I tumours. Type-III tumours are sporadic and the most aggressive (Rindi *et al*, 1993), with greater metastatic potential. In patients with carcinoid tumours larger in diameter than 2 cm associated with gastrin production, antrectomy and local resection is the best option. For those with sporadic gastric tumours, local resection is undertaken.

2.9.3 Carcinoid tumours of the ileum and small intestine

Most small-bowel carcinoids occur in the terminal ileum. Tumours larger in diameter than 2 cm are more likely to cause symptoms and are also more likely to metastasise

especially if invasive. The treatment for non-metastatic and metastatic small-bowel carcinoids is resection with adjuvant therapy for the latter group (Caplin *et al*, 1998 ₁).

2.9.4 Carcinoid tumours of the colon

Most colonic carcinoids are found in the right colon (Rothmund *et al*, 1994) and these patients present with abdominal pain and weight loss, though some present late with liver metastases. Tumours are detected by colonoscopy and those smaller in diameter than 2 cm on a pedicle may be removed by polypectomy; otherwise, local resection is required (Caplin *et al*, 1998 ₁).

2.9.5 Carcinoid tumours of the rectum

These tumours are usually small, do not produce symptoms, and are often found incidentally by endoscopy. Unless the tumours are deeply invasive, they rarely metastasise (Rothmund *et al*, 1994) and local excision is the treatment of choice (Caplin *et al*, 1998 ₁).

2.9.6 Carcinoid tumours of the appendix

These tumours are usually found incidentally and are slow-growing, benign tumours. Most carcinoid tumours occur in the distal appendix and hence do not cause any difficulties. The management of patients with carcinoids of the appendix is removal of appendix and right hemicolectomy (Caplin *et al*, 1998 ₁).

2.9.7 Carcinoid syndrome

The most common systemic syndrome caused by carcinoid tumours is the carcinoid syndrome (Table 2.6). It occurs when hormonal tumour products reach the systemic circulation. During the "first pass," the liver is able to remove from the blood stream

even large amounts of a primary tumour's hormonal products before they reach the systemic circulation. This usually implies the presence of disease that has venous drainage in the systemic circulation in such a way as to circumvent the liver and its "first-pass" effect. Such is the case with metastatic disease in the liver itself or primary disease in the bronchi. Hepatic metastasis is the most frequently associated condition in patients with carcinoid syndrome. Because tumours of the jejunum, ileum, appendix, and ascending colon are the most common and frequently metastasize, they account for about 80% of the carcinoids that cause the carcinoid syndrome (Norton et al, 1993).

Clinical features	Frequency	Characteristics	Mediators
Flushing	90%	With foregut tumours-prolonged purple hue, predominantly on the face and neck Mid gut tumours-short lived and pink-red	5-hyroxytryptamine, histamine, kalleikrien, substance –P, prostaglandins
Abdominal pain	40%	Long history	Tumour obstruction, hepatomegaly, intestinal ischemia
Diarrhoea	70%	Secretory	5-hyroxytryptamine ,histamine, gastrin, vasoactive intestinal peptide, prostaglandins
Wheezing	15%		5-hyroxytryptamine, Histamine
Heart disease	Right-30%, Left-10%		Substance-P, Neurokinin-A, 5-hyroxytryptamine
Telangiectasia	25%	Face	Unknown
Pellagra	5%	Dermatitis, diarrhoea, dementia	Niacin deficiency

----

Table 2.6 Characteristics of carcinoid syndrome (Kaplan et al, 1991; Moertel, 1992; Caplin et al, 1998 [1,2])

2.10 Standard Diagnostic Modalities

Carcinoid tumours show varying tumour biology, patients often present with-distinct clinical symptoms. Certain investigations (Table 2.7), aid the clinician in the diagnosis of carcinoid tumours.

Biochemical	Pathological	Imaging	Others
Urinary excretion of 5-HIAA	*Biopsy/FNAC*	*Chest X ray*	*Intra-arterial stimulation with secretin (for gastrinomas)*
Chromogranin concentration	*Surgical pathology*	*Endosonography*	
	Endoscopic biopsy	*Ultrasonography*	*Intra operative gamma detecting probes*
Blood serotonin concentration		*Echocardiography*	
		CT scans	
		MRI	*Intra-arterial stimulation with calcium (for insulinomas)*
Gut hormone Peptide		*Nuclear Medicine* ^{99m}Tc-MDP Bone scan ^{123}mIBG ^{111}In-pentetreotide ^{99m}Tc (V) DMSA ^{99m}Tc-Depreotide ^{99m}Tc-vapreotide PET imaging	*Portal venous sampling*

Table 2.7 Diagnostic modalities in detecting neuroendocrine tumours.

2.10.1 Histopathology

The histopathological diagnosis of carcinoids is based on silver, argyrophil staining which is a general marker for neuroendocrine differentiation, and argentaffin staining to demonstrate content of serotonin (Fig 2.1-2.4). However, these two methods have recently been mostly replaced by immunohistochemistry using antibodies against

chromogranin A and synaptophysin. In order to show the content of serotonin, specific antibodies are used (Oberg, 1998). Almost all well-differentiated neuroendocrine gastrointestinal tumors show positive staining for chromogranin A, except for some insulin-producing tumours which may be stained by chromogranin B antibodies. Synaptophysin shows similar sensitivity, but these antibodies have to be used on frozen sections rather than formalin-fixed material, which limit their clinical use. Staining for Neuron-specific enolase has been used routinely in many laboratories for staining of neuroendocrine tumours, but it is not quite specific and should therefore be combined with chromogranin A immunocytochemistry (Oberg, 1998; Wilander *et al*, 1989; Solcia *et al*, 1989). A correct histopathological diagnosis is the prerequisite for therapeutic considerations.
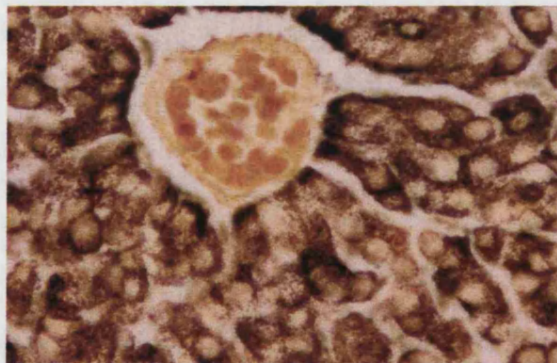
Fig 2.1 Grimelius silver staining showing the granules (Bax *et al*, Image courtesy AP Dillon)
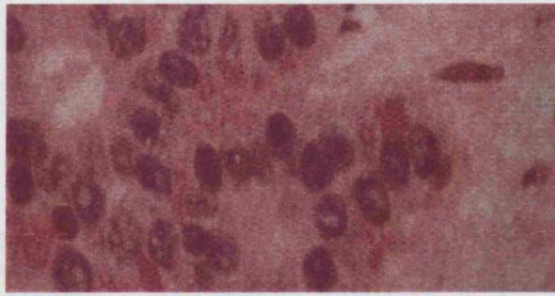
Fig 2.2 Haematoxylin & eosin (H&E) staining showing granules (Bax *et al*, Image courtesy AP Dillon)
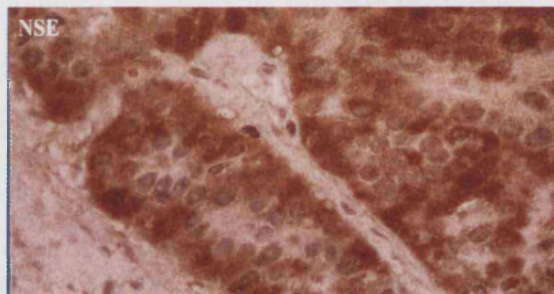
Fig 2.3 Neuron specific enolase (NSE) to categorise cells of neuroendocrine origin (Bax *et al*, Image courtesy AP Dillon)
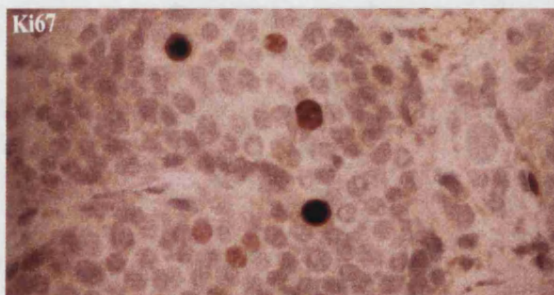
Fig 2.4 Immunostained cells for the Ki67 proliferate marker (Bax *et al*, Image courtesy AP Dillon)

2.10.2 Biochemical Diagnosis

2.11.2.1 There have been numerous investigations into identifying serum factors that may aid in the diagnosis and management of patients with carcinoid tumours (Feldman *et al*, 1986; Stridsberg *et al*, 1995). Most research has focused on neurotensin, substance P, 5HIAA and the chromogranins (A, B and C) since these factors are usually found within tumour cells and assist in histochemical diagnosis. Measurement of 24 h urine 5-hydroxyindoleacetic acid by high-performance liquid chromatography is highly specific (Stridsberg *et al*, 1995). Fruits such as bananas and avocados, and certain cough medications, can cause false-positive results whereas other drugs such as levodopa, aspirin, and phenothiazines can cause false-negative results, and this is especially highlighted by the non-specific colorimetric method for measurement of 5-hydroxyindoleacetic acid.

2.10.2.2 Chromogranins (Cg) are found in neural and neuroendocrine cells, but not endocrine tissues in general. While the full physiological role of chromogranins is not known, several cleavage products have been identified lending credence to the hypothesis that the chromogranins are primarily pro-hormones (Eriksson *et al*, 2000_2). However, use of these factors as markers for carcinoid disease is limited by specificity since pancreatic neuroendocrine tumours may also have elevated levels. False positive elevations may occur with liver or kidney failure, inflammatory bowel disease, atrophic gastritis, or the chronic use of proton pump inhibitors (Eriksson *et al*, 2000_2). There appears to be a direct correlation between tumour burden and serum chromogranin A (CgA) levels (Jenson *et al*, 1997) and a rising serum level of chromogranin A (CgA) can precede radiographic evidence of recurrence (Bajetta *et al*, 1999).

2.10.3 Conventional Imaging

There is great variability in the detection rate of the primary carcinoid tumour, and this is often dependent on its location.

2.10.3.1 Chest X-ray

Chest radiography is usually the first imaging modality to detect bronchial carcinoids and is performed to investigate non-specific respiratory complaints. Since the tumours are slow growing, they may compress airways and induce an obstructive pneumonia or atelectasis and may appear as opacities with notched margins (Nessi *et al* 1991).

2.10.3.2 Ultrasonography/ Doppler sonography

Abdominal ultrasound is frequently used as a first-line investigation in the diagnosis of GEP tumours but is relatively insensitive in the detection of GEP tumours. In one series, abdominal ultrasound detected only 15% of gastrinomas from 1 to 3 cm in size (London JF *et al*, 1991). Echo-enhanced power Doppler sonography is a non-invasive procedure that has been increasingly used for the differential diagnosis of pancreatic tumours. It has high sensitivity (94%) and high specificity (96%) for the differentiation of neuroendocrine lesions from other pancreatic tumours (Rickes *et al*, 2003).

2.10.3.3 Endosonography

Endosonography (EUS) is a sensitive method to image neuroendocrine tumours located in the pancreas and in the gastrointestinal wall (Zimmer *et al*, 1994 [1, 2]). Foregut NETs are frequently smaller than 2cm in diameter and mainly located in the

Pancreas or the gastric and duodenal wall. These NETs can be visualised in great detail with high resolution. Small pathological structures of 2-3mm in size can be detected by EUS. Endoscopic ultrasound has been reported to be very sensitive in detecting endocrine pancreatic tumours, even when CT or transabdominal ultrasound fails to show the tumour (Rösch *et al*, 1992). Various studies indicate that NETs of the pancreas can be localised by EUS in about 80-100% of cases (Rosch *et al*, 1992; Glover *et al*, 1992; Lightdale *et al*, 1991; Palazzo *et al*, 1992; Yamada *et al*, 1991; Zimmer *et al*, 1994 [1,2]). Combination of Somatostatin receptor scintigraphy and EUS increases the sensitivity even further (Zimmer *et al*, 1994 [1,2]).

2.10.3.4 Echocardiography

Regurgitation and stenosis of the tricuspid and pulmonary valve, leading to right heart failure, are the most common cardiac manifestations of the carcinoid heart disease. Echocardiography is quite useful in carcinoid heart disease, which is frequently encountered in mid-gut type of carcinoid tumours (Lundin *et al*, 1994). The characteristic pattern is involvement of mural and valvular endocardium with a plaque-like or diffuse distribution. The most frequent echocardiographic abnormalities in patients with carcinoid syndrome are functional and morphological abnormalities involving the tricuspid valve. Tricuspid regurgitation is seen in nearly 80% of these patients (Lundin *et al*, 1994). Echocardiographic findings are important for timing of valve replacement. Echocardiography is easily performed and it is suitable for screening and follow-up of patients with malignant carcinoid disease (Lundin *et al*, 1994).

2.10.3.5 Computerised Tomography (CT)

CT is relatively more sensitive for detecting insulinomas and less sensitive for detecting gastrinomas. The information obtained from the CT scan varies according to the type of scanner used. For CT scanning to be useful for the detection of NETs, advanced dynamic scanning techniques with rapid contrast injection are required. Contrast enhancement of the peritumour vessels permits identification of tumour involvement of the adjacent arterial and venous structures, and also identifies tumours greater than 2 cm in diameter and metastases of regional lymph nodes or in the liver (Fig 2.5). Approximately 30–75% of solitary gastrinomas may be detected at CT scanning (Wank *et al*, 1987) (Table 2.8 and 2.9). However, a major drawback of both CT scanning and MR imaging is that only suspected specific anatomical sites such as the abdomen or chest are usually imaged (Shi *et al*, 1998). CT scans can also be used to precisely guide a biopsy needle into a suspected metastasis. The main disadvantage of this technique is that whole body imaging is both time-consuming and expensive to perform.
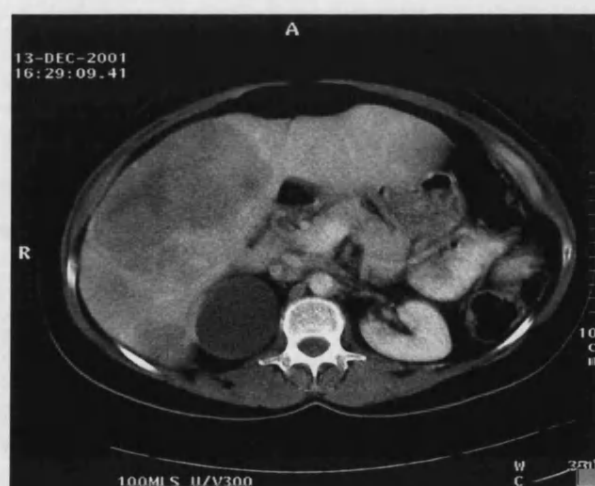
Fig 2.5 CT of liver showing multiple carcinoid metastases in the liver

2.10.3.6 Magnetic resonance imaging (MRI)

MRI has been shown to be effective for detecting tumours in both the liver and pancreas and is more sensitive than a CT scan (Shi *et al*, 1998; Reinig *et al*, 1987; Chezmar *et al*, 1991). MRI of the liver is a valuable tool for the diagnosis and follow-up of patients with metastatic carcinoid (Kvols, 1994). The boundaries of hepatic metastases are sometimes better visualized with MRI of the liver than dynamic contrast-enhanced CT scans. Liver metastases are usually seen as homogeneous lesions of medium intensity on T2-weighted images. Occasionally necrosis and hemorrhage may also be identified within the metastases (Kvols, 1994).

However, these techniques also have limitations for localizing and staging tumours. The pancreas is one of the most difficult abdominal organs to visualize, even by MR imaging. Although pancreatic endocrine tumours have significantly longer T1 and T2 relaxation times compared to normal pancreas tissue, the potential advantage of the improved tissue contrast of MR imaging has been overshadowed by the presence of motion artifacts. As a consequence, small pancreatic endocrine tumours are not detected, and the sensitivity is less than 50 % (Steiner *et al*, 1989). Since pancreatic endocrine tumours are frequently vascular, contrast agents such as gadolinium-DTPA can improve imaging. The disadvantage of MRI is availability and cost.

2.10.3.7 Angiography

Neuroendocrine tumours are seen on arteriography as diffusely enhancing masses without tumour vessels and without arteriovenous shunting. The sensitivity of angiography was 68% for extra pancreatic and 86% for hepatic lesions. Hepatic metastasis is easier to demonstrate arteriographically because of the absence of overlying bowel (Doppman *et al*, 1999). Angiography is of value for pre-operative

and pre-embolisation vascular mapping, and localising small pancreatic apudomas (Aspestrand *et al*, 1993). It is an invasive test and should be considered in the clinical context of its effect on management (Aspestrand *et al*, 1993). The role of angiography for diagnosis is very minimal.

2.10.3.8 Other methods

Other methods that are also used to localise GEP tumours include intraoperative Ultrasound, intraoperative transillumination, portal venous sampling, intra-arterial stimulation with calcium (for insulinomas) and intra-arterial stimulation with secretin (for gastrinomas). These techniques can be useful for detecting occult tumours. For ethical reasons relating to their invasive nature, however, these methods have not been used in large studies of unselected patients with GEP tumours (OctreoScan, Medicare sevices Advisory Committee, 1999).

Sensitivity	EUS	US	CT	MRI	SRS
Total	88%	32%	36%	24%	52%
<2cm	88%	6%	12%	0%	35%
>2cm	87%	87%	87%	75%	87%
Pancreas	94%	41%	47%	29%	47%
Extra-pancreatic	75%	12%	12%	12%	62%

Table 2.8 Comparison of sensitivities of different imaging procedures in detecting primary Nets depending on size and site (Kaltsas *et al*, 2001 [1,2])

Sensitivity	US	CT	MRI	SRS
Primary tumour localisation	46%	64%	42%	80%
Metastases	83%	88%	79%	90%

Table 2.9 Comparison of ultrasonography and somatostatin receptor imaging computed tomography in the detection carcinoid tumours (Eriksson *et al*, 2002).

2.11 Nuclear Medicine Imaging

Many neuroendocrine tumours can be visualised successfully with ^{123}I- MIBG, ^{111}In-pentetreotide and PET imaging (Chapter 3). These agents are taken up by normal tissues and by the neuroendocrine tumours by different mechanisms.

2.12 Standard Treatment Options

Successful treatment of malignant carcinoid tumours requires a multimodality approach. Therapeutic strategy of neuroendocrine tumours is complex, due to their heterogeneity and to the fact that although generally slow growing, a significant proportion demonstrates aggressive tumour growth (Ducreux *et al*, 2002). Chemotherapy was considered the standard for treatment of neuroendocrine tumours during the 1970s and 1980s. During the 1980s both alfa-interferon and somatostatin analogue therapies were developed and significantly improved the clinical management of malignant neuroendocrine tumours (Oberg *et al*, 1998 [1]). Somatostatin analogues are the mainstay of symptomatic medical treatment of carcinoid syndrome.

There are various treatment options available for the management of carcinoid tumours (Table 2.10). Surgery should always be considered in the treatment of

neuroendocrine GEP tumours. It may be more effective if performed in earlier stages of the disease process.

TREATMENT OF NEUROENDOCRINE TUMOURS	
SURGICAL MANAGEMENT	**MEDICAL MANAGEMENT**
Cytoreductive Hepatic Surgery *Surgical Management of Carcinoid Heart Disease* *Vascular occlusion therapy* *Liver transplantation for Hepatic metastases*	*Life style* *Chemotherapy* *Interferon* *5-hydroxytryptamine receptor antagonists* *Inhibitors of 5-hydroxytryptamine release*
RADIOTHERAPY *Control of local symptoms*	**RADIONUCLIDE THERAPY** ^{131}*mIBG* ^{111}*In-(DTPA) octreotide* ^{90}*Y-DOTATOC* ^{90}*Y-lanreotide* ^{177}*Lu-octreotate*

Table 2.10 Therapeutic modalities

2.12.1 Symptomatic

2.13.1.1 Life-style

Patients should be aware of precipitating factors such as alcohol, spicy foods, and strenuous exercise may trigger symptoms and these should be avoided (Caplin *et al*, 1998 [1]).

2.12.1.2 Inhibitors of 5-hydroxytryptamine releases

5-hydroxytryptamine receptor antagonists have been used with limited success. Methysergide (Melmon *et al*, 1965) lost favour because of the incidence of retroperitoneal fibrosis. Ketanserin and cyproheptadine (Moertel *et al*, 1991) have been shown to provide some control of symptoms.

Other antagonists such as ondansetron (Platt *et al*, 1992) may be even more effective, but await controlled trials. Octreotide, a somatostatin analogue, is the best therapy for controlling symptoms. It reduces flushing in more than 70% of patients and diarrhoea in more than 60% (Arnold *et al*, 1995). Additionally, in a minority of patients, there are several reports, including prospective trials, of an inhibitory effect of octreotide on tumour growth (Arnold *et al*, 1996).

2.12.2 Surgical treatment

Surgical removal of carcinoid tumours is often curative when the disease is detected at an early stage (Table 2.11). Surgery may also provide significant palliation for selected patients with metastatic disease (Kvols *et al*, 1994).

2.12.2.1 Cytoreductive hepatic surgery

Debulking surgery for metastatic carcinoid tumours is quite appealing as these tumours usually have an indolent course and may produce incapacitating symptoms from excess hormone production (Kvols *et al*, 1994). Palliative surgery should be considered only when at least 90% of tumour bulk could be safely excised.

2.12.2.2 Surgical management of carcinoid heart disease

Carcinoid heart disease should be suspected in patients with the carcinoid syndrome when they develop signs or symptoms of right-sided failure and such patients should be diagnosed before valvular dysfunction leads to diastolic overload and decrease of functional aerobic capacity (Kvols *et al*, 1994). Only a minority of patients with carcinoid heart disease require cardiac surgery. The patients most likely to benefit from cardiac surgery are those with worsening cardiac status but with an indolent course with relatively stable metastases (Kvols *et al*, 1994).

Carcinoid tumours of the appendix	**The management of carcinoids of the appendix are surgical. If the base of the appendix is involved, a right hemicolectomy should be considered.**
Carcinoid tumours of the ileum and small intestine	**The treatment for non-metastatic and metastatic small-bowel carcinoids is resection (adjuvant therapy for the latter group)**
Carcinoid tumours of the stomach	***Carcinoid tumours* >2 cm associated with gastrin production, antrectomy and local resection is the best option.** *Sporadic gastric tumour:* **local resection and clearance of metastatic lymph nodes (if applicable)**
Carcinoid tumours of the colon	**Polypectomy or local resection**
Carcinoid tumours of the rectum	**Local excision**
Carcinoid tumours of the bronchus	**Surgical resection**

Table 2.11 Local surgical management of neuroendocrine tumours (Caplin *et al*, 1998[1])

2.12.2.3 Liver transplantation

Liver transplantation has become routine treatment for a large number of end stage liver diseases. Liver metastases of neuroendocrine tumours are still thought to be an appropriate indication for liver transplantation with their slow growth rate and comparatively low-grade malignancy (London NJ *et al*, 1991; Gores, 1993). There are other factors which have to be considered and assessed critically before going further, such as the degree of radicality of the surgical procedure.

Not only should all macroscopic tumours be removed, but the margins of resection should be proven to be within the healthy tissue. However the number of patients with neuroendocrine tumour metastases only in the liver is comparatively low. The best indication for transplantation seems to be patients with metastases restricted to the liver who are unresponsive to adjuvant therapy after aggressive surgical resection, including excision of the primary lesion and reduction of hepatic metastases.

In such highly selective patients, liver transplantation remains a high-risk operation, but it can yield long-term survival (Dousset *et al*, 1995). In selected patients, liver transplantation for non-resectable neuroendocrine hepatic metastases may provide not only long-term palliation but also cure. In view of the shortage of donor organs, liver grafting for neuroendocrine metastases should be considered solely in patients without evidence of extra-hepatic tumour manifestation and in whom all other treatment methods are no longer effective (Lang *et al*, 1997).

2.12.3 Medical Management

Medical treatment includes chemotherapy and biotherapy. Chemotherapy is particularly useful for patients with more aggressive pancreatic tumours with high proliferation capacity, whereas alpha interferon is beneficial in classical midgut

carcinoids with low proliferation capacity. In experienced hands, hepatic artery embolisation is an effective treatment for hepatic metastasis.

2.12.3.1 Interferon therapy

Alpha–interferon is used in the treatment of carcinoid tumours because of its ability to stimulate natural killer cell function and to control secretion, clinical symptoms and tumour growth (Oberg *et al*, 1983). The anti-tumour effects of alpha-interferon include anti-proliferation, apoptosis, differentiation, and cytotoxic/cytostatic effects (Oberg *et al*, 1991). Alpha–interferon also clearly demonstrates an immunomodulatory effect by increased expression of class I antigens on tumour cells and induction of autoimmunity (Oberg *et al*, 1991; Ronnblom *et al*, 1991). Another effect of alpha-interferon is induction of fibrosis within liver metastasis. With time, the number of tumour cells decreases, and are replaced by fibroblasts, without any change in the tumour size, and therefore not recognised by conventional radiology methods (Andersson *et al*, 1990). The antiproliferative effect of alpha-interferon is mainly due to a block of the cell cycle in the G0/G1 phase with very low numbers of S-phase cells detectable after alpha-interferon administration (Chaudhry *et al*, 1992 [2]). There are some dose-related adverse effects in the alpha-interferon therapy such as weight loss, flu-like symptoms, anaemia, fatigue, leukopenia, hepatotoxicity, thrombocytopenia and increased blood lipids. The treatment with alpha-interferon is life-long and it is important to realise that the therapy is not curative but can control the disease for an extended period of time and improve quality of life.

2.12.3.2 Somatostatin and Somatostatin analogues

2.12.3.2a Somatostatin (SS) is a small regulatory peptide (Fig 2.6); it was isolated in the ovine hypothalamic gland in 1973 as a growth hormone (GH) release-inhibiting factor (Brazeau *et al*, 1973). SS is widely distributed in the human body and is found not only in the hypothalamus but also in various parts of the gastrointestinal tract, indicating that inhibition of GH is not its only function (Lucey *et al*, 1986). Apart from its function as a neurotransmitter in the central nervous system, it also has inhibitory effects on the secretion of hormones by the pancreatic islets (insulin, glucagon) and on exocrine pancreatic function. SS also inhibits normal gastrin production, and consequently gastric acid and pepsin production. A number of observations have suggested an antiproliferative effect of SS and its stable analogues (Schally *et al*, 1988; Kvols *et al*, 1986; Lamberts *et al*, 1991). Somatostatin has represented a real breakthrough in the treatment of patients with neuroendocrine gastroenteropancreatic neoplasms (Anthony *et al*, 1999). Symptomatic carcinoid syndrome and various pancreatic endocrine tumours with symptomatic syndromes are well controlled with somatostatin analogues. Somatostatin (SS) and its octapeptide analogues exert their effects through interaction with somatostatin receptor (sst) subtypes 1 to 5 (sst_{1-5}) (de Herder *et al*, 2002). Natural somatostatins (SS14, SS28) bind with high affinity to all 5 human somatostatin receptor subtypes, sst_{1-5}. However, the therapeutic use of somatostatin peptides is limited by the, rapid proteolytic degradation in plasma.

A number of short synthetic somatostatin analogs with improved metabolic stability have been synthesized in the past but Sandostatin (octreotide) and Somatuline (lanreotide) are the only two synthetic somatostatin analogs approved for clinical use

(Bruns *et al*, 1996; Bruns *et al*, 2002; Hoyer *et al*, 1994; Bauer *et al*, 1982; Murphy *et al*, 1987).

Ala-Gly-Cys-Lys-Asn-Phe-Phe-Trp-Lys-Thr-Phe-Thr-Ser-Cys

Fig 2.6 Structure of somatostatin (Fichna *et al*, 2003)

2.12.3.2b Octreotide is a synthetic octapeptide analog of somatostatin. Its major effects include inhibition of the release of pituitary growth hormone and, under certain conditions, prolactin. Octreotide also suppresses the secretion of serotonin and the endocrine secretions of the pancreas, stomach, and intestine (including gastrin, vasoactive intestinal peptide, insulin, glucagon, secretin, motilin, and pancreatic polypeptide). Octreotide also has a direct antiproliferative action, probably by blocking the action of epidermal growth factor (EGF) (CCO Formulary 2000).

Octreotide acetate is a long-acting octapeptide with pharmacologic actions mimicking those of the natural hormone somatostatin (Novartis data sheet, 1999) (Fig 2.7). Octreotide has an apparent half-life of 1.7 hours. The duration of action of Sandostatin (octreotide acetate) is variable but extends up to 12 hours depending upon the type of tumor. About 32% of the dose is excreted unchanged into the urine (Novartis data sheet, 1999). Octreotide has been successfully used in patients with functioning tumours. Long-term therapy with the mainly sst_2-specific, long-acting SS analogs octreotide and lanreotide suppresses GH release by GH-secreting pituitary adenomas, and this control of hormone release also normalizes IGF-I levels in two-thirds of patients with acromegaly (Lamberts, 2002 [1,2]).

D-Phe-Cys-Phe-D-Trp-Lys-Thr-Cys-Thr-(ol)
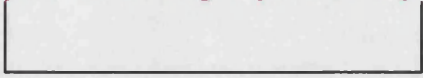
Fig 2.7 Structure of Octreotide (Fichna *et al*, 2003)

Other than instant clinical improvement, notable tumor shrinkage also occurs in most patients, based on a decrease in the size of individual pituitary tumour cells, which no longer synthesize and secrete hormone. In addition, the proliferation marker Ki-67 is lowered in octreotide-treated GH-secreting tumours, but there is no change in the apoptotic index (Losau *et al*, 2001).

In most patients with metastatic carcinoid disease and islet cell tumours, octreotide therapy also improves clinical symptoms. Control of diarrhea and flushing attacks, caused by an overproduction of serotonin or tachykinin(s), was reported in 70–90% of patients with metastatic carcinoid tumors (Lamberts *et al*, 2002 [1, 2]). Diarrhea, dehydration and hypokalemia in patients with tumours secreting vasoactive intestinal peptide, and peptic ulceration, hypoglycemic attacks and necrolytic skin lesions in patients with tumours secreting gastrin, insulin and glucagon, respectively, were also well controlled in 50–80% of patients treated with octreotide (Lamberts *et al*, 1996). Results from studies also suggest a temporary stabilization of (metastatic) tumour growth during SS analog therapy in one- to two-thirds of patients with carcinoids and/or islet cell tumors (Arnold *et al,* 2000; Shojamanesh *et al*, 2002).

The observed prolonged survival in octreotide-treated patients with these metastasized gastroenteropancreatic (GEP) tumours seems to be related, at least in part, to this temporary inhibition of tumour growth, but might also be attributed to the improvement in the quality of life of these patients (Lamberts *et al*, 2002 [1,2]).

The acceptance of the use of SS analogs such as octreotide and lanreotide by the patients further improved as monthly long-acting depot formulations of these compounds became available. Recently, significant improvement in the management of the disease has been demonstrated with long-acting repeatable (LAR) octreotide. This new formulation requires only one monthly intramuscular injection, and shows better acceptability and patient compliance to therapy (Dogliotti *et al*, 2001).

The availability of long-acting molecules has permitted the exploration of high-dose therapy in increasing tumour shrinkage and prolonging survival (Dogliotti *et al*, 2001). Octreotide acetate may be administered subcutaneously or intravenously. Subcutaneous injection is the usual route of administration of Sandostatin (Novartis Pharmaceuticals, 1999).

2.12.3.2c   Lanreotide is similar to the natural chemical Somatostatin (Fig 2.8). Somatostatin itself is chemically very unstable and is broken down within minutes of its release in the body. Lanreotide, by comparison, is extremely stable and consequently much longer acting. It is for this reason that lanreotide is preferred for medicinal use. The recommended initial dose of lanreotide LA is one 30mg injection (2ml) given intramuscularly every 14 days.

D-2-NaI -Cys-Tyr-D-Trp-Lys-Val-Cys-Thr-NH$_2$

Fig 2.8 Structure of lanreotide (Fichna *et al*, 2003)

2.12.4 Chemotherapy

Chemotherapy has been used for many years in the treatment of carcinoid tumours. The efficacy of chemotherapy in neuroendocrine tumours (NET) depends on primary site and histological differentiation. Many reports have suggested a superior activity of chemotherapy for pancreatic NET than for metastatic carcinoid tumours (Rougier *et al*, 2000). Chemotherapy has been particularly active in patients with rapidly proliferating neuroendocrine tumours such as endocrine pancreatic tumours and lung carcinoids. So far a combination of stretozotocin and 5-flurouracil or doxirubicin seems to be the most successful. Streptozotocin-based combinations including 5-flourouracil and doxorubicin have generated partial remissions in 40%-60% of patients giving a median survival of about two years in patients with advanced disease. Cisplatinum plus etoposide has demonstrated significant anti-tumour effects in anaplastic endocrine pancreatic tumours and lung carcinoids. However, in low proliferating tumours such as classical midgut carcinoids the response rates with the same combinations of cytotoxic agents have only generated short-lasting responses in fewer than 10% of patients. In some of these patients, biological treatment has been of benefit (Oberg, 2001).

2.12.5 Radiotherapy for neuroendocrine tumours

Radiotherapy has a role only for regionally advanced or metastatic disease. Carcinoid and islet tumours grow in a region with complex anatomy, containing various sensitive tissues and organs such as the kidneys, liver, stomach, small intestine and the spinal cord (Bernhard *et al*, 1994). Adequate care has to be taken not to exceed the tolerance doses for irradiation of these sensitive organs kidneys (20Gy), liver (25Gy) and stomach (45Gy) (Bernhard *et al*, 1994). Exceeding these doses will result in high-

risk complications like tissue necrosis, ulceration, perforation and neurological effects. But radiation therapy has a potential to arrest tumour growth and hormone secretion. Radiotherapy also causes pain relief and improvement of compression symptoms caused by bone and spinal metastases (Bernhard *et al*, 1994).

2.12.6 Radio-frequency ablation of liver tumours

Radio-frequency thermal ablation is receiving increasing attention as an alternative to standard surgical therapies for the treatment of liver neoplasms. Radio-frequency thermal ablation (RFA) of liver tumours is undertaken by both radiologists and surgeons using different techniques for a variety of indications. RFA of hepatic malignancies can be carried out using a percutaneous, laparoscopic, or open approach. Local control appears superior for tumours less than 4 cm when an open surgical approach is used (Kuvshinoff *et al*, 2002). Radio-frequency ablation treatment for carcinoid metastases refractory to hepatic artery embolisation may represent a useful adjunct for symptomatic control, decreased octreotide dependence, and slowing of disease progression (Wessels *et al*, 2001).

2.12.7 Radionuclide therapy

The expression of neuroendocrine peptide receptors on carcinoid tumours, and their avid uptake of ^{111}In-labelled octreotide and [123]Iodine-labelled MIBG for scintigraphic scanning, has led to the development of receptor-targeted therapy **(Chapter 4).**

2.12.8 Hepatic arterial chemoembolisation

The introduction of hepatic artery embolisation for treatment of hepatic metastases from carcinoid and other neuroendocrine tumors has demonstrated excellent palliation and cytoreduction in patients with unresectable tumors (Brown *et al,* 1999; Clouse *et al,* 1994; Gates *et al,* 1999; Lunderquist *et al,* 1982; Marlink *et al,* 1990 and Wangberg *et al,* 1993). Ethiodized oil is less morbid than embolisation with particulate matter alone and is more convenient, less costly, and less morbid than the effects of systemic chemotherapy (Clouse *et al,* 1994). Vascular occlusion therapy results in prolonged control of symptoms, biochemical response, and also tumour regression.

2.13 Prognosis

2.13.1 Foregut carcinoids

Foregut tumours rarely cause carcinoid syndrome, so the treatment usually is directed to the primary tumour. The 5-year survival after resection of patients with type I gastric carcinoids is more than 98%. Type 2 gastric carcinoid usually has a benign course. The 5-year survival in patients having type 3 or sporadic gastric carcinoids is only 20 % (Vinik *et al,* 1989; Neary *et al,* 1997; Akerstrom *et al,* 1996). The prognosis of patients with bronchial neuroendocrine tumours varied with the degree of malignancy; the 5-year survival rate ranged from 87% for patients with typical carcinoids (Skuladottir *et al,* 2002).

2.13.2 Appendiceal carcinoid tumours

Appendiceal carcinoids are the most common type of carcinoid tumours, making up 36%. Carcinoid syndrome is rare and the overall 5-year survival rate approaches 99% (Stinner et al, 1996; Neary et al, 1997).

2.13.3 Small-bowel carcinoid tumours

Carcinoid syndrome is common among patients having these tumours. The overall 5-year survival rate of small-bowel carcinoids is 50% to 60%. Disease confined to the bowel is associated with a 75% survival rate, whereas regional disease and liver metastases carry 60% and 35% 5-year survival rates respectively (Stinner et al, 1996).

2.13.4 Hindgut carcinoid tumours

Colonic carcinoids are rare, and rarely present with carcinoid syndrome. Standard colonic resection for all sizes of colonic carcinoid tumours is the treatment of choice. These tumours tend to behave as adenocarcinomas, with a 5-year patient survival ranging from 20% to 50%, depending on the stage of the tumour (Neary et al, 1997; Memon et al, 1997; Stinner et al, 1996). Rectal carcinoids are the third most common carcinoid tumour and make up to 3% of rectal tumours. Like appendiceal carcinoids, they have a favorable size-dependent prognosis (5-year survival rate, 70% to 85%).

2.13.5 Advanced metastatic carcinoid tumours

The most common cause of carcinoid syndrome is metastatic liver disease arising from a small-bowel carcinoid tumour. When carcinoid tumours from other embryological sites metastasize to the liver, the prognosis is uniformly dismal. Historical data has provided a baseline, suggesting a 5-year survival rate of less than

20% for patients with carcinoid liver metastases (Godwin *et al*, 1975) compared with other cancers. However, progression tends to be slow and it has been found that the "debulking" the tumour and thereby lessening production of syndrome-producing amines can improve both quality and length of life. In a large series of studies from the Mayo clinic (Que *et al*, 1995) of 70 patients with resected neuroendocrine liver metastases, 50 were found to have carcinoid disease, operative mortality was 2.7% and 4-year survival was 73%. Of the 57 patients who had hormone-related symptoms preoperatively, actual symptom-free survival at 4 years was 30%.

2.14 Future

2.14.1 Transfection of somatostatin receptors (SSR)

New developments in molecular biology have made it possible to transfect R-negative tumour cells with an SSR gene. There has been a new approach using sst_2 gene transfer in the treatment of pancreatic cancer (Slooter *et al*, 2001; Rauly *et al*, 1996). By inducing the SSR on the tumour cells, antitumour effects are obtained which might be attributed to several mechanisms. Firstly, an autocrine negative feedback loop in which transfected tumour cells start to produce SS, which binds in an autocrine manner to the induced SSR, may provide an inhibitory effect on tumour cell growth. Secondly, the binding of SS to sst_2 may upregulate p27, a tumour suppressor gene, which leads to cell cycle arrest in the G0-G1 phase, and subsequently causes apoptosis. Local and distant bystander effects have also been noted (Rochaix *et al*, 1999). The local bystander effect might be attributed in part to apoptosis. When type sst_2-positive cells undergo apoptosis, these cells release apoptotic vesicles and enzymes, which in turn may kill neighbouring cells. The distant bystander effect is be explained by a paracrine effect. SS can upregulate the expression of sst_1 on parental

tumour cells, thereby rendering them sensitive to the antiproliferative effect of SS. All the above mentioned mechanisms may contribute to successful treatment of certain types of cancers with gene therapy. Another reason why transfection of tumour cells with an SSR gene may be beneficial involves radionuclide therapy (Slooter *et al*, 1999). By inducing the SSR on SSR-negative tumours, treatment with radionuclides should be possible. Moreover, transfection of SSR-positive tumours with an SSR gene can increase the homogeneity of distribution of tumour cells expressing the SSR and thereby increase the efficacy of therapy; at present this strategy is currently being investigated. Transfecting tumour cells with SSRs in combination with radionuclide therapy are a new modality in the treatment of cancer; however, it is experimental and its full potential remains to be elucidated in the near future. (Slooter *et al*, 2001).

2.14.2 Newer somatostatin analogue: SOM-230: A universal ligand

The incorporation of structural elements of somatostatin-14 in a stable cyclohexapeptide template in the form of modified unnatural amino acids resulted in the identification of the novel cyclohexapeptide SOM-230 (Bruns *et al*, 2002).

It is a promising new metabolically stable cylohexapeptide with broad SRIF receptor binding and is currently under investigation in phase I clinical trials (Bruns *et al*, 2002). SOM-230 exhibits a very different binding pro-file to human somatostatin receptors hsst1–5. It binds with a high affinity to sst1, sst_2, sst_3 and sst_5, and with a lower affinity to sst_4. When compared with Sandostatin and Somatuline, SOM-230 exhibits a 20 to 30 times higher binding affinity to sst1, and a 40 to 100 times higher binding affinity to sst_5, respectively. Interestingly, SOM-230 demonstrates one of the highest binding affinities to sst_5 ever reported for an SRIF analog, which is even two times higher than that measured for SRIF-14. SOM-230 has very potent inhibitory

effects on GH and IGF-I release. SOM-230 has a very long plasma half-life of nearly 24 hours (Bruns *et al*, 2002). Therefore, SOM-230 is a promising development candidate with several potential advantages over currently used SRIF analogs. SOM-230 may also, at last, give an answer to the long-standing question, whether the sst_1- and sst_3- mediated anti-tumour effects (cell cycle inhibition, induction of apoptosis) have a clinically beneficial effect not only in patients with inoperable carcinoids and islet cell tumours, but also in patients with otherwise non treatable somatostatin receptor-positive breast, prostate and colonic cancers (Lamberts *et al*, 2002_1).

2.14.3 Vascular–targeting agent

Dependence of tumour cells on a functional blood vessel system for survival, proliferation, and metastatic dissemination leads to a fascinating concept called vascular-targeted anticancer therapy. There is a possibility of indirectly inhibiting tumour growth and survival by interfering with neo-vessel formation or function (Carmeliet *et al*, 2000; Benezra *et al*, 2001; Micheletti *et al*, 2003). Unlike anti-angiogenic agents, aimed at preventing vessel formation, the vascular-targeting agents aim to compromise the integrity and functionality of already existing tumour vessels, leading to shutdown of the tumour vascular system and consequent tumour cell death (Chaplin *et al*, 1999). Vascular targeting is made possible by the structural, phenotypic, and functional differences between vessels in tumour and normal tissues (Brown *et al*, 1998; Ruoslahti *et al*, 2000; St Croix, 2000). The tubulin-binding agent ZD6126 is a novel vascular-targeting agent in clinical development for the treatment of solid tumours (Micheletti *et al*, 2003). The colchicine derivative ZD6126 is a water-soluble phosphate pro-drug. It is converted *in vivo* into *N*-acetylcolchinol (ZD6126 phenol), which binds to the colchicine-binding site on tubulin, and causes

disruption of microtubules. In animal models, ZD6126 selectively induces tumour vascular damage and massive tumour necrosis at well-tolerated doses (Blakey *et al*, 2002). ZD6126 is currently in early phase clinical trial (Micheletti *et al*, 2003).

2.15 Discussion

Diagnosis of neuroendocrine tumours is challenging and interesting. Today there are various diagnostic modalities available for diagnosis starting from biochemical markers (5-HIAA, Chromogranin A and B, tachykinins, pancreastatin and subunits of HCG) histopathology (silver staining, argyrophil and argentaffin staining) and imaging modalities. But all these modalities have advantages and drawbacks related to their sensitivity and specificity. Conventional radiological techniques such as CT scan, MRI, and angiography are well-established tools for the identification of NETs. But these modalities are helpful in only in certain types of neuroendocrine tumours depending on their size and site. Nuclear medicine with its diagnostic and therapeutic potential had made significant impact in the diagnosis and treatment of these tumours (Chapter 3 and 4). Today increasing number of investigative procedures and therapeutic options are available to diagnose and treat these complex neuroendocrine tumours. To treat these tumours effectively we need a multidisciplinary neuroendocrine team. A general consensus on the best evidence-based management of a patient needs to be discussed and agreed. If a patient requires surgery the appropriate surgeon should be consulted. All scintigraphic and radiological scans should be reviewed in a joint meeting with an interventional radiologist and nuclear medicine physicians. We should have protocols for serial haematological, biochemical, urinary, and radiological assessment. These protocols enable formal

assessment of therapeutic response and audit of management, as well as the opportunity to carry out controlled trials.

2.16 Conclusion

Patients with neuroendocrine tumours are uncommon, and optimum management should therefore be done in centres of expertise with a multimodality approach. Endocrinologist, medical/surgical oncologist, interventional radiologist and nuclear medicine experts should take part in the assessment and care of these patients. This will help to provide the much needed multidisciplinary approach in diagnosis and treatment.

Chapter 3

Nuclear Medicine imaging in neuroendocrine tumours

3.1 Introduction

Cancer diagnosis is one of the clinical dilemmas every physician faces in spite of

advances in diagnostic modalities. Most of the techniques have very good sensitivity

but very few have good specificity. In general, the smaller the tumour at the time of

diagnosis, the better the prognosis. Accurate early detection of the tumour gives us a

chance to plan and treat appropriately.

Neuroendocrine tumours offer a new diagnostic and therapeutic challenge. These

patients can be evaluated by anatomical imaging studies, such as computed

tomography (CT) or magnetic resonance imaging (MRI), and the functional status of

these tumours are assessed using physiological imaging by scintigraphy.

Neuroendocrine tumours can be visualized by several nuclear medicine modalities

based on different mechanisms of cellular uptake (Table 3.1). The most widely used

radiopharmaceutical is Iodine-metaiodobenzylguanidine (^{123}I-mIBG) and Indium–

pentetreotide (^{111}In-pentetreotide). Recently positron-emmiting agents have been used

for imaging neuroendocrine tumours.

3. 2 Radionuclides

The selection of an appropriate radionuclide is very important in developing any

diagnostic or a therapeutic radiopharmaceutical. Important factors should be

considered, which include half-life of the radioactive nuclide, mode of decay, cost

and availability (Table 3.2).

Radionuclide half-life is a critical factor. For diagnostic imaging the half-life of a radionuclide must be long enough to facilitate the accumulation in the target tissue, while allowing clearance through the non-target organs.

Radiopharmaceutical	Mechanism of uptake
[111]In-Pentetreotide	Somatostatin receptor level uptake and localises primarily on the tumour cells of neuroendocrine origin.
[123]I -metaiodobenzylguanidine	Primarily an active uptake-1 mechanism in the cell membrane. It localises in the catecholamine storage granules and adrenergic nerve endings.
[18]F-fluoro-2-deoxy-D-glucose (18F-FDG)	Increase in glycolytic metabolism accounts for an increase of the FDG uptake
[11]C-labeled 5-HTP	Metabolic pathway converting 5-HTP (5-hydroxy-tryptophan) to 5-HT

Table 3.1 Radiopharmaceuticals for imaging neuroendocrine tumours

3.2.1 Technetium [^{99m}Tc]

^{99m}Tc is used in most of the nuclear medicine diagnostic procedures. It has ideal properties for gamma camera imaging. It has a half-life of 6 hours which is long enough to synthesize the ^{99m}Tc-labeled radiopharmaceuticals and perform imaging studies. ^{99m}Tc emits a 140 keV gamma-ray with 89% abundance which is close to optimum for imaging. ^{99m}Tc is readily available at low costs from its parent nuclide ^{99}Mo ($t_{0.5}$ = 66 h) from a ^{99}Mo/^{99m}Tc generator (Fichna et al, 2003; Sattelberger et al, 1999).

3.2.2 Iodine [^{123}I]

^{123}I has a half-life of 13 hours. It has the most favorable physical properties of any radioisotope of iodine. ^{123}I decays by electron capture with the emission of gamma

photons of 159 keV and has no beta particles. Disadvantages of ^{123}I are its limited availability, cost and short half-life.

3.2.3 Indium [^{111}In]

^{111}In has a half-life of 67 hours which makes it an ideal isotope for labelling peptides and immunoglobulins, where imaging is performed over several days. ^{111}In nuclide decays by electron capture with emission of gamma-photons of 173 and 247 keV (89% and 95% abundance, respectively), which is used in gamma-scintigraphy. ^{111}In is often used as an equivalent for ^{90}Y in scintigraphic imaging in humans for dosimetry studies, since ^{90}Y does not emit gamma-rays (Fischman *et al*, 1993).

Technetium [^{99m}Tc] Main emissions							
	Gamma or X		Beta (Emax)		Electrons		Alpha	
	E	%	E	%	E	%	E	%
E1	18	6			120	9		
E2	21	1			138	1		
E3	141	89						
% omitted		1				1		
Iodine [^{123}I] Main emissions							
	Gamma or X		Beta (Emax)		Electrons		Alpha	
	E	%	E	%	E	%	E	%
E1	27	71			127	14		
E2	159	83			154	2		
E3	529	1			158	<1		
% omitted		17				4		
Indium [^{111}In] Main emissions							
	Gamma or X		Beta (Emax)		Electrons		Alpha	
	E	%	E	%	E	%	E	%
E1	23	69			145	9		
E2	171	90			219	5		
E3	245	94						
% omitted		15				2		

Table 3.2 Showing main emissions from the diagnostic radionuclides (Delacroix, 1998)

3.3 Radiopharmaceuticals

3.3.1 Radiopharmaceuticals are drugs containing atoms of some radioactive elements. They are designed for diagnostic or therapeutic purposes, to deliver small doses of ionizing radiation to the disease sites in the body. Therapeutic radiopharmaceuticals, unlike classical chemotherapeutics, may act against malignant cells with high specificity (Fichna *et al*, 2003). In the past decade significant progress has been made in the development of peptide-based target-specific radiopharmaceuticals for imaging and radionuclide targeted therapy. The peptide that has attracted the greatest interest as an imaging agent is somatostatin (SS). Somatostatin is a tetra-decapeptide that regulates the secretion of numerous hormones. In addition, receptors for somatostatin are expressed on a variety of human tumours and that fact has become a basic principle for the use of somatostatin analogues in radiochemistry, tumour imaging and treatment (Lamberts *et al*, 1988; Lamberts *et al*, 1991; Thakur *et al*, 1997; de Jong *et al*, 1999). Presently somatostatin analogues that are more resistant to biological degradation are available. The cyclic octapeptide, octreotide (Anderson *et al*, 2001) is a good replacement for somatostatin in the clinical application, since it shows similar bioactivity, it has a relatively high metabolic stability and its pharmacokinetic properties are better. Octreotide is less susceptible to enzymatic degradation in vivo due to the incorporation of the N-terminal D-Phe and the C-terminal amino alcohol, Thr (ol), into its molecule (Lewis *et al*, 1999, Bauer *et al*, 1982). The pharmacophoric group in octreotide is a sequence of four amino acids: -Phe^3-D-Trp^4-Lys^5-Thr^6-, which organized into a beta-turn conformation by a disulfide bond, formed between cysteine residues at the N- and C-terminus of the peptide backbone (Signore, 1995). Many octreotide analogues have been synthesized and some of them have proved to be useful as targeting molecules (Bakker *et al*, 1990).

3.3.2 Synthesis of target specific radiolabeled peptides for diagnostic neuroendocrine imaging

Once we have an ideal radionuclide and a targeting molecule, we need good labelling methods to bring them together. Peptides are labelled with a variety of radionuclides for specific, diagnostic or therapeutic applications. This is commonly done, by using both conventional and novel chelating moieties. High specific-activity peptides are prepared and used to minimize unwanted physiologic effects (Weiner *et al*, 2001). These radiolabeled peptides have revolutionised the diagnosis and treatment of neuroendocrine tumours. Peptides can be synthesized easily and inexpensively, they have fast clearance and rapid tissue penetration, and they are less likely to be immunogenic than antibodies. Most peptides have a high affinity for characteristic receptor molecules that are overexpressed on malignant mammalian cells (Weiner *et al*, 2001). Peptides can be labelled in different ways and each method has some advantages and disadvantages over the other (Table 3. 3).

Labelling method	Principle	Targeting molecule	Advantages	Disadvantages
Direct labelling	Radionuclide binds directly to active groups present in the targeting molecule	High molecular weight molecules	Easy to perform	1.Chemistry is unknown 2.unknown geometry of radionuclide-targeting molecule complex 3. Posible damage to targeting molecule during labelling process.
Chelate methods *Pre-labelling*	Labelling of BFCA followed by conjugation with the targeting molecule	Small peptides	1.Relatively easy to control 2.Well defined chemistry 3.Targeting molecule functional groups remains unlabeled	1.Time consuming 2. complicated purification of obtained radiopharmaceutical
Chelate methods *Post-labelling*	Conjugation of BFCA to targeting molecule followed by labelling of conjugate	Small peptides	1.Most popular method 2.Well defined chemistry 3.possible use of classical solid phase or solution methods of peptide synthesis	1. Possible damage to targeting molecule during labelling process

Table 3.3 Overview of peptide Labelling Methods (Fischman *et al*, 1993; Liu *et al*, 1997; Eisenwiener *et al*, 2000; Baidoo *et al*, 1998; Thakur *et al*, 1995 and Fichna *et al* 2003)

3.4 Bifunctional Chelating Agents (BFCAs)

BFCAs are used to connect a radionuclide and a targeting molecule to form a radiopharmaceutical. An ideal BFCA should coordinate with radionuclide with a high yield, to form a relatively stable complex. The agent must comply with the nature and oxidation state of a radionuclide and should prevent any accidental changes in its redox potential (Fichna *et al*, 2003). It is important to carefully choose a proper BFCA, as the conjugation with targeting molecule requires specific conditions: pH, temperature, reaction time. The stereochemistry of a BFCA is important when synthesizing radiopharmaceuticals for targeting specific receptors. (Fichna *et al*, 2003).

3.4.1 DTPA

DTPA (diethylenetriaminopentaacetic acid) belongs to the group of polyaminocarboxy chelates (Fichna *et al*, 2003). It is a strong chelating group, mostly linked with ^{111}In, a trivalent radionuclide. It can also be attached to larger proteins like albumins and antibodies (Meares *et al*, 1986; McMurry *et al*, 1998; Hnatowich *et al*, 1983) as well as to small peptides, like somatostatin analogues (Bakker *et al*, 1991, Krejcarek *et al*, 1977). A great obstacle in the efficient radiolabeling of DTPA conjugates is the presence of trace metals in the preparation, which compete with radionuclides in the process of labelling. For that reason a significant, 40- to 70-fold molar excess of peptide conjugate and ultra-pure radionuclide derivative of the highest possible specific activity are required (Bakker *et al*, 1991). Many research groups put much effort into the synthesis of kinetically stable DTPA-peptide conjugates that form complexes with ^{90}Y (Brechbiel *et al*, 1991). Substitutions, particularly in the carbon atoms of the DTPA backbone, sterically hinder the opening of the chelate ring that must occur during radionuclide complex dissociation and

increase the in vivo stability of the radiopharmacutical. ^{99m}Tc is less suitable for the labelling of DTPA-peptide conjugates, as this radionuclide, even at high concentrations, has low affinity and poor selectivity to the binding sites of this BFCA (Blok *et al*, 1999).

3.4.2 DOTA

DOTA (1, 4, 7, 10-tetraazacyclododecane-N, N', N'', N'''-tetraacetic acid) and its derivatives is a good alternative for DTPA. They play an important role in clinical applications, as they form very stable complexes with a variety of trivalent radionuclides, such as ^{66}Ga (gallium), ^{67}Ga (gallium), ^{68}Ga (gallium), ^{86}Y(yttrium), ^{90}Y(yttrium), ^{111}In (indium), ^{149}Pm (promethium), ^{177}Lu (lutetium) (de Jong *et al*, 1997, Virgolini *et al*, 1998; Otte *et al*, 1997; DeNardo *et al*, 1995; DeNardo *et al*, 1998; McMurry *et al*, 1992). Two different approaches for DOTA conjugation with peptides have been developed. In the first approach one of the four carboxy groups in DOTA is activated to facilitate the reaction with primary amines in the peptide and form a stable amide bond linkage. In the second approach DOTA derivatives with additional side chains are used. The conjugation of all DOTA derivatives to a peptide is performed through an amino group of a peptide. DOTA and derivatives are successfully conjugated to a number of somatostatin analogues (Otte *et al*, 1997; Virgolini *et al*, 1998; Keire *et al*, 2001; Otte *et al*, 1998; Smith-Jones *et al*, 1998; Heppeler *et al*, 1998; Stolz *et al*, 1998). DOTA conjugates are especially suitable for radionuclide therapy, as they can be radiolabeled with ^{67}Ga (*75*), ^{90}Y (DeNardo *et al*, 1995; Smith-Jones *et al*, 1998) and ^{111}In (Virgolini *et al*, 1998). However, ^{90}Y conjugates the chelate situated closer to the peptide, so that the labeled conjugate is more rigid and less flexible, which makes binding with the receptor more difficult.

3.4.3 TETA

TETA (1, 4, 8, 11-tetraazacyclotetradecane-1, 4, 8, 11-tetraacetic acid) is one of the most studied chelating agents for copper (^{64}Cu)in peptide targeted radiotherapy. TETA has been successfully used as a BFCA with somatostatin analogues (Anderson et al, 1999).

3.4.4 HYNIC

HYNIC (2-hydrazinonicotinic acid) has been used as a BFCA for radiolabeling of different groups of molecules, such as γ-globulins (Abrams et al, 1990, Schwartz et al, 1991) chemotactic peptides (Babich et al, 1993; Babich et al, 1995) and somatostatin analogues (Krois et al, 1996; Bangard et al, 1998; Decristoforo et al, 1999; Decristoforo et al, 2000). The structural organization of HYNIC determines its application, as it can only occupy one or two coordination sites of the radionuclide. That is the reason why a coligand such as tricine or EDDA (ethylenediaminodiacetic acid) should be also coordinated to complete the coordination sphere of a radionuclide (Edwards et al, 1997; Liu et al, 1998). The conjugation of co-ligands helps in modifying the properties of obtained radiopharmaceutical, such as hydrophilicity or pharmacokinetics. However, the requirement for the use of coligands makes the chemistry of the synthesis more complicated, and multiple possible products and side-products can be obtained. HYNIC is often used as a BFCA for somatostatin analogues. The desired amide bond formation should occur between the carboxy group of HYNIC and the N-terminal amino group of a peptide. However, in somatostatin analogues the presence of lysine makes it difficult to obtain a mono-substituted product. The available methods of HYNIC-octreotide conjugation have been compared and none of them seemed efficient (Krois et al, 1996).

3.5 Somatostatin receptor scintigraphy (SRS)

Peptide receptor scintigraphy is a sensitive and specific technique to show in vivo the presence and abundance of somatostatin receptors on various tumours. With this technique primary tumours and metastases of neuroendocrine cancers as well as of many other cancer types can be localised (Krenning *et al*, 1999). The high level expression of somatostatin receptors (SSTR) on various tumour cells has provided the molecular basis for successful use of radiolabeled somatostatin analogs as tumour tracers in nuclear medicine. The vast majority of human tumours seem to over express the one or the other of five distinct Somatostatin receptors sub-types (Table 3.4). Whereas neuroendocrine tumours frequently over express sub-types 2, intestinal adenocarcinomas seem to over-express more often sub-types 3 or sub-types 4, or both of these subtypes (Virgolini *et al*, 2001).

3.5.1 ^{123}I Tyr-3 octreotide

In 1987, researchers from the University Hospital Dijkzigt Rotterdam introduced I-123-labeled Tyr-3 octreotide. Using this agent, neuroendocrine tumours were visualized, in vivo, based upon the identification of somatostatin receptors (Lamberts *et al*, 1990, Krenning *et al*, 1989; Kvols *et al*, 1993). However, disadvantages of this particular agent included limited availability, the expense and short half-life of I-123, difficult labelling chemistry, and high abdominal background of radioactivity, due to the principle clearance of this agent through the liver.

3.5.2 ^{111}In- pentetreotide

To overcome the difficulties associated with I-123 Tyr3-octreotide, a second radiolabeled analog of octreotide was developed, which was formulated by

conjugating diethylene triamine penta-acetic acid (DTPA) to the basic octreotide molecule, which allowed radiolabeling by chelation with [111]Indium (Krenning et al, 1993). This radiopharmaceutical was known as OctreoScan. Visualization of SSR-positive neuroendocrine tumours, with [^{111}In-diethylenetriaminopenta-acetic acid (DTPA)] pentetreotide (Octreoscan, Mallinckrodt Medical BV, Petten, Netherlands) has been used for more than 10 years (Krenning et al, 1989, 1995). Various tumours with somatostatin receptors can be imaged with ^{111}In-pentetreotide. Successful scanning depends on receptor-mediated internalization of (^{111}In-DTPA) octreotide, which results in degradation to the final radiolabeled metabolite ^{111}In-DTPA-D-Phe in the lysosomes (Duncan et al, 1997). This metabolite is not capable of passing through the lysosomal or other cell membrane(s) and will, therefore, stay in the lysosomes, causing the long intracellular retention time of [111]In (Duncan et al, 1997). This internalization process of (^{111}In-DTPA) octreotide is essential for successful scintigraphy and radionuclide therapy of tumours, because various radionuclides that are suitable for radiotherapy (e.g., those emitting conversion and Auger electrons such as ^{111}In) are only effective over a short distance of only a few nanometres to micrometers from their target, the nuclear DNA. ^{111}In-labeled (DTPA) octreotide has an appropriate distribution profile in humans and long biologic half-life for ^{111}In in tumour tissue, for scintigraphy and radionuclide therapy (Kwekkeboom et al, 2000). The efficacy of SRS using ^{111}In-labeled (DTPA) octreotide in patients with histologically or biochemically proven endocrine pancreatic tumours or carcinoids was evaluated in a European multicentre trial (Krenning et al, 1995).

The highest success rates were observed with glucagonomas (100 %), vipomas (88 %), gastrinomas (73 %), 'non-functioning' islet cell tumours (82 %) and carcinoids (87 %). Insulinomas were detected in only 46 % of cases (owing to the low incidence of

sst$_2$ on insulinoma cells) (Table 3.5). The low sensitivity in this study found for some

tumours could be related to important differences in scanning procedures, such as the

amount of radioligand administered, the duration of the acquisition and the use of

single photon emission computed tomography (SPECT) (Valkema *et al*, 1996;

Krenning *et al*, 1995; Slooter *et al*, 2001).

Neuroendocrine with somatostatin receptors	Non-neuroendocrine with somatostatin receptors
- Adrenal medullary tumours (pheochromocytoma, neuroblastoma, and ganglioneuroma) - Gastroenteropancreatic tumours (e.g., gastrinoma, insulinoma, glucagonoma, vasoactive intestinal polypeptide secreting tumour [VIPoma], and non-functioning gastroenteropancreatic tumours). - Carcinoid tumours. - Medullary thyroid carcinoma. - Melanoma. - Merkel cell tumour of the skin. - Paraganglioma. - Pituitary adenomas. Small cell lung carcinoma	- Astrocytomas. - Benign and malignant bone tumours. - Breast carcinoma. - Differentiated thyroid carcinoma (papillary, follicular, and Hürthle cell). - Lymphoma (Hodgkin's and non-Hodgkin). - Meningioma. - Non–small cell lung carcinoma. - Prostate carcinoma. - Renal cell carcinoma. - Sarcomas. - Autoimmune diseases (e.g., rheumatoid arthritis, Graves' disease, and Graves' ophthalmopathy). - Bacterial pneumonia. - Cerebrovascular accident. - Fibrous dysplasia. - Granulomas (e.g., tuberculosis and sarcoid). - Radiation pneumonitis.

Table 3.4 Indications for ^{111}In-pentetreotide imaging (Helena *et al*, 2001)

Neuroendocrine tumours	^{111}In-pentetreotide sensitivity
Islet cell tumours (gastrinomas, insulinomas, vasoactive intestinal polypeptide-secreting tumours, and glucagonomas)	75%–100% (except for Insulinoma, 50%–60%)
Pheochromocytomas, neuroblastomas, and paragangliomas	> 85%
Medullary thyroid carcinoma	65%–70%
Carcinoid	86%–95%
Small cell lung cancer	80%–100%

Table 3.5 ^{111}In-pentetreotide sensitivity in various neuroendocrine tumours (Helena *et al*, 2001; Krenning *et al*, 1995)

3.5.3 Principle of imaging

[111]Indium-pentetreotide is a (^{111}In-DTPA-D-Phe-) conjugate of octreotide, a somatostatin analog that binds to somatostatin receptors (predominantly somatostatin receptor subtypes sst_2 and sst_5). This octapeptide concentrates in neuroendocrine and some non-neuroendocrine tumors containing somatostatin receptors (Fig 3.1, 3.2).

3.5.4 Imaging protocol: [111]Indium is labelled with pentetreotide (Octreo scan, Tyco Healthcare, Petten, Netherlands). Approximately 120-150 MBq is injected intravenously. Whole body imaging and SPECT of liver or any other abnormal sites detected on the planar imaging are performed 24 hours later (Table 3.6).

Study	Whole body somatostatin imaging	SPECT imaging
Radiopharmaceutical	^{111}In-pentetreotide	^{111}In-pentetreotide
Activity administered	120-150 MBq	120-150 MBq
Patient preparation	None	None
Patient positioning	Supine, arms to side using the arm rest	Supine, arms to side using the arm rest
Collimator	Medium energy general purpose	Medium energy general purpose
Energy and window	170+250 keV with 15% window offset	170+250 keV with 15% window offset

Table 3.6 Somatostatin imaging protocol used at the Royal Free Hospital
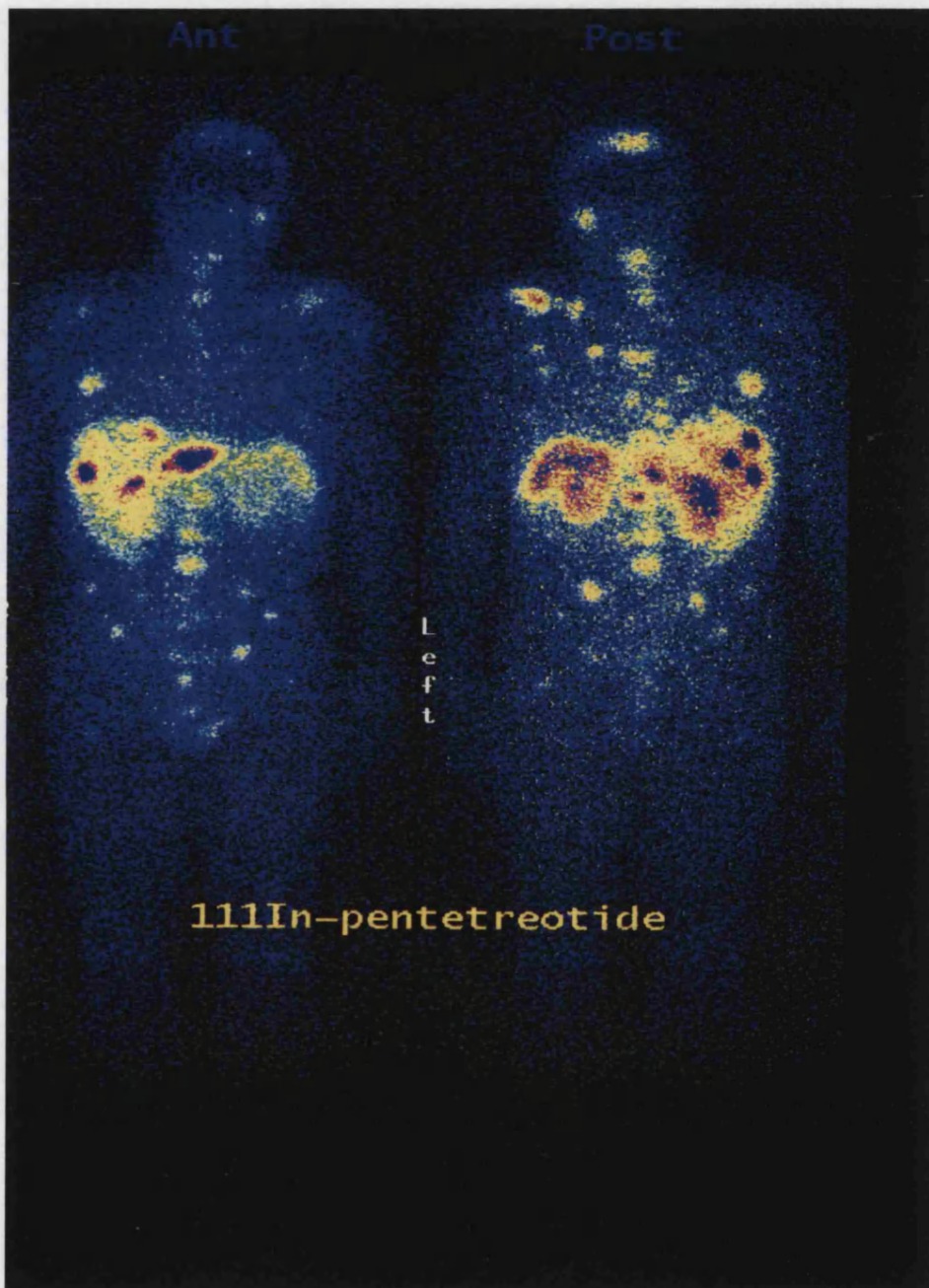
Fig 3.1 Whole body [111]Indium-pentetreotide scan showing multiple somatostatin receptor positive tumours all over the body
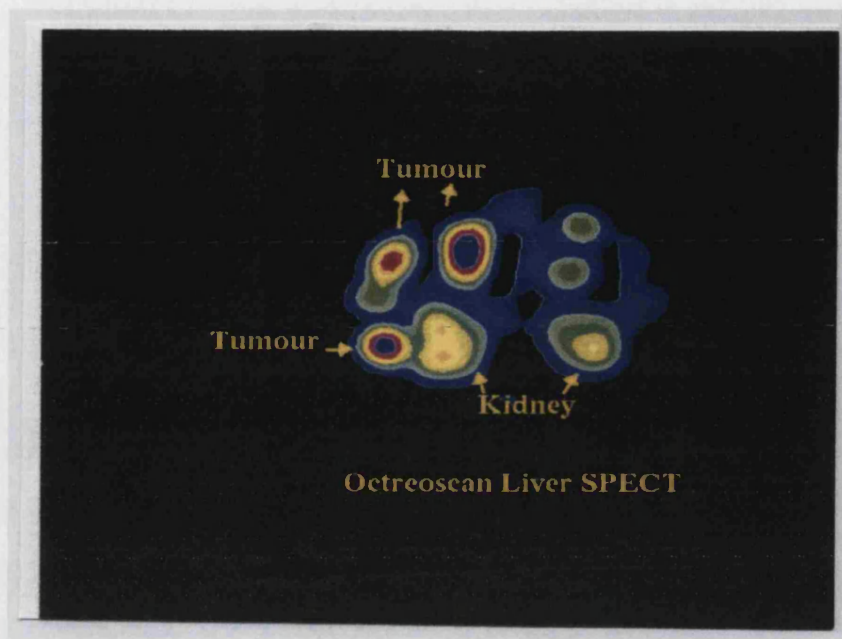
Fig 3.2 Octreoscan liver SPECT demonstrating multiple lesions in the liver

3.5.5 Normal distribution and artefacts: Normal scintigraphic features include visualization of the thyroid, spleen, liver, kidneys, and in part of the patient's pituitary (Table 3.7). In addition, the urinary bladder and the bowel (to a variable degree) are often visualized .The visualization of the pituitary, thyroid, and spleen occurs because of receptor binding (Kwekkeboom *et al*, 2000). Uptake in the kidneys is for the most part from reabsorption of the radiolabeled peptide in the renal tubular cells after glomerular filtration, although somatostatin receptors have been demonstrated in human renal tubular cells and vasa recta (Reubi *et al*, 1993). There is a predominant renal clearance of the somatostatin analog, although hepatobiliary clearance into the bowel also occurs, which necessitates later images and SPECT to facilitate the interpretation of abdominal image.

Potential causes of a false-positive interpretation	Potential causes of a false-negative interpretation
1. Accumulation of ^{111}In-pentetreotide in the nasal and pulmonary hilar areas can be seen with respiratory infections. 2. Diffuse pulmonary or pleural accumulation of ^{111}In-pentetreotide can be observed after radiation therapy to the lung or bleomycin therapy. 3. The tracer may accumulate at recent surgical and colostomy sites. 4. Accumulation of the tracer in normal structures (pituitary, thyroid, liver, spleen, kidneys, bowel, gallbladder, ureters, bladder, or stimulated adrenal glands) must be kept in mind. 5. Caution must be used to avoid interpreting physiologic gallbladder activity as hepatic metastasis.	1. Presence of unlabeled somatostatin, either as a result of octreotide therapy or because production of somatostatin by the tumour itself may lower tumour detectability; however, there are also literature reports of improved tumour-to-background ratio after pre-treatment with nonradioactive octreotide. 2. Different somatostatin receptor subtypes have different affinities for the radioligand; variable tumour differentiation/receptor expression also influences tumour detectability. This is a consideration, especially with insulinomas and medullary thyroid carcinomas. 3. Liver metastases of neuroendocrine tumours may appear isointense because of a similar degree of tracer accumulation by the normal liver. Correlation with anatomic imaging or subtraction scintigraphy with sulphur colloid may be considered.

Table 3.7 Potential causes for false-positive and false-negative interpretation in ^{111}In-pentetreotide imaging (Helena *et al*, 2001).

3.6 Meta-iodobenzylguanidine (mIBG) scintigraphy

3.6.1 The guanethidine analog mIBG and its molecular structure share some characteristics with the adrenergic hormone-neurotransmitter, norepinephrine (Sisson *et al*, 1986). Norepinephrine is synthesized by normal adrenergic neurons and cells in the adrenal medulla, is stored in adrenergic granules, and is secreted by exocytosis. Some of the norepinephrine that is secreted is taken up by the same adrenergic cells and stored again in granules. During this uptake process, mIBG can enter the metabolic pathway of norepinephrine. The scintigraphic distribution of mIBG would be expected to occur in organs with adrenergic innervations, and in organs that process catecholamines for excretion, such as the liver and urinary bladder (Hanson *et al*, 2001). In day-to-day practice, ^{123}I-labeled mIBG is used for diagnosis and ^{131}I-labeled mIBG for therapy (Fig 3.3, Table 3.8).

3.6.2 Normal distribution

In early images heart and lungs are seen. The salivary glands, liver, spleen and urinary bladder are seen throughout the scanning period. Colonic activity may be seen in 20% of the patients. Normal adrenals may be seen in 16% of patients at 48 hours with[131]I-labeled mIBG images. ^{123}I-labeled mIBG shows a somewhat different pattern, with the adrenals seen in more than 30% of patients because of greater photon flux afforded by the administration of higher activity. In adults the uterus, spleen, lacrimal glands and neck muscles may be demonstrated with ^{123}I–mIBG (Beierwaltes, 1991; Elgazzar *et al*, 1995).

3.6.3 Imaging protocol

Study	Whole body imaging	SPECT imaging
Radiopharmaceutical	^{123}I-mIBG	^{123}I-mIBG
Activity administered	120 MBq	120 MBq
Patient preparation	Thyroid blockade with potassium iodide tablets 60mg twice daily for 3days (start one day before the injection date)	Thyroid blockade with potassium iodide tablets 60mg twice daily for 3days (start one day before the injection date)
Patient positioning	Supine, arms to side using the arm rest	Supine, arms to side using the arm rest
Collimator	Low energy general purpose	Low energy general purpose
Energy and window	159 keV and 15% window	159 keV and 15% window

----

Table 3.8 Imaging protocol of mIBG whole body and SPECT protocol

----
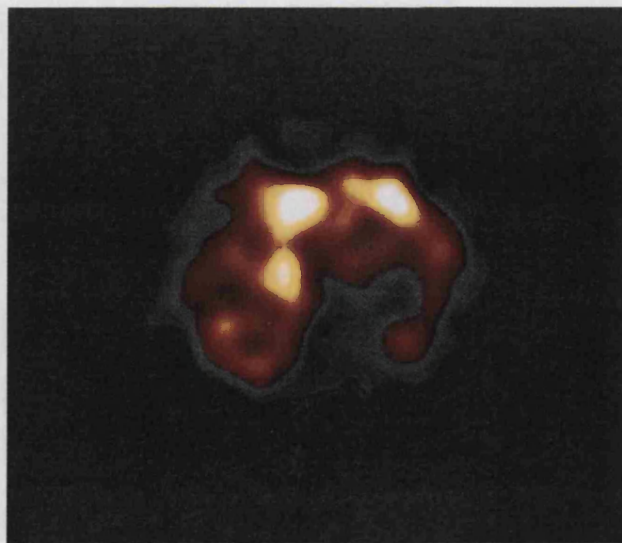
Fig 3.3 ^{123}mIBG SPECT (transverse section) showing multiple lesions in the liver

3.7 ^{99m}Tc-MDP Bone scan

The bone scan is commonly used for the detection of bone metastases (Fig 3.4).

However recent reports indicate that octreoscan detects more lesions than bone scan,

so the role of bone scans in neuroendocrine tumours may be limited (Gibril *et al*,

1998) (Fig 3.5).
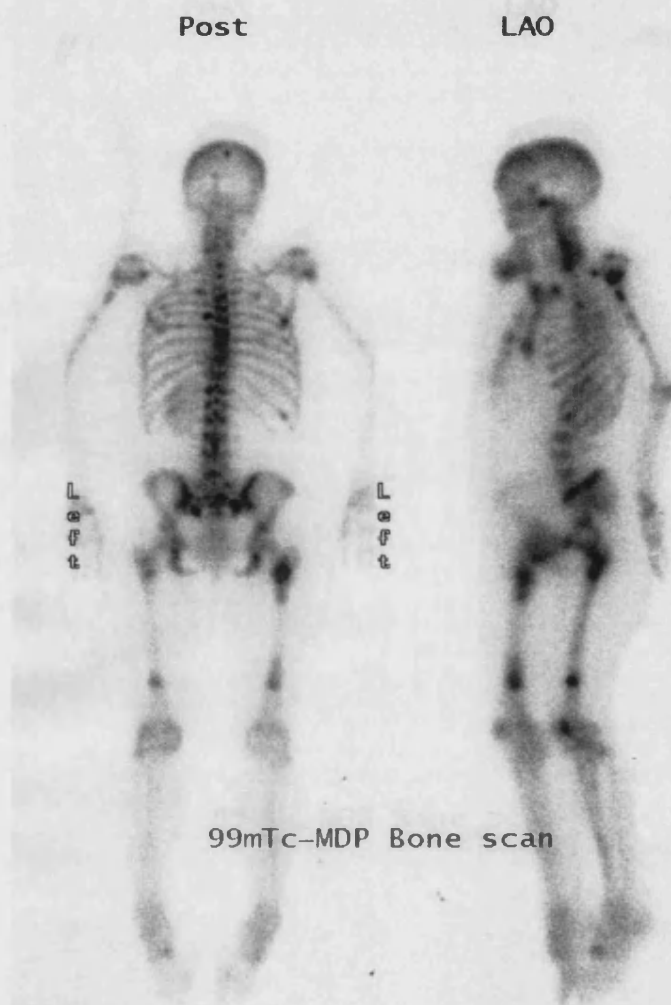
Fig 3.4 ^{99m}Tc-MDP Bone scan showing multiple metastases in the bones
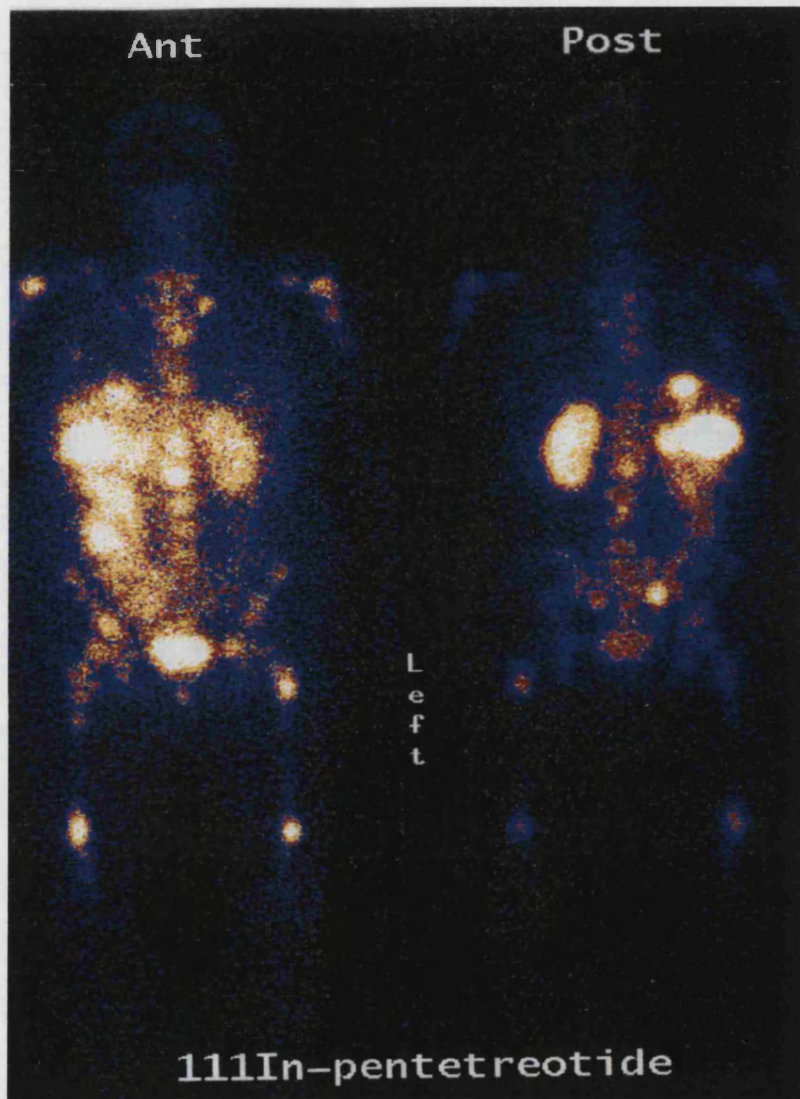
Fig 3.5 ^{111}In-pentetreotide scans showing multiple metastases in the same patient with carcinoid tumour

3.8 Pentavalent ^{99m}Tc-dimercaptosuccinic acid [99Tcm-(V) DMSA]

Pentavalent ^{99m}Tc-dimercaptosuccinic acid [^{99m}Tc-(V) DMSA] has established uses in the detection and diagnosis of medullary thyroid carcinoma (MTC), osteosarcoma, amyloidosis and many soft tissue tumours (Leah *et al*, 1999). It is not only helpful for the diagnosis of primary tumours but also for residual tumour and metastasis of medullary carcinoma of thyroid. However ^{111}In-pentetreotide is superior to ^{99m}Tc- (V) DMSA for the detection of tumour foci in patients with MTC (Arslan *et al*, 2001).

3.9 ^{99m}Tc- depreotide scintigraphy (NEOSPECT)

^{99m}Tc-depreotide is a peptide analogue of a somatostatin and preferentially binds to somatostatin receptors 2, 3, and 5 (Grewal *et al*, 2002) Its ability to form complexes with ^{99m} technetium results in higher resolution images and lower cost in comparison to octreotide scintigraphy. The somatostatin receptor is relatively over-expressed in pulmonary neoplastic tissue when compared to most benign tissue processes (Fig 3.6). A somatostatin analog-technetium ligand (^{99m}Tc-depreotide) has shown significant promise in the rapid, convenient, accurate and cost effective characterization of pulmonary nodules (Blum *et al*, 2002). The sensitivity and diagnostic accuracy compare favourably with that reported for FDG-PET (Blum *et al*, 2000).

3.10 ^{99m}Tc -Vapreotide (RC-160)

RC-160, a somatostatin analogue with enhanced binding affinity to somatostatin receptors subtypes 4 has been labelled with ^{99m} Tc (Decristoforo *et al*, 1999). It seems to be an important alternative to ^{111}In labelled pentetreotide for the targeting of

somatostatin receptor positive tumours. However there is very little data available regarding its efficacy over the routinely used ^{111}In labelled pentetreotide.
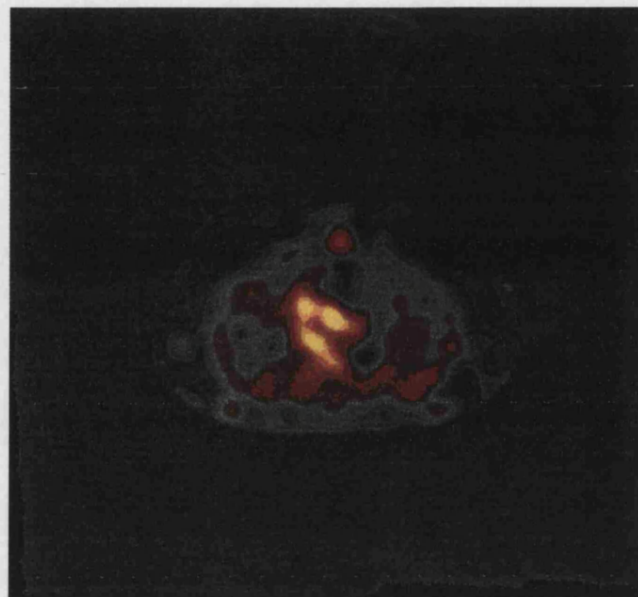
Fig 3.6 [99m]Tc- depreotide scintigraphy of lung showing lesion in the lung

3.11 Positron emission tomography (PET)

The first routinely used PET tracer in oncology, (18) F-labeled deoxyglucose (FDG), was successfully used for diagnosis of cancer, reflecting increased expression of glucose transporter in cancerous tissue (Eriksson *et al*, 2002 [1]). Positron emission tomography (PET) is an imaging method that identifies tumour based on uptake of radiolabeled tracers that are dependent on metabolic activity or pathways. Generally tumours have higher than normal rate of glycolysis. However, since carcinoid tumours are indolent and slow growing, they have a low metabolic rate and are not usually visualized with this tracer (Erasmus *et al*, 1998).

Serotonin (5-HT) synthesis occurs in all carcinoid tumours, but is also carried out by other neuroendocrine tumours with much less consistency. The metabolic pathway

converting 5-HTP (5-hydroxy-L-tryptophan) to 5-HT can be used for PET imaging. ^{11}C–5-HTP is specifically trapped by serotonin-producing tumours. Non-specific accumulation of tracer in the renal pelvis can cause a streaky artefact (Eriksson *et al*, 2002 $_1$). This renal excretion is caused by peripheral decarboxylation of 5-HTP by amino acid decarboxylase and is blocked by concomitant administration of oral carbidopa (Orlefors *et al*, 1998). With PET it is also possible to quantify the metabolic rate of the tumour and its response to therapy which is reflected as rate of tracer uptake (Orlefors *et al*, 1998; Sundin *et al*, 2000). Since SRS is unable to visualize tumour in the 10% of carcinoid tumours that do not express somatostatin receptors, a PET scan with ^{11}C–5-HTP may prove to be a superior method to visualize carcinoid tumours, but to date no studies have directly compared SRS and PET.

3.12 Discussion

^{123}mIBG and SRS with ^{111}In-pentetreotide have made a tremendous impact in management of neuroendocrine tumours. The overall sensitivity of SRS in localising neuroendocrine tumours is high and the majority of pancreatic endocrine tumours can be localised by SRS (Kwekkeboom *et al*, 2002). Scintigraphy with ^{111}In-pentetreotide in general detects more metastatic lesions than ^{123}I-mIBG in patients with neuroendocrine tumours. In occasional patients' scintigraphy with ^{123}I-mIBG demonstrated lesions not evident with ^{111}In-pentetreotide (Kaltsas *et al*, 2001$_2$). In patients with a strong suspicion of a neuroendocrine tumour and in whom all imaging modalities were negative, scintigraphy with ^{111}In-pentetreotide identified more lesions than ^{123}I-mIBG, although the detection rate was still low (Kaltsas *et al*, 2001$_2$).

Inspite of all these advances in the sensitivity of imaging modalities, we are still lagging behind specificity. This is not only true in neuroendocrine tumours but also in

other tumours. The diagnostic scenario of NETs is changing rapidly and there is need for multidisciplinary approach to improve the sensitivity and specificity in imaging neuroendocrine tumours.

3.13 Conclusion

[111]In- pentetreotide is a radiopharmaceutical with a great potential for the visualization of somatostatin receptor–positive tumours. The overall sensitivity of SRI to localize neuroendocrine tumours is high. In several neuroendocrine tumour types, inclusion of SRI in the localization or staging procedure may be very beneficial and effective in terms of cost, patient management, or quality of life.

Radionuclide therapy in Neuroendocrine Tumours

4.1 Introduction

Nuclear medicine therapy is based on the deposition of therapeutic doses of ionising radiation in tumours or organ tissues. In principle, to achieve the desired therapeutic effect, a particular radionuclide should exhibit adequate physical, chemical and biological properties (Vucina *et al*, 2001). Radionuclide therapy delivers continuous irradiation at relatively low dose rates (Flower, 1998). The dose rate varies during therapy, decreasing at a rate which generally depends on two factors (a) the physical half-life of the radionuclide and (b) the biological clearance of the labelled product (Flower, 1998).

The therapeutic strategy in neuroendocrine tumours is complex, both due to their heterogeneity and to the fact that, although generally slow-growing, a significant proportion demonstrates aggressive tumour growth. Presently, there are various radiopharmaceuticals available for treating patients with neuroendocrine tumours (de Jong *et al*, 2002 [1]) (Table 4.1).

---

^{131}I-mIBG (Meta-iodobenzylguanidine)
[^{111}In-diethylenetriaminepentaacetic acid (DTPA)]-pentetreotide
[^{90Y}-dodecanetetraacetic acid (DOTA), Tyr^3] octreotide (^{90}Y-DOTATOC)
[^{90}Y-DOTA]-lanreotide
[^{177}Lu-DOTA, Tyr^3] octreotate

Table 4.1 Radionuclide therapeutic agents

4.2 General principles of radionuclide therapy

There has been a significant effort in radionuclide therapy to improve tumour targeting together with simultaneous reduction of physiological organ uptake. New routes of administration of radiopharmaceuticals (intratumoral, intra-arterial) have enhanced the treatment of malignancies. Another significant tendency in radionuclide therapy is its evolution from monotherapy towards a combined application with other anticancer modalities (Valdes Olmos *et al*, 2001). The accurate assessment of bio-distribution and radiation dose delivered during radionuclide therapy is difficult and challenging. The therapeutic outcome depends on various complex factors of the radionuclide used (Table 4.2).

4.2.1 Choice of radionuclide

The choice of radionuclide depends on the range of principle radiation emitted, size of the tumour, availability and cost. The radionuclides are usually grouped according to the range of principle radiation emitted (Flower, 1998).

Alpha (α) emitters have a short range (50-90μm) and traverse up to 10 cell diameters from the point of radioactive decay (Humm, 1986; Flower, 1998). The therapeutic potential of α emitters lies in the energy loss within their short path. The alpha (α) emitters deposit 400 times more energy per unit distance than beta (β) radiation. The high linear energy transfer (80-100 keV/μm) deposit approximately 1.0 MeV upon traversing the diameter of a cell nucleus. This is sufficient to break the double stranded DNA, with little subsequent chance of repair (Humm, 1986).

Beta (β) emitters have a wide range from less than 200μm to greater than 1mm. The beta range is important in relation to the size of the tumour to be treated.

Radionuclides that decay by internal conversion and electron capture are also used in radionuclide therapy. Many of these have a very short range (<10Å) and they can cause significant radiobiological damage only if the emission take place very close to the cellular DNA (Humm, 1986).

4.2.2 Radiopharmaceutical uptake and retention

The uptake of the radiopharmaceutical at the tumour site is affected by various factors such as changes in blood supply, interstitial pressure, permeability and increase in the extra-vascular space (Ackery, 1998). The efficacy of radionuclide therapy will be lowered if the blood flow to the affected area is reduced. This is because less radiopharmaceutical is available to the viable cells; the functional integrity of tumour cells decreases so the demand for the metabolic substrate decreases and finally the hypoxic state of the cells reduces the sensitivity of the affected tissue to the radiation effects. The amount of radiopharmaceutical taken up at the tumour site and its retention at the tumour site is very important in the assessment of cumulative absorbed radiation dose to organ or the tumour to be treated (Ackery, 1998). In radionuclide therapy planning, the physical half-life of the radionuclide label should be studied very carefully as a short acting agent will not take full advantage of its residence time at the tumour site, where as a radionuclide label of a long physical half life will give unnecessary dose to normal tissues (Ackery, 1998). In practice no radiopharmaceutical is entirely selective and other tissue will generally compete for its uptake, thereby reducing the final concentration at the required tumour site (Ackery, 1998).

Choice of radionuclide
Uptake and retention of radiopharmaceutical
Chemical conjugation/labelling
Radiation dosimetry
Radiation related toxicity

Table 4.2 Common factors affecting the therapeutic outcome

4.2.3 Chemical conjugation/labelling

Combination of radionuclide with a tissue or tumour specific pharmaceutical is a very complex process. Direct labelling is possible only in very few circumstances (Ackery, 1998). Most of the time a conjugating molecule (usually a chelate) needs to be attached to the pharmaceutical. But the problem is, attachment of a chelate could alter the behaviour and bio-distribution of the radiopharmaceutical. This may lead to reduced concentration in tumour/target tissue. Chelates which bind with radio-metals in-vitro may release them in-vivo, giving unwanted and increased radiation burden from free radionuclide. The radioconjugates are subject to high radiation fluxes and may undergo self-irradiation radiolysis. Decomposition into a variety of radiolabeled sub-species can be minimised by dilution or freezing the radiopharmaceutical solution, thereby preventing the release of free radionuclide (Giap *et al*, 1995). Finally the timing between synthesis of the radiopharmaceutical and injecting them into the patient is a very important factor.

4.2.4 Radiation dosimetry

It is practically very difficult to calculate precisely the magnitude and biodistribution of the internal dose delivered from unsealed sources. In view of the large inherent uncertainties individual patient dosimetry is not always performed (Flower, 1998). For targeted radionuclide therapy, the level of activity to be administered is often determined from whole-body dosimetry performed on a pre-therapy tracer study. The largest potential source of error in this method is due to inconsistent or inaccurate activity retention measurements (Flux *et al*, 2002). However, with recent advances in imaging and counting techniques, internal dose estimations are becoming more common and challenging.

4.2.5 Assessment of Radiation related toxicity

The assessment of radiation related toxicity is very important. The bone marrow stem cells are the critical sites in most of radionuclide therapies and it takes 4-6 weeks to recover from their initial damage. Normal tissues are always at risk if they lie close to the tumour site (Ackery, 1998).

To avoid these complications utmost care should be taken to analyse all the above mentioned factors before planning radionuclide therapy.

4.3 Radionuclides

4.3.1 Iodine [^{131}I]

^{131}I is a beta-emitting radionuclide with a physical half-life of 8.04 days, a principal gamma ray of 364 KeV (81% abundance) and beta particles with a maximum energy of 0.61 MeV and an average energy of 0.192 (Table 4.3).

4.3.2 Yttrium [^{86}Y, ^{90}Y]

There are two radionuclides of yttrium used in the radiopharmaceutical labelling. ^{86}Y ($t_{0.5}$ = 14.7 h) is a β^+emitting radionuclide, often used as an equivalent for ^{90}Y in PET imaging. ^{90}Y ($t_{0.5}$ = 64 hours) is a β^- emitter, which is the most frequently used radionuclide for targeted radionuclide therapy. ^{90}Y is obtained in high-specific activity from ^{90}Sr (Herzog *et al*, 1993; Wester *et al*, 1997; Rosch *et al*, 1999; Fichna *et al*, 2003).

4.3.3 Lutetium [^{177}Lu]

The more frequently used radionuclide of lutetium is ^{177}Lu ($t_{0.5}$ = 160.8 h) which is a short range beta and a gamma-emitter (Firestone *et al*, 1996). It has the physical characteristics similar to ^{131}I (113 and 208 keV gamma photons) and forms stable complexes with chelating agents such as DOTA. It has an average energy of 148 keV and a maximum range of 1.5mm

Iodine [131 I] Main emissions							
	Gamma or X		Beta (Emax)		Electrons		Alpha	
	E	%	E	%	E	%	E	%
E1	284	6	248	2	46	4		
E2	365	82	334	7	330	2		
E3	637	7	606	90				
% omitted		11		1		2		
Yttrium [90Y] Main emission							
	Gamma or X		Beta (Emax)		Electrons		Alpha	
	E	%	E	%	E	%	E	%
E1			523	<1				
E2			2284	100				
E3								
% omitted				0				

Table 4.3 Showing main emissions from the therapeutic radionuclides (Delacroix, 1998)

4.4 Radionuclide therapy and Neuroendocrine Tumours

One of the interesting concepts in radiation oncology today is the delivery of high radiation dose to the tumour, while sparing the surrounding and normal tissues. NETs have the possession of neuroamine uptake mechanisms or they express specific receptors at the cell membrane (Lamberts *et al*, 1991). When a β-emitting radioisotope is coupled to mIBG or an SMS analogue, it may specifically target tumour cells and deliver an effective radiation dose to the involved cell and neighbouring tissue to within a few millimetres or so, thus selectively sparing non-tumour tissue (Lamberts *et al*, 1991). The avid uptake of ^{111}In-labelled pentetreotide and ^{123}I-labelled mIBG by the NETs in scintigraphic scanning, led to the development of receptor-targeted therapy. Various radiopharmaceuticals have moved from the laboratories to the patient, which has changed the therapeutic scenario.

4.4.1 Meta-iodobenzylguanidine (mIBG) therapy

4.4.1.1 Meta-iodobenzylguanidine is a meta isomer of the guanethidine derivative iodobenzylguanidine (EANM Radionuclide Therapy Committee guidelines). Eligible patients will have mIBG positive tumours, documented by quantitative tracer scintigraphy. It is essential that all known tumour sites are mIBG positive. The administered activity range is between 3.7-11.2 GBq (EANM Radionuclide Therapy Committee guidelines). Thyroid blockade with potassium iodate is essential prior to administration to prevent thyroidal uptake of free radio-iodine. Unlike patients with metastatic catecholamine-secreting tumours, experience with ^{131}I-mIBG for carcinoid tumours is limited. A global experience of the treatment of 52 patients was reported in 1994, where an objective tumour response was recorded in 15% and symptomatic responses in 65% (Hoefnagel, 1994).

4.4.1.2 Side effects and drawbacks: Nausea and vomiting may occur during the first two days post-therapy. Temporary myelosupression typically occurs 4-6 weeks post-therapy. Bone marrow depression is more likely in patients who have bone marrow involvement at the time of ^{131}I-mIBG therapy.

Fig 4.1 Post-therapy ^{131}I-mIBG scan confirming excellent uptake of therapy dose in tumour site

4.4.2 Radiolabeled Somatostatin analogue therapy

Radiolabelled Somatostatin analogue therapy is gaining much-needed recognition in the treatment of neuroendocine tumours. Clinical studies are being performed using different agents. Results from pre-clinical and clinical multicenter studies have shown encouraging results (Table 4.4). In most radionuclide therapies, bone marrow toxicity is dose limiting but after radionuclide targeted therapy using Somatostatin analogues labelled with ß-emitters such as ^{90}Y and ^{177}Lu, the kidney is the dose-limiting organ because of high tubular reuptake of the peptide analogs after glomerular filtration and retention of the radionuclides in the tubular cells (de Jong *et al*, 2002 ₁).

4.4.2.1 ^{111}In-DTPA-pentetreotide

4.4.2.1a ^{111}In-pentetreotide is known to be internalised by the NET cell (Andersson *et al*, 1996); therefore, if given in sufficient activities, ^{111}In-pentetreotide, which produces an Auger electron with a range of about 80–200 nm, could have a therapeutic effect.

Recent studies have shown that ^{111}In-pentetreotide can be given in activities of up to 5 GBq with minimal toxicity (McCarthy, 1998; Caplin *et al*, 2000). Many research groups used multiple doses of (^{111}In-DTPA) octreotide, up to 160 GBq, to treat patients with somatostatin receptor–positive tumours (Kwekkeboom *et al*, 2000). The therapeutic effects included partial and minor remissions in a few patients and, mostly, stabilization of previously progressive tumours. In a series of patients, Buscombe et al reported that 31% of the patients had an objective response from the treatment of their disease with high-activity ^{111}In-pentetreotide, and 44% had a period of tumour stability, with no growth in tumour size for at least 6 months after the end of treatment. Therefore, in this study at least 75% of patients showed some benefit

from the treatment (Buscombe *et al*, 2003). This finding compares well with the results of de Jong where about 67% of patients showed either stability or a response (de Jong *et al*,1999).

4.4.2.1b Side effects and drawbacks: Toxicity generally consisted of mild bone marrow toxicity, but a myelodysplastic syndrome or leukaemia developed in few patients who received >100 GBq. In view of this, a 100 GBq dose was considered the maximal tolerable dose of (^{111}In-DTPA) pentetreotide (de Jong *et al*, 2002 [1, 2]). The major drawback of ^{111}In is the short range of the therapeutic Auger electrons emitted. The radiation emitted from a receptor-positive tumour cell cannot kill neighbouring receptor-negative cells in tumours with receptor heterogeneity, because the path length of the Auger electrons is less than a cell diameter. Also the cost is very high. Presently very few centres use ^{111}In-octreotide to treat their patients.

4.4.2.2 ^{90}Y-DOTATOC

4.4.2.2a It is an effective radiopharmaceutical for treating patients with neuroendocrine gastroenteropancreatic and bronchial tumours. The results of the initial phase II study reported by Waldherr *et al* are encouraging. They treated patients with 4 intravenous injections of a total of 6,000 MBq/m^2 ^{90}Y-DOTATOC, administered at intervals of 6 wk, and all patients had renal protection through co-infusion of amino acid infusion. The overall response rate was 24%. In the later phase of the trial the patients were treated with higher doses of ^{90}Y-DOTATOC (7.4 GBq/m^2 in 4 equal injections at intervals of 6 wk, with renal protection using Hartmann-HEPA 8%) (Waldherr *et al*, 2002). An objective response occured in 23% of the patients (WHO criteria), complete remission in 5%, partial remission in 18%, stable disease in 69%, and progressive disease in 8%. An overall 63% clinical benefit in terms of clinical symptoms was obtained. These promising tumour responses after

therapy are essentially similar to those found in other ^{90}Y-DOTATOC studies, despite differences in therapy regimens (Paganelli *et al*, 2001; Valkema *et al*, 2001).

4.4.2.2b Side effects and drawbacks: Renal toxicity, thrombocytopenia, liver toxicity was observed in some patients. Nausea and vomiting were observed in patients treated with amino acids (de Jong *et al*, 2002 [1]). The radiation dose that can be administered safely to the kidneys during these therapies remains to be established. There is no real consensus regarding amino acid infusions for reducing the renal toxicity. Also disadvantage is ^{90}Y is a pure ß-emitter isotope; ^{90}Y-DOTATOC cannot provide quantitative imaging outside the body.

4.4.2.3 ^{90}Y-DOTA-lanreotide (MAURITIUS)

4.4.2.3a ^{90}Y-DOTA-lanreotide is a universal Somatostatin (SST) receptor subtype ligand that binds to a large variety of human tumours (Smith-Jones *et al*, 1999). In the MAURITIUS (Multicenter Analysis of a Universal Receptor Imaging and Treatment Initiative, a European Study) trial cumulative treatment doses up to 8584 MBq ^{90}Y-DOTA-lanreotide were given as short-term intravenous infusion. Preliminary treatment results in 154 patients indicate stable tumour disease in 41% (63 of 154) of patients and regressive tumour disease in 14% (22 of 154) of tumour patients with different tumour entities expressing Somatostatin receptors (Virgolini *et al*, 2002).

4.4.2.3b Side effects and drawbacks: No severe acute or chronic haematological toxicity, change in renal or liver function parameters caused by ^{90}Y-DOTA-lanreotide treatment were reported for patients in the MAURITIUS trial (Virgolini *et al*, 2002).

4.4.2.4 (^{177}Lu-DOTA, Tyr3) octreotate

4.4.2.4a (^{177}Lu-DOTA, Tyr3) octreotate is recently developed peptide (in which the C-terminal threoninol is replaced with threonine), and has been used for the treatment of neuroendocrine tumours (Kwekkeboom *et al*, 2001). This agent seems show the highest tumour uptake of all tested octreotide analogues so far, not only in rats but also in patients with neuroendocrine tumours (de Jong et al, 2001). The interim results show that (^{177}Lu-DOTA, Tyr3)-octreotate is also most promising for PRRT of somatostatin receptor–positive tumours. Amino acids are co-infused to reduce the kidney dose to less than 23 Gy. By CT assessment, minor tumour shrinkage was reported in 6% of 18 patients; partial remission, in 39%; tumour progression in 11%; and no change, in 44% (de Jong *et al*, 2002 $_2$).

4.4.2.4b   Side effects and drawbacks: Mild nausea, vomiting, and mild abdominal discomfort were present in some patients (de Jong *et al*, 2002). Tumour response is dependent on tumour size (de Jong *et al*, 2002 $_2$). ^{177}Lu would be optimal for small tumours, whereas ^{90}Y would be better for large tumours. In patients with tumours of more than one size, combinations of radionuclides might be used (de Jong *et al*, 2002 $_2$). Since only a small group was treated with ^{177}Lu, more patients need to be treated to evaluate the clinical outcome.

4.4.3 ^{131}I- Lipiodol therapy

Many patients with disseminated neuroendocrine tumours have metastases limited to their livers. These tumours may be very symptomatic as in the case of the carcinoid syndrome where there is over production of serotonin. Though slow growing, these tumours are malignant and can grow to sufficient size to block the portal vein and

inferior vena cava causing portal hypertension. They can disrupt the liver synthetic function as a result of their bulk and this can lead to liver failure and death.

There is a wide experience in treating hepatocellular cancer (HCC) using I-131 iodinated poppy seed oil (^{131}I-Lipiodol, CIS-Schering, Saclay, France). The technique involves injecting 500-1000 MBq of ^{131}I-Lipiodol directly into the hepatic artery under angiographic control. The group from Rennes, our group and those from Hong Kong have found evidence for efficacy with little evidence for toxicity (Roul et al, 1997). We know from triple phase CT imaging that neuroendocrine tumours in the liver have a good vascular supply like an HCC and unlike colonic cancer metastases in the liver. Therefore it was logical to attempt the use of ^{131}I- Lipiodol in untreatable symptomatic and growing neuroendocrine tumours within the liver.^{131}I Lipiodol has also been used in an adjuvant setting to treat patients with 0.9 GBq ^{131}I Lipiodol 6 weeks after surgical resection. The reason for this is that as the post-surgical liver starts to regenerate, small microscopic daughter tumours can be stimulated to grow. If these were pre-cleared by ^{131}I Lipiodol then there would be a lower chance of recurrence. It has been shown that at 24 months after administration of ^{131}I Lipiodol a significant 50% increase occurs in both the disease free interval and overall survival in those receiving ^{131}I Lipiodol compared to age matched controls (Lau et al, 1999).

Within the angiography suite the right and left hepatic artery is identified via a femoral artery puncture. Once this has been identified 800-1000 MBq of ^{131}I-Lipiodol was infused in about 5 minutes using a 5 French catheter into the hepatic artery. Care is taken to avoid reflux up the gastro-duodenal artery. To ensure this did not occur, the ^{131}I- Lipiodol was infused under fluoroscopic control. If the tumour was predominately on the right the right hepatic artery was catheterised, if on the left the left hepatic artery. If bilateral, the catheter was placed at the junction of the two

arteries. Before sending the patient home, whole body imaging was performed to determine the level of retention of ^{131}I- Lipiodol in the tumour. Shunting into the lungs is a concern and images are performed at 48-96 h after administration of the ^{131}I Lipiodol for assessment. If shunting of 15% or more has occurred the right lung may have received about 12 cGy. This normally causes no problems but repeated radio-lipiodol treatment is not recommended (Buscombe *et al*, 2002).

Radio pharmaceuticals	[111]Indium-pentetreotide	[90]Yttrium-pentetreotide	[90]Yttrium-lanreotide	[177]Lutitium-octreotate
Type of radiation	Auger electrons $t_{1/2}$ = 67 hours	high-energy ß-emitter (>1mm) $t_{1/2}$ = 64 hours	high-energy ß-emitter (>1mm) $t_{1/2}$ = 64 hours	low-energy ß- and γ (<200µm) $t_{1/2}$ = 160.8 hours
Chelator	DTPA	DOTA	DOTA	DOTA
Dose	up to 5 GBq/cycle	1 to 4.4 GBq/cycle	1.2 GBq/cycle	3.7-7.4 GBq/cycle
Amino acid co-infusion	NO	YES	NO	YES
Reported response rates	70% had benefit for 6 months after treatment, and 31% had sustained benefit at 18 months.	Objective response in 23% ,complete remission in 5%, partial remission in 18%, stable disease in 69%, and progressive disease in 8%. Overall clinical benefit was 63%.	Stable tumour disease in 35% and regressive tumour disease in 10%	Minor tumour shrinkage in 6%, partial remission in 39%, tumour progression in 11% and no change in 44%.
Side-effects	Minimal bone marrow toxicity has been reported.	1. Renal toxicity, thrombocytopenia, liver toxicity is reported in some patients. 2. Nausea and vomiting were reported in patients treated with amino acids.	1. No renal, haematological or liver toxicity was reported were reported in the MAURITIUS trial.	1. Mild nausea, vomiting, and mild abdominal discomfort has been reported.
Advantages	1.Imaging can be performed 2. Binds to SS receptor 2 and 5 with high affinity	1. Better for large tumours 2. Binds to SS receptor 2 and 5 with high affinity	1. Binds to SS receptors 2, 3, 4, and 5 with high affinity. 2. Better for large tumours	1. Highest tumour uptake of all SS analogues 2. Octreotate has nine-fold higher affinity for the SS receptor 2 as compared with octreotide. 3. Imaging can be performed
Disadvantages	1. Short path length of Auger electrons 2. Bind to SS receptor 3 with moderate affinity does not bind to receptor 1 and 4 3. Presently very few centres use ^{111}In-pentetreotide to treat their patients.	1. Quantitative imaging cannot be performed 2. Bind to SS receptor 3 with moderate affinity does not bind to receptor 1 and 4	1. Quantitative imaging cannot be performed 2. Binds to receptor 1 with lower affinity	1. Tumour response is dependent on tumour size. 2. 177Lu would be optimal only for small tumours 3. So far only a small group has been treated with [177]Lu

Table 4.4 Summary of targeted therapy with radiolabeled somatostatin analogues [(Kwekkeboom *et al*, 2000; Buscombe *et al*, 2003 ; de Jong *et al*, 1999; de Jong *et al*, 2002 [1,2]; Waldherr *et al*, 2002; Paganelli *et al*, 2001; Valkema *et al*, 2001)

4.5 Controversies in radiolabeled somatostatin analogue therapy

Even though many radionuclide peptides have reached the clinical/ treatment phase, we need more clinical data to assess the real therapeutic outcome to move higher up in the treatment algorithm. Another major drawback is that no general consensus exists between various groups regarding optimisation of treatment factors. In most radionuclide therapies, bone marrow toxicity is dose limiting. In Peptide receptor radionuclide therapy, the bone marrow is also at risk, but after Peptide receptor radionuclide therapy using somatostatin analogs labelled with ß-emitters such as ^{90}Y and ^{177}Lu, the radiosensitive kidney is the dose-limiting organ because of high tubular reuptake of the peptide analogs after glomerular filtration and retention of the radionuclides in the tubular cells (de Jong *et al*, 2002 1). Since there is no clear-cut method of accessing the risk to the kidneys, thereby toxicity and dose limits to the kidneys are complicated .

Serial images after injection of 111 MBq ^{111}In-DOTATOC has been used to calculate the radiation dose to the kidneys (Waldherr *et al*, 2002). A drawback of this method is that small structural modifications in somatostatin analogs, for example, chelator substitution or metal replacement, can considerably affect the somatostatin receptor binding affinity (Reubi *et al*, 2000, de Jong *et al*, 2002 1). On the other hand, the major part of the reuptake process in the kidney is not somatostatin receptor mediated, probably resulting in a comparable kidney residence time for ^{111}In- and ^{90}Y-labeled DOTATOC. To reduce radiation exposure to the kidney, different groups have tested several regimens of amino acid co-infusion, but these solutions have some disadvantages, in particular their hyperosmolarity and their propensity to cause vomiting and metabolic changes. There was also some question regarding the type of amino acids and the dose to be administered. Most centres use arginine and lysine, but

still there is no universal consensus regarding this issue. A few studies have reported D-lysine in preference to L-lysine for the reduction of renal uptake of radioactivity during scintigraphy and therapy because of its lower toxicity and because it should not interfere with the natural amino acid metabolic balance (Bernard *et al*, 1997) Presently co-infusion of Lysine and Arginine is advocated , which seems to result in a significant inhibition of renal radioactivity in therapy, allowing higher treatment doses and thus resulting in higher tumour radiation doses (Rolleman *et al*, 2003).

4.6 CONCLUSION

Use of combinations of radionuclides would be of greatest interest to obtain the widest range of tumour curability. The problem of balancing benefits (clinical response to radionuclide therapy) and risks (renal radiotoxicity) is significant; therefore, careful assessment of biodistribution, dosimetry and toxicity is important, preferably on an individualised basis. There should also be a method to monitor and assess the treatment response. Finally every patient ideally should receive a "tailor-made" therapy based on his or her particular tumour biology profile.

Chapter 5

^{90}Yttrium brehmsstrahlung imaging

5.1 Introduction

Patient specific radiation dosimetry requires quantitative imaging of the pharmacokinetics and biodistribution of the radionuclides. ^{90}Yttrium (^{90}Y), a pure beta-emitter is an attractive radionuclide for targeted radionuclide therapy. It has gained considerable attraction in targeted radionuclide therapy because of its long range beta emission. Furthermore it lessens radiation safety concerns since it does not emit gamma radiations. Treatment of neuroendocrine tumours with ^{90}Y labelled somatostatin analogues is popular.

Imaging ^{90}Y could be relevant for the assessment of the therapeutic plan and outcome in patients undergoing therapy, because it would allow the treatment plan to be modified on the basis of localisation and biodistribution of the radiopharmaceuticals. The beta particles emitted from ^{90}Y interact with the tissue to produce brehmsstrahlung radiation. Brehmsstrahlung means "braking radiation" and is retained from the original German to describe the radiation which is emitted when electrons are de-accelerated or "braked" when they pass near nuclei in their path.

Delerated charges give off electromagnetic radiation, and when the energy of the bombarding electrons is high enough, that radiation is in the x-ray region of the electromagnetic spectrum. Brehmsstrahlung is characterised by a continuous distribution of radiation, which becomes more intense and shifts toward higher frequencies when the energy of the bombarding electrons is increased.

Conventional gamma photon imaging methods cannot be easily applied to imaging of ^{90}Y-bremsstrahlung because of its continuous energy spectrum (Shen *et al*, 1994).

Furthermore, quantitation of ^{90}Y by brehmsstrahlung imaging is difficult because of the poor image quality that results from septal penetration and scatter secondary to the broad brehmsstrahlung energies (Shen *et al*, 1994). The choice of collimation and energy window are complex as broad spectrums of energies from brehmsstrahlung are present. However, brehmsstrahlung emissions can be utilized to acquire an image of beta sources using a gamma camera (Shen *et al*, 1994).

The absence of gamma emissions from ^{90}Y for imaging has led researchers to use ^{111}In, a radionuclide with similar chemical properties and good imaging photons, as a tracer for the assessment of pharmacokinetics and radiation dosimetry of ^{90}Y (Shen *et al*, 1994). Although the chemical properties of ^{90}Y and ^{111}In are identical, ^{111}In may not predict the behaviour of ^{90}Y with complete accuracy. There are studies reported regarding the use of brehmsstrahlung imaging in patients undergoing radiation synovectomies for rheumatoid arthritis and more recently to assess the pharmacokinetics and radiation dosimetry of the ^{90}Y-labeled antibody (Smith *et al*, 1988; Shen *et al*, 1994). In the past there have been efforts to obtain radiation dosimetric data by imaging brehmstrahlung from pure beta emitting radionuclides using different type of collimation. Clarke *et al* used long bore high energy collimators (57-285 keV window) for imaging ^{32}P (Clarke *et al*, 1992) and Siegel *et al* used a medium energy (ME) collimator (53-148 keV) for imaging ^{89}Sr (Siegel *et al*, 1992). However, due to enhanced photon scattering and penetration through the collimator septa the images obtained by brehmstrahlung experience greater blurring.

In our initial experiment (Gnanasegaran, 2001) the energy and windows were determined empirically after acquiring the energy spectrum from a patient, using a high energy collimator. The brehmstrahlung spectrum was seen as a continuous spectrum with more photons present in the lower part of the spectrum. A peak of

75keV was just discernable. It was decided for our experiments that optimum energy would be 75 keV with ± 50% window offset. Broad energy windows employed were empirically determined. We later used them in the assessment of biodistribution of radiolabelled somatostatin analogues (Chapter 6). But from the experience of others (Shen *et al*, 1994, Clarke *et al*, 1992; Siegel *et al*, 1992) and ours (Gnanasegaran, 2001) the choice of collimation and energy window requires a practical compromise between the sensitivity and spatial resolution for specific requirements and circumstances. We used a HEGP collimator empirically after imaging a phantom with all the 3 types of collimators (LEHR, MEGP and HEGP) (Fig 5.1). With this basic background from our previous experience we went further to investigate lesion detectability and uniformity of response by examining the contrast and uniformity in brehmsstrahlung imaging using a Williams phantom filled with ^{90}Y. The experiment was split into 2 areas (a) to investigate the effect of different energy and windowing (b) to investigate the effect of different thickness of scattering material.

LEHR	**MEGP**	**HEGP**
(Low energy high resolution collimator)	(Medium energy general purpose collimator)	(High energy general purpose collimator)
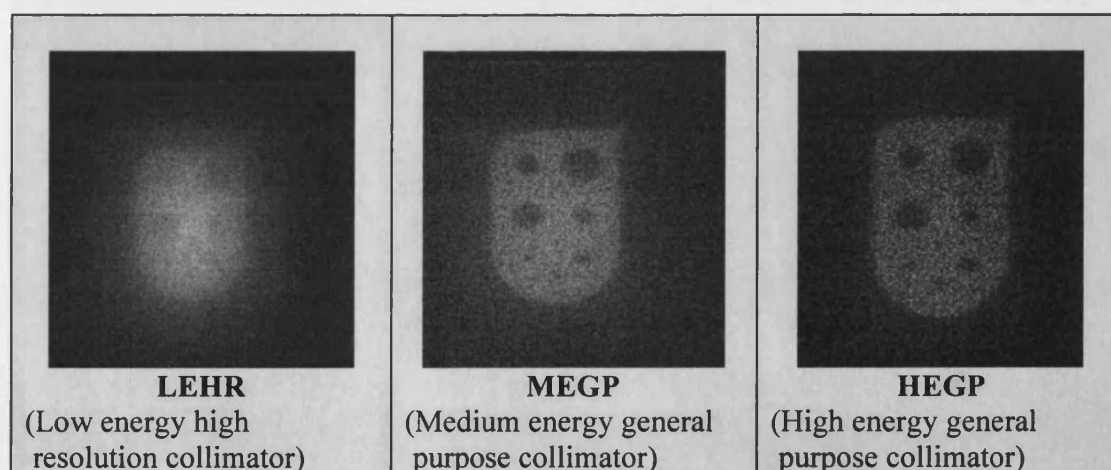
Fig 5.1 Showing Williams phantom images using different collimators

5. 2 Experiment 1

5.2.1 Aim

To investigate the effect of scattering material and different energy windows in brehmsstrahlung imaging using Williams phantom filled with ^{90}Y.

5.2.2 Material and methods

The experiments were conducted after filling the Williams phantom with 256 MBq of ^{90}Yttrium (Fig 5.2). The Internal dimensions of the phantom are 20 x 13 x 1 cm (excluding the curvature). The phantom consists of 8 cylindrical lesions of different sizes. The differently sized lesions are solid perspex cylinders, which represents zero activity (cold lesions).

The images were acquired on a Prism 2000XP dual head gamma camera (Picker International, Inc. Cleveland Ohio, USA). The head was rotated to 180^0 with the sensitive face directed vertically upwards. Tissue equivalent blocks (scatter material) were placed directly onto the centre face of the camera face (Fig 5.3).

5.2.2a Using a high energy collimator, the phantom was imaged at 0cm with different width energy windows and different central energy (Table 5.1). All acquisitions were terminated after 500,000 counts (Fig 5.4). An assessment of lesion detectability and uniformity of response was performed. Contrast and uniformity (coefficient of variation) was determined by equations (5.1 and 5.2) respectively.

Contrast = <u>Mean count in the background ROI -Minimum count value in lesion ROI</u> X 100
                          Mean count in the background ROI

Equation 5.1 Contrast measurements

$$\text{Coefficient of variation (CoV)} = \frac{\text{S.D (standard deviation)}}{\text{Mean}} \times 100$$

Equation 5.2 Coefficient of variation
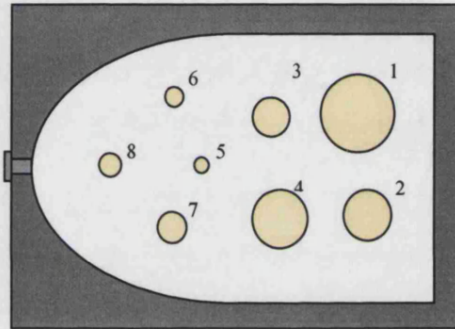
Internal dimensions: 20 x 13 x 1 cm
(excluding the curvature)
Lesion diameter (cm): 1:   4.0
                      2:      2.5
                      3:      2.0
                      4:      3.0
                      5:      0.7
                      6:      1.0
                      7:      1.5
                      8:      1.2

Fig 5.2 Diagrammatic representation of Williams's phantom with internal dimension of the 8 lesions (coloured yellow).
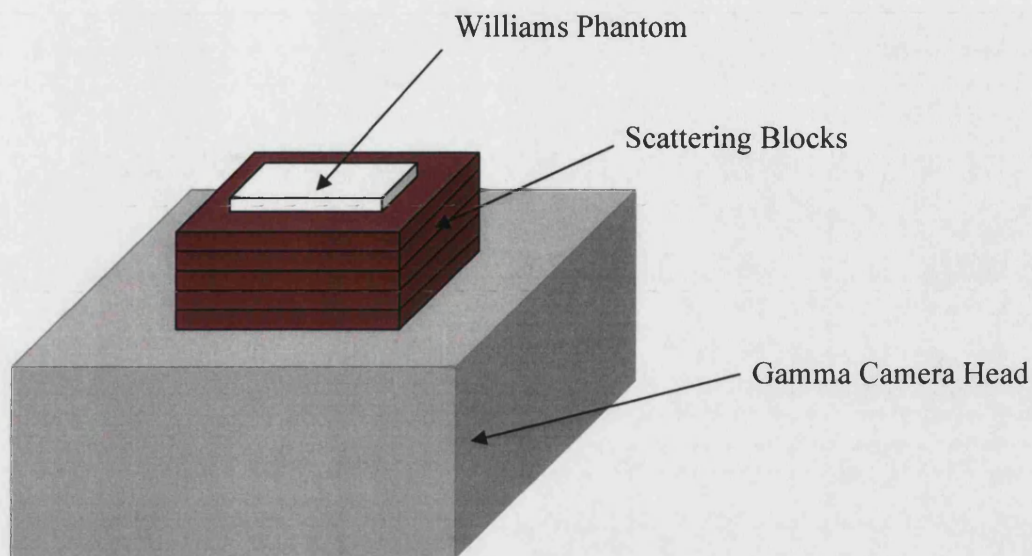
Fig 5.3 Diagrammatic representation of imaging Williams's phantom using a gamma camera (experiment arrangement)

Energy keV	Windows	Collimator
90	60	HEGP
85	60	HEGP
80	60	HEGP
75	60	HEGP
90	50	HEGP
85	50	HEGP
80	50	HEGP
75	50	HEGP
90	40	HEGP
85	40	HEGP
80	40	HEGP
75	40	HEGP

Table 5.1 Williams phantom was imaged with several different energy windows for a fixed count rate of 500,000 counts using high energy collimators.

Visual analyses of the images were done by four blinded observers and In-house IDL code (Version 5.5) (IDL Research system Inc, Boulder, CO, USA) was used for the quantitative analyses of the final images. Firstly a large ROI was drawn over the phantom to mask out all the background. Irregular ROI were drawn over the lesions visible (Minimum pixel) to assess the minimum pixel and remove the lesions for uniformity measurements. The ROIs were drawn over all the lesions. The minimum pixel values in these regions were used, since determining the ROI over the lesions was difficult for lesion with poor resolution. With the same computer software, we were able to get the mean pixel value and the standard deviation pixel value of the area within the mask, but excluding the lesions used, to calculate uniformity. The same procedure was repeated for all the images acquired. Equation 5.2 was used in the calculation of uniformity to reduce the error as the single pixel calculation such as that from the integral uniformity has a greater degree of error for this application.
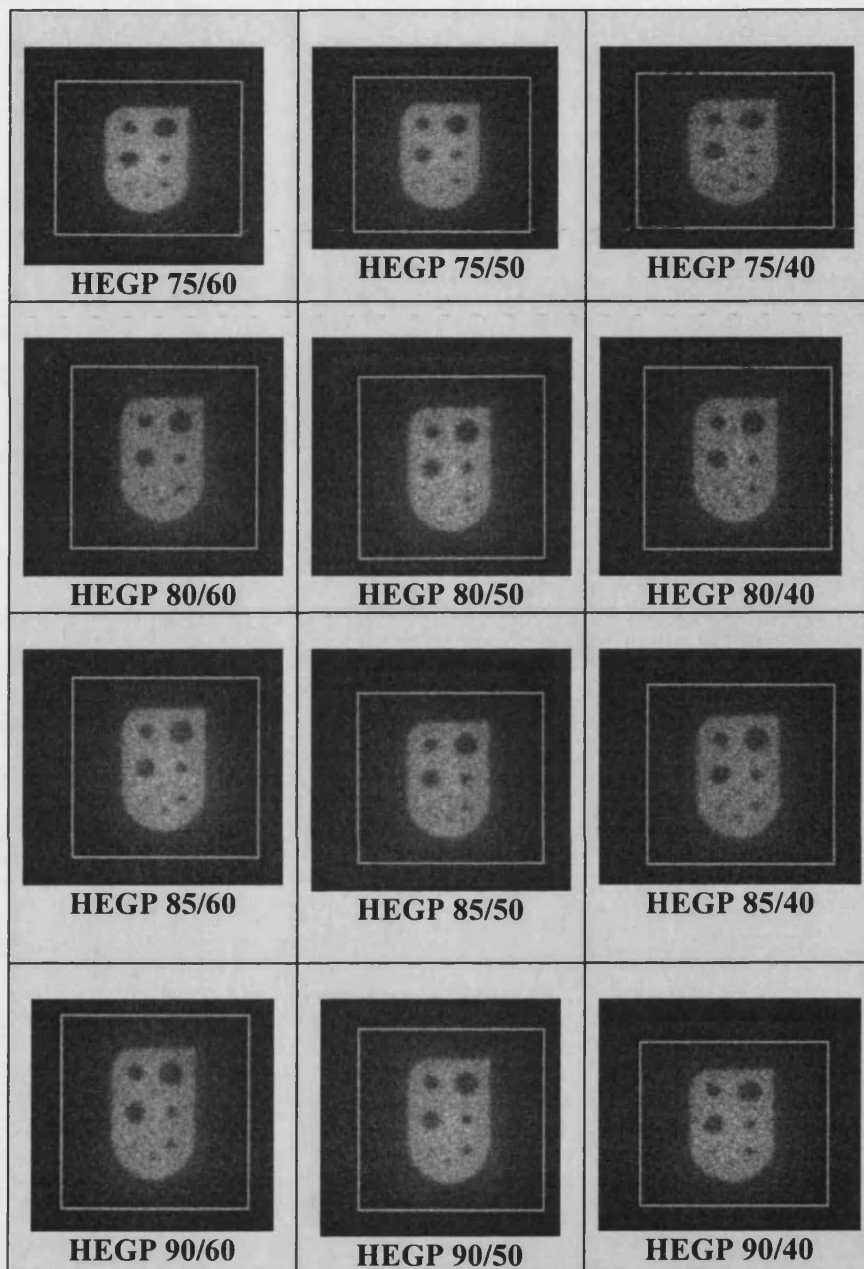
Fig 5.4 Images of Williams's phantom at different central energy and window width (Example: HEGP 90/60=High Energy General Purpose Collimator at central energy 90keV with energy width 60%)

5.2.2b In order to investigate how the image quality would change with increased scattering material. The Williams's phantom was positioned in the centre of the FOV (field of view). Using a high energy collimator (90 keV, 60% window), measurements of contrast and uniformity were taken with several different thicknesses of scattering blocks. Varying thicknesses (1, 2, 4, 6, 8, 10 and 15 centimetre) of Perspex were placed between the phantom and the camera face (Fig 3). Using a high energy general purpose (HEGP) collimator the image was acquired for a fixed count of 500,000 counts using a matrix of 256 x 256 (Fig 5.5).
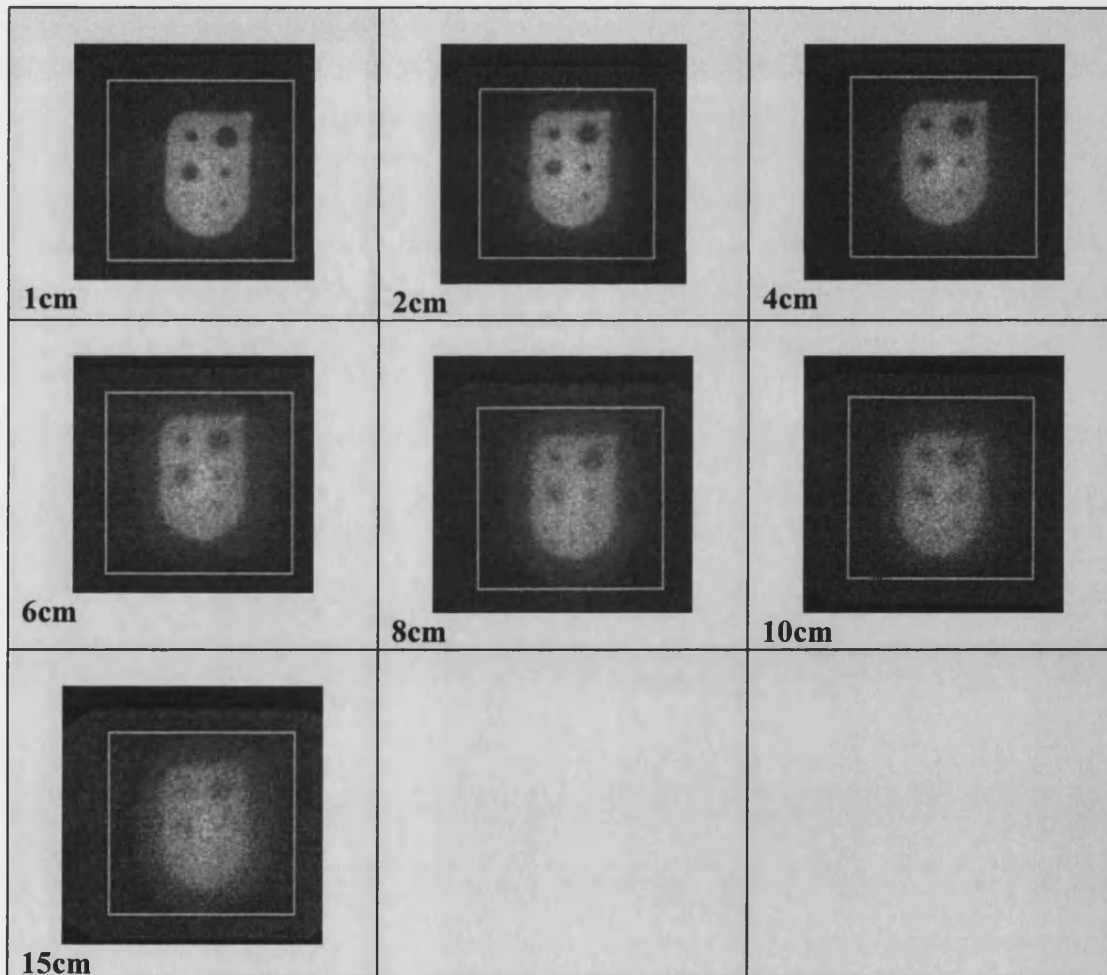
Fig 5.5 Imaging of ^{90}Y filled Williams's phantom with various depth of scattering material (90/60 = centred at energy 90keV with energy width 60)

5.2.3 Results

5.2.3a Contrast with different energy and windows

The average number of lesions visualised by 4 observers varied with central energy and window width (Fig 5.6). The contrast results for each lesion and window are shown in figure 5.7, 5.8, 5.9. To assess the best energy window with relation to contrast, for each lesion, we ranked the best energy window (1) to the worst energy window (12). The median ranking for each lesion was calculated for 3 window widths (60%, 50%, and 40%) and four central energies (75, 80, 85, 90 keV). A summary of the median ranking for each lesion and window width and central energy are given in the table 5.2. The results of visual analysis and quantitative analysis agree and show that for the energy windows investigated there is no optimal window in terms of contrast.
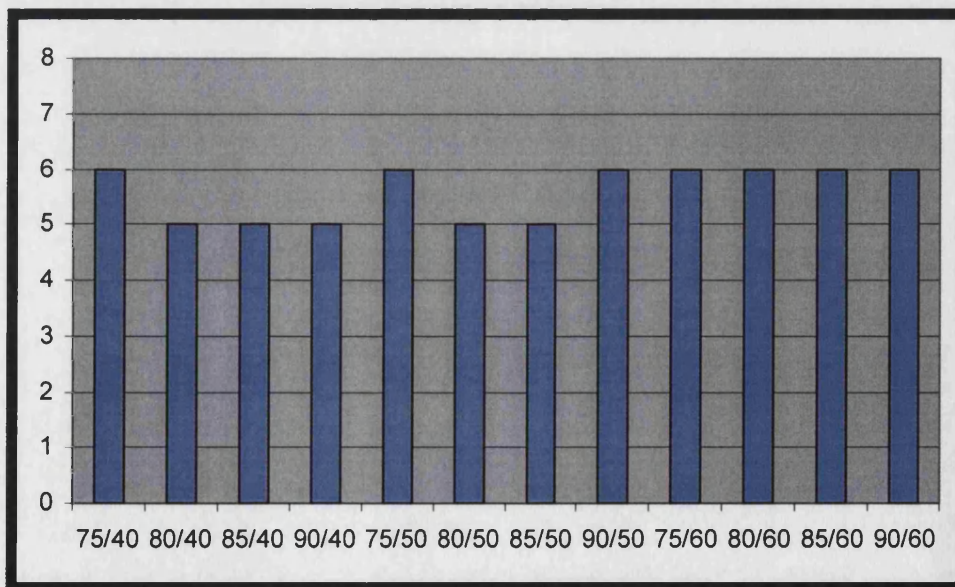
Fig 5.6 Shows the average number of lesions detected by four observers at different window and energies.

Central Energy	Lesion 1	Lesion 2	Lesion 3	Lesion 4
75keV	2	10	4	7
80keV	8	3	10	9
85keV	9	5	6	5
90keV	7	8	7	4
Window width	Lesion 1	Lesion 2	Lesion 3	Lesion 4
40%	4.5	6.5	6	6
50%	9	6.5	4.5	4.5
60%	8	6.5	8.5	8.5

Table 5.2 Median ranking for each lesion was calculated for 3 window widths and four central energies
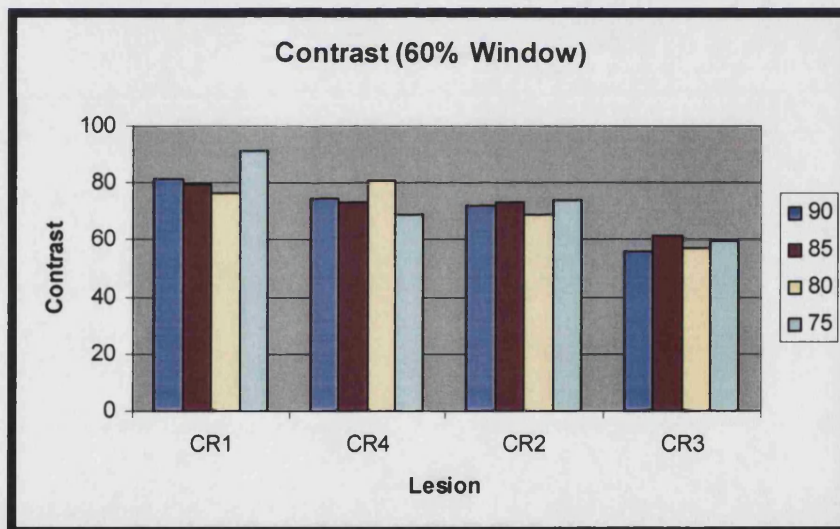
Fig 5.7 Showing contrast of 4 lesions imaged with 60% window with different energy
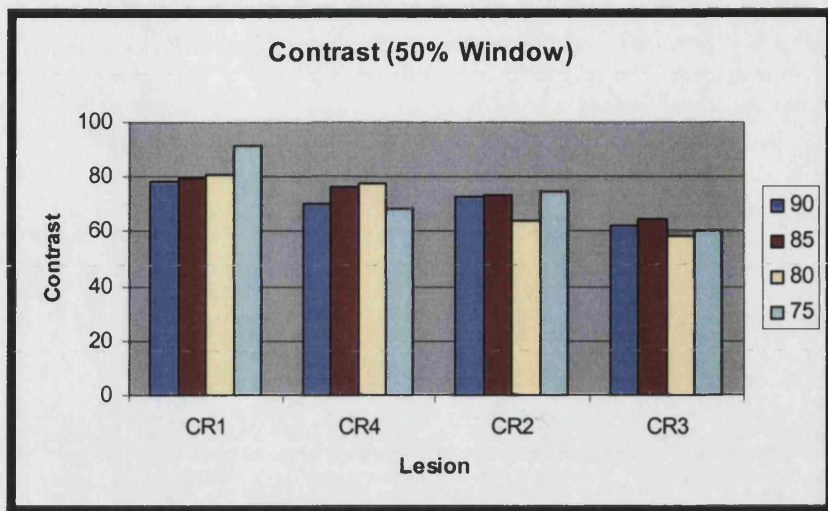
Fig 5.8 Showing contrast of 4 lesions imaged with 50% window with different energy
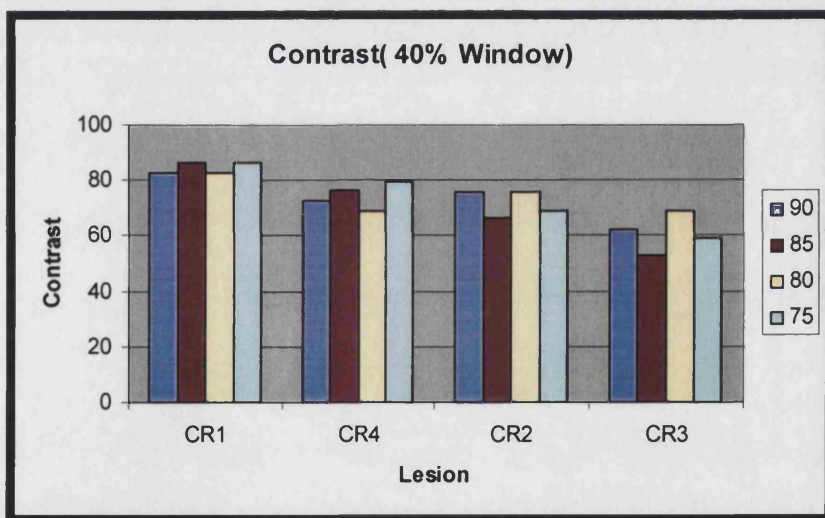
Fig 5.9 Showing contrast of 4 lesions imaged with 40% window with different energy

5.2.3b Contrast in relation to depth

In the experiment to assess the image contrast over varying depth using the scatter materials, we could see that the there is degradation (downward trend) of the image with increasing depth even for the biggest lesion in the phantom (Fig 5.5, 5.10, 5.11).
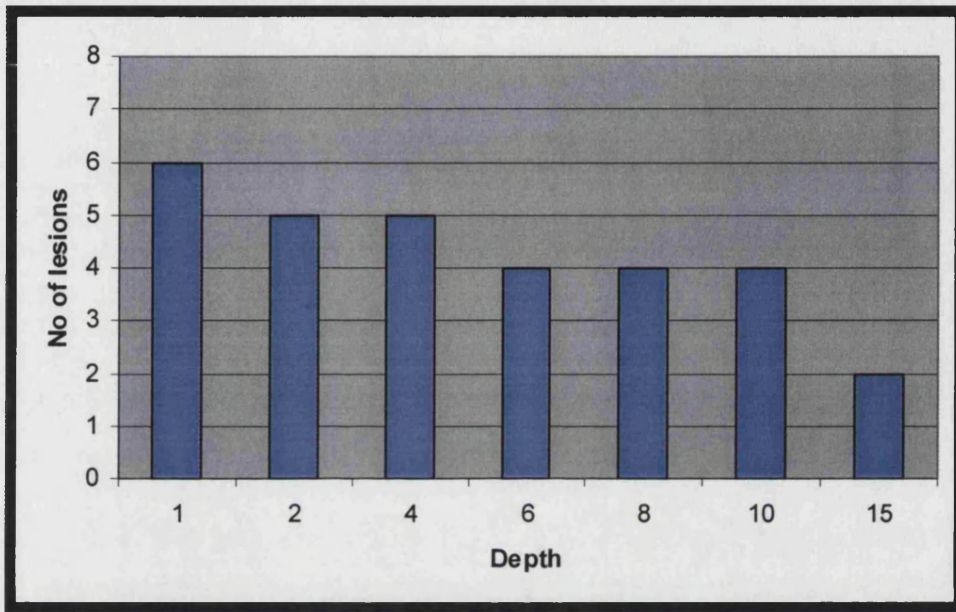
Fig 5.10 Number of lesions detected over varying depths on visual analysis
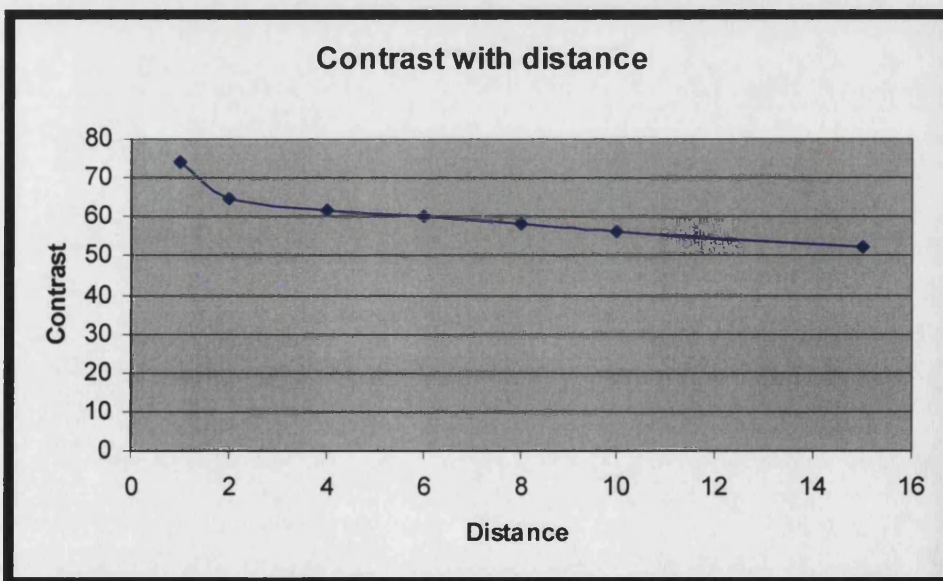
Fig 5.11 Showing degradation of contrast with increase in scattering material

5.2.3c Uniformity

The figure 5.12 and table 5.3 shows that how uniformity varies with different energy and window settings. The best uniformity is with smallest value, which is in this case is with energy centred at 75 keV with 60% window width. The figure 5.13 shows the changes in uniformity with increasing scatter.
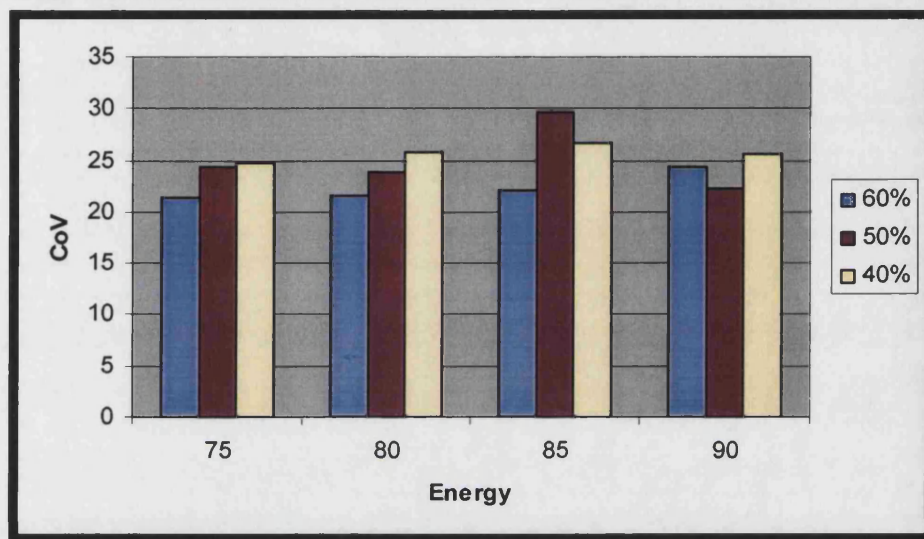
Fig 5.12 Shows uniformity with varying window and energy

Energy	Window	Collimator	CoV
90	60	HEGP	24.33
85	60	HEGP	22.01
80	60	HEGP	21.51
75	60	HEGP	21.46
90	50	HEGP	22.22
85	50	HEGP	29.69
80	50	HEGP	23.81
75	50	HEGP	24.4
90	40	HEGP	25.69
85	40	HEGP	26.67
80	40	HEGP	25.86
75	40	HEGP	24.80

Table 5.3 Shows uniformity with varying window and energy
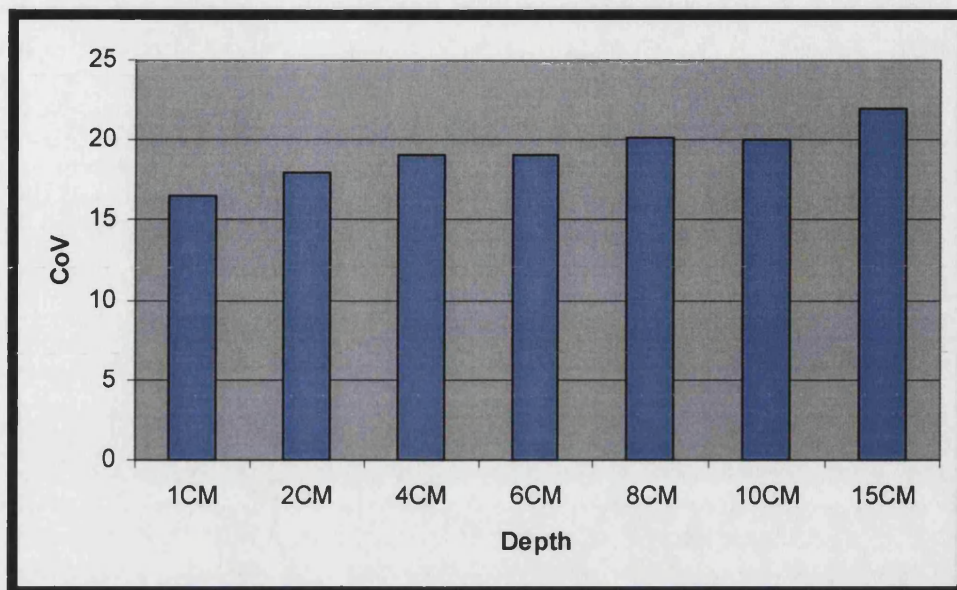
Fig 5.13 Showing changes in uniformity with depth

5.2.4 Discussion

Imaging with ^{90}Y is relevant in therapy planning because the plan can be modified if there is instability of the radiopharmaceutical. In the past imaging of brehmsstrahlung has been reported by other researchers using gamma cameras (Smith *et al*, 1988; Clarke *et al*, 1992; Siegel *et al*, 1992; Shen *et al*, 1994).

Our initial clinical experiments were conducted using a High Energy General Purpose collimator (HEGP) because it has better resolution and signal to noise ratio than other collimators (Shen *et al*, 1994). We empirically centred the energy at 75 keV with a 50% window off-set for our post therapy imaging.

In the assessment of contrast using different central energy and window widths. The lesions were visually analysed by 4 blinded observers, over all 6 lesions were visible ranging in size from 1.2-4 cm in diameter. These lesions were visible with varying contrast. Visual assessment and quantitative assessment of contrast were in

agreement; suggesting that in terms of contrast there is no optimal energy window in the range investigated.

We also saw a downward trend in the visualisation of the lesions while using scattering material i.e. the lesion outline or the margins were clearly defined with minimal scatter (1cm), where as with increasing scatter material (max of 15cm) the lesion margins were more poorly defined (Fig 5.5). None of the lesions below 1.2 cm was visualised by the 4 observers even with the minimum scatter of 1cm. Quantitative assessment of contrast supports this observation. This is clinically relevant even though we looked at the cold lesions in our experiments, in our observation we could not see lesions less than 3cm in diameter with 15cm scatter. At the more clinically relevant depth of 10cm no lesion less than 2cm diameter were seen. In a clinical situation, this means that organs will be well defined, but lesions at increasing depth will not be clearly seen.

Uniformity of response is an important parameter for quantification. In my experiments uniformity varies with energy and depth. Visual analysis shows no significant difference in uniformity with different central energy and window widths. Quantitatively the optimal uniformities were found at lower central energies and higher window widths with optimal window of 60% width. On assessment of uniformity over increasing scatter the optimal uniformity is obtained at 1cm depth (Fig 5.13).

The physics of brehmsstrahlung imaging is complex and still not fully understood (Gandon, 2003) and the argument about optimal imaging is still ongoing. For example Shen et al, with their extensive research reported that spatial resolution and signal to noise ratio of the medium energy (ME) collimators were lower than the high energy (HE) collimators, but the sensitivity of ME collimator was two times greater than the

HE collimator thereby confirming the advantage of using ME collimators. Clarke *et al* proposed that HE collimators with empirically selected broad energy window were sufficient for imaging patients with therapy doses of ^{90}Y and ^{32}P.

The difficulties here are that the characteristics of collimators such as HEGP collimators differ quite greatly from manufacturer to manufacturer making the generalised agreement of an optimal collimator problematic. Our experiments have shown that MEGP collimator has too much septal penetration (Gandon, 2003). Other influences in detector design and their resulting character will also make it difficult to optimise imaging parameters for all systems. Finally patient factors such as patient weight could also affect optimal imaging parameters.

The final quality of image in nuclear medicine is determined by various factors, including resolution, sensitivity and the amount of scatter and the uniformity of response across the detector. As of today many researchers have given different views, the choice of collimator, energy and window is complex and practical compromise has to be made for specific circumstances. In our experiments there was no optimal window for contrast, however in terms of uniformity of response imaging using HEGP with energy centred at 75 keV with 60% window width would be optimal.

5.2.5 Conclusion

Contrast of the image is most important because it allows visualisation of the lesion and uniformity is related to the consistency and accuracy of the image. Our experiments suggest that although there is no optimal window in terms of contrast in the range we have assessed, in terms of uniformity of the window 75 keV with 60% window is optimal.

To apply these methods clinically, a more realistic model for localised variations of brehmsstrahlung generation in tissue and for related photon transport mechanisms is required. Even then evaluation of radiation dosimetry could be difficult as it lacks primary photon emission. But with the present experiments we have found that it is possible to access the general biodistribution of the ^{90}Y labelled compounds. Further more we were able to confirm in patients that we are targeting the right organs. In terms of dosimetry, further experiments are required to assess the viability of these methods.

5.2.6 Future plan

(a) To acquire planar and SPECT images under the proposed imaging protocol and test the accuracy as to whether it is possible to quantify the injected ^{90}Y activity. Initial experiments are presently in progress using an anthropometric phantom.

(b) To acquire planar images using wider windows with increasing energy following the preliminary experiments conducted by (Gandon, 2003).

Chapter 6

^{111}Indium-pentetreotide and Brehmsstrahlung Imaging in the assessment of biodistribution and bone marrow toxicity of radiolabelled somatostatin analogues

----

6.1 Introduction

The value of radionuclide therapy is largely determined by the predictability of the patterns of biodistribution of the radiopharmaceutical. Radio-labelled receptor binding peptides have emerged as an important class of radiopharmaceuticals and these peptides transmit their biological function by binding to their specific receptor on the target cell. This specific receptor-binding property is exploited when the radiolabelled peptide is used as a radiopharmaceutical. The high-binding affinity for its receptor facilitates retention of the peptide in receptor-expressing tissues, whereas its relatively small size facilitates rapid clearance from the blood and other non-target tissues.

^{111}In and ^{90}Y radiolabeled somatostatin analogues are commonly used in the treatment of neuroendocrine tumours. After administration, a large amount of the compound is excreted via the urinary tract, while a variable part is trapped in the tumours. Unfortunately, the compound may also be trapped in critical tissues such as kidney or bone marrow. As a consequence, a method for assessment of individual biodistribution and pharmacokinetics is required to predict the maximum dose that can be safely injected into patients (Walrand *et al*, 2003).

The absence of gamma emissions from ^{90}Y for imaging has led researchers to use ^{111}In, a radionuclide with similar chemical properties and good imaging photons, as a tracer for the assessment of pharmacokinetics and radiation dosimetry of ^{90}Y (Shen *et al*,1994). However, it may be that a diagnostic radiolabelled somatostatin analogue such as ^{111}In-pentetreotide will have a biodistribution, which is similar enough to

allow for this agent to predict the biodistribution of a therapeutic radiolabelled somatostatin analogues, ^{90}Y-lanreotide and ^{90}Y-SMT.

6. 2 Experiment 1

6.2.1 Aim

The aim of this study was to compare the biodistribution of ^{111}In-pentetreotide and ^{90}Y-lanreotide and secondly to determine whether this biodistribution was close enough to allow ^{111}In-pentetreotide to be used to predict toxicity and for ^{90}Y-lanreotide treatment.

6.2.2 Material and methods

6.2.2a Inclusion criteria

Fourteen patients with somatostatin receptor-positive neuroendocrine tumours were included in this study, 6 males and 8 females (30-79years) (Table 6.1). All the patients were referred to the Nuclear Medicine Department from the Neuroendocrine Tumour Clinic of Royal Free Hospital, London. Of the 14 patients, 12 patients had carcinoid tumour 1 patient had medullary carcinoma of thyroid and 1 patient had small cell lung carcinoma. All had been assessed as unsuitable for surgery, chemotherapy or ^{131}I-mIBG therapy and had been offered ^{90}Y-lanreotide therapy for symptom control or control of growing tumour.

6.2.2b Preparation of agents

The ^{111}In-pentetreotide was labelled according to manufacturer's instructions and was released for injection if the thin layer chromatography showed labelling efficiency of greater than 95%.

The ^{90}Y-lanreotide was produced by dissolving 100mcg of DOTA lanreotide peptide residue (Biomedica, Vienna, Austria) in 0.4ml of 1M ammonium acetate buffer using

a low metal shedding needle for fluid transfer (to avoid transfer of other trace elements). After mixing at room temperature for 3-5 minutes, the solution was added to the vial containing 1.2 GBq of ^{90}Y-chloride (Amersham Health, Amersham Berks, UK) and the vial placed in a water bath containing boiling water for 10 minutes. Before administration the product was filtered through a 0.2 micron low-protein-binding filter. The labelling efficiency was checked to be above 95% by both HPLC and thin layer chromatography before it was administered.

Patient	Age in years	Sex	Diagnosis
1 CK	67	F	Non secretory-carcinoid tumour
2 CS	52	M	Secretory-carcinoid tumour
3 SP	50	M	Secretory-carcinoid tumour
4 MC	47	F	Non secretory-carcinoid tumour
5 SH	45	M	Non secretory-carcinoid tumour
6 JB	77	F	Non secretory-carcinoid tumour
7 EB	43	F	Non secretory-carcinoid tumour
8 SS	56	F	Non secretory-carcinoid tumour
9 LM	79	F	Medullary carcinoma of thyroid
10 MR	57	F	Secretory-carcinoid tumour
11 LC	57	F	Small cell lung carcinoma
12 BP	62	M	Non secretory-carcinoid tumour
13 DV	59	M	Secretory carcinoid tumour
14 MQ	30	M	Non secretory-carcinoid tumour

Table 6.1 Patients with somatostatin receptor-positive neuroendocrine tumours

6.2.2c Imaging

The patients were assessed for the presence of somatostatin receptors by the use of commercially available ^{111}In-pentetreotide (Octreoscan, Tyco Healthcare, Petten Netherlands). For analysis of the biodistribution of ^{111}In-pentetreotide, whole body imaging at 24 hours post injection of 120 MBq ^{111}In-pentetreotide (maximum allowed in the U.K) was used (Fig 6.1.1). Imaging was performed on a two headed gamma camera fitted with medium energy collimators (Phillips-Marconi Prism 2000,

Cleveland, Ohio). Anterior and posterior views were obtained into a 256 X 256 matrix at a scanning rate of 20 minute/metre and peak energies of 170 and 250 keV with 15% window.

Within 8 weeks of this scan all 14 patients received 1-1.2 GBq ^{90}Y-lanreotide followed by whole-body brehmsstrahlung imaging 24 hours later (Table 6.2). All the images were acquired using the same gamma camera, fitted with high-energy collimators, with a 75 keV photopeak and 50% windows (Gnanasegaran, 2001) (Fig 6.1 and 6.2). The same matrix size and acquisition time were used as in the ^{111}In-pentetreotide imaging.

In view of the limited resolution of the brehmsstrahlung imaging it was not possible to identify all tumour sites and many of the patients had multiple small tumours. Total tumour uptake was therefore not calculated as part of this study.

Study	Whole body somatostatin imaging	^{90}Y brehmsstrahlung
Radiopharmaceutical	^{111}In- pentetreotide	^{90}Y-lanreotide
Activity administered	120 MBq	1-1.2 GBq
Patient preparation	None	None
Patient positioning	Supine, arms to side using the arm rest	Supine, arms to side Using the arm rest
Collimator	Medium energy general purpose 170 + 250 keV with 15% window	High energy general purpose 75 keV with 50% windows

Table 6.2 Whole body imaging protocol for ^{111}In- pentetreotide and ^{90}Y-lanreotide
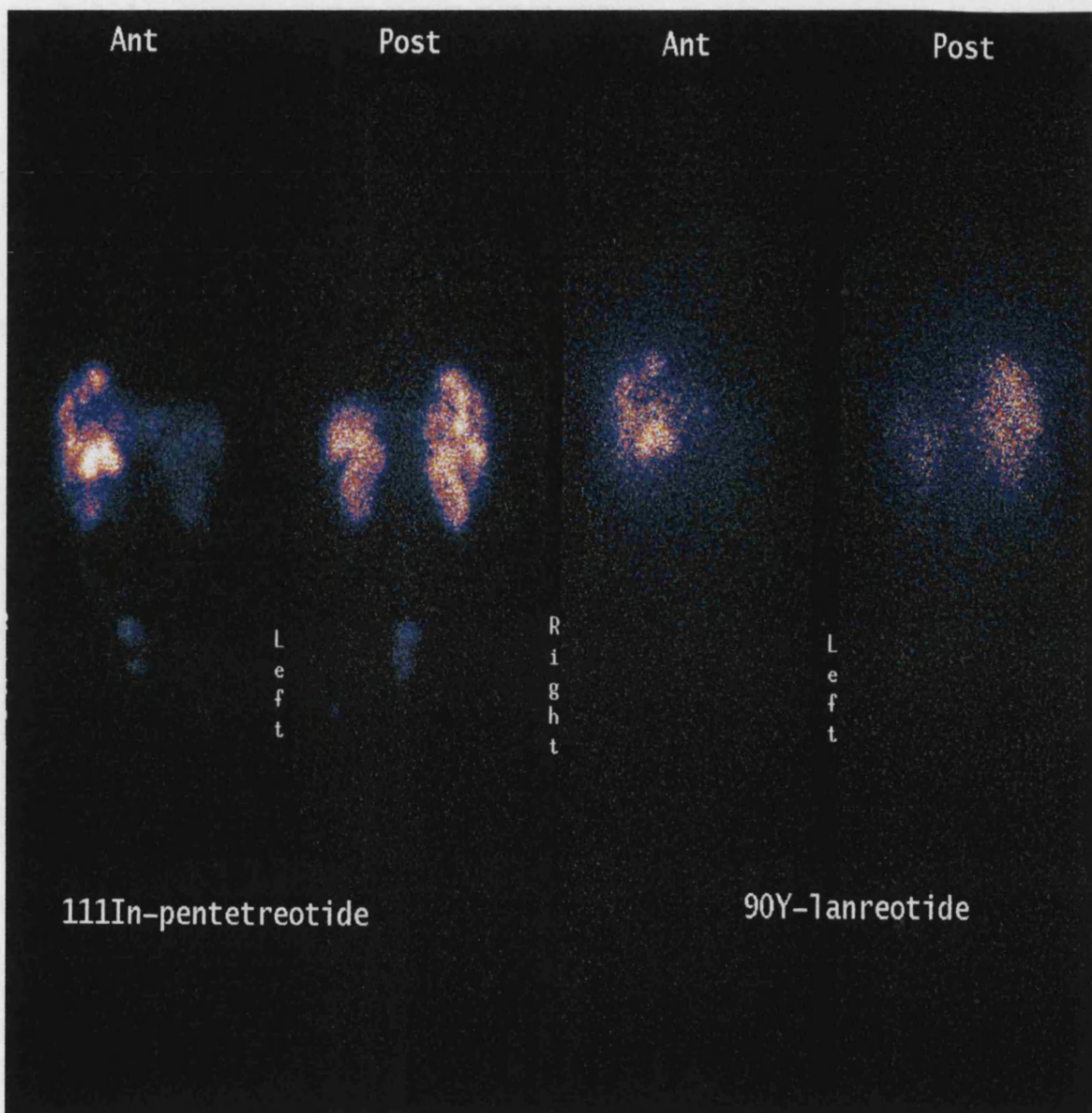
Fig 6.1 Anterior and posterior 24 hour post injection whole body images showing a similar distribution of ^{111}In pentetreotide and ^{90}Y-lanreotide in tumour around the liver. However, note the uptake of the ^{90}Y-lanreotide is less in the kidneys, bladder and colon.
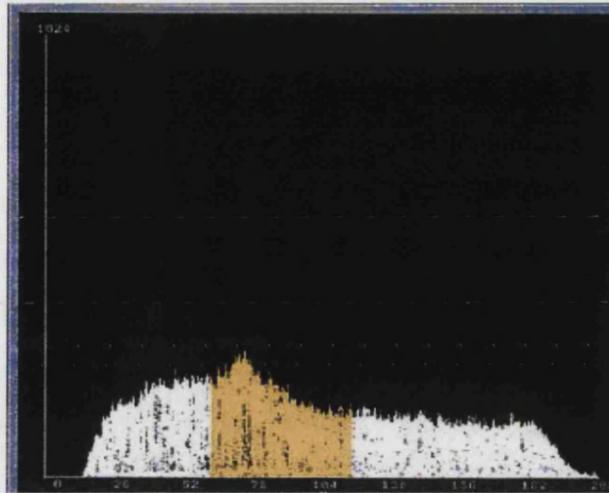
Fig 6.2 Brehmsstrahlung Spectrum

6.2.2d Biodistribution and dosimetry

The whole body ^{111}In-pentetreotide and the ^{90}Y-lanreotide (brehmsstrahlung) images were then used for the calculation of the biodistribution of each radio-labelled somatostatin. Irregular regions of interest (ROI) were drawn over the ^{111}In-pentetreotide images in all the patients. The ROIs were drawn, manually, on the anterior whole body image over the liver, spleen (except in one patient who had undergone splenectomy), heart, bone marrow (spine), and the kidneys. These regions were then stored and applied to the posterior image after "flipping" the images (Fig 6.3). The organ sites were defined by the appearances of that organ on the ^{111}In-pentetreotide scan. The whole body uptake was calculated using a geometric mean (Formula 6.1) and then the geometric mean uptake was calculated for the liver, spleen, heart, bone marrow, left kidney and the right kidney by counting the activity from the anterior and posterior images (Formula 6.2) (Table 6.3). The whole procedure was then repeated for the ^{90}Y-lanreotide images using the same regions as those applied in the ^{111}In-pentetreotide images (Table 6.4) and the geometric mean

was used. The absorption correction for the brehmsstrahlung has not yet been defined and verified and therefore a depth correction technique could not be employed.

$$\text{Geometric mean} = \sqrt{\text{Anterior counts} \times \text{Posterior counts}}$$

Formula 6.1 Calculation of Geometric mean

$$\text{Organ uptake \%} = \frac{\text{Counts (geometric mean) of organ}}{\text{Counts (geometric mean) of whole body}} \times 100$$

Formula 6.2 Calculation of organ uptake as percentage of whole body uptake
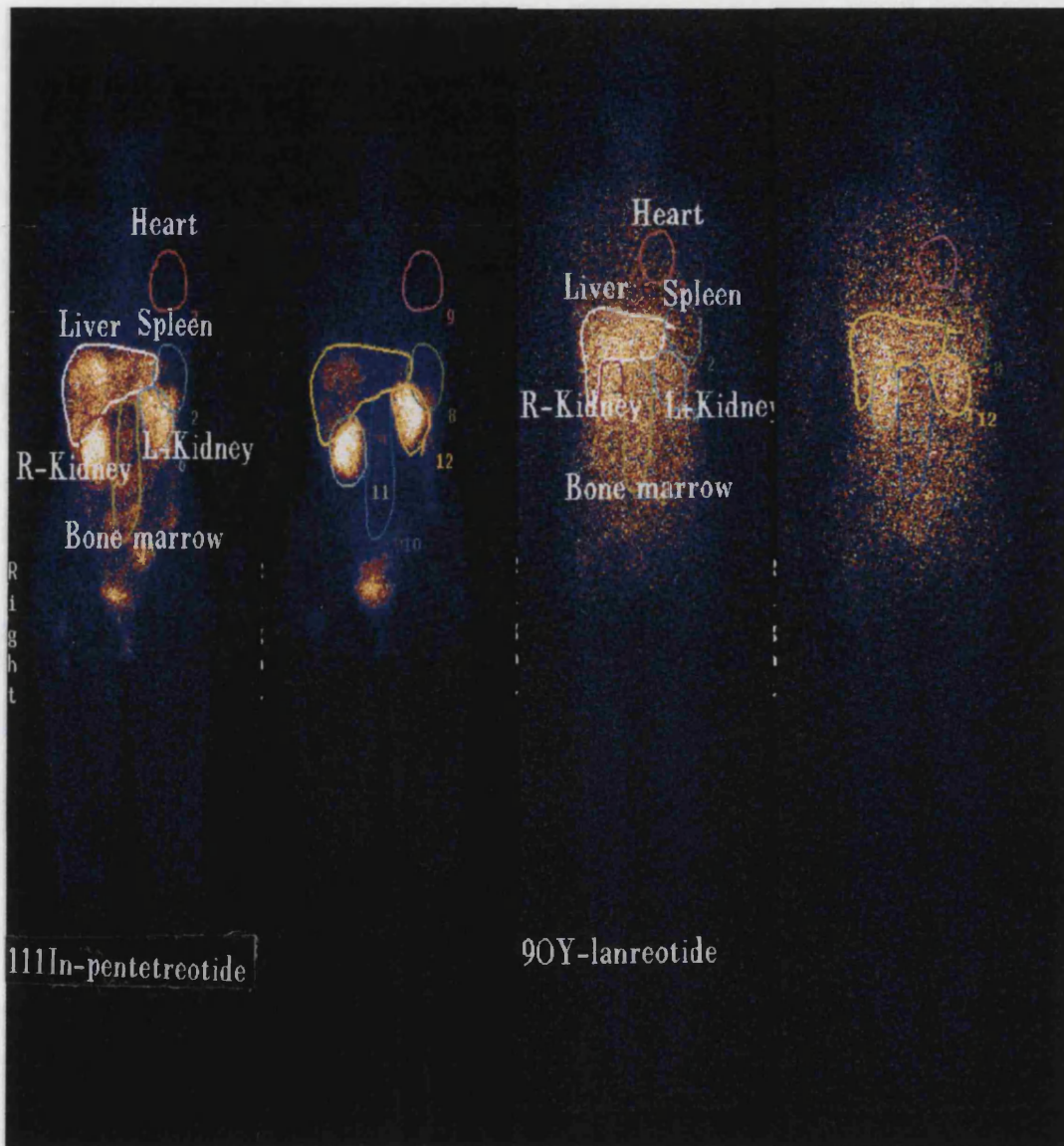
Fig 6.3 Anterior and posterior whole body image of ^{111}In-pentetreotide and ^{90}Y-lanreotide image showing regions drawn for calculation of percentage of whole body uptake in various organs

	Liver	Spleen	Heart	Bone marrow	Kidney
1CK	10.5	2.9	1.5	2.2	12.9
2CS	6.5	3.9	1.3	2.7	18.6
3SP	24.3	7	1.2	2.1	11.2
4MC	23.1	8	1.1	3.4	18.9
5SH	10.6	1.2	1.1	2.8	25
6JB	21	12.5	2.4	3.5	7.6
7EB	8.9	1.6	1.8	1.9	4.9
8SS	12.7	Splenectomy	0.9	2	13
9LM	19.5	21	1.9	4.5	27.5
10MR	68	2.2	0.5	1.5	6.6
11LC	26	4.2	0.8	3.5	10
12BP	53.4	4.3	1.9	1.4	13.1
13DV	23.7	6.3	1.4	2.6	14.1
14MQ	18.7	5.9	0.5	0.9	7.7

Table 6.3 Percentage of uptake in different organs with ^{111}In-pentetreotide

	Liver	Spleen	Heart	Bone marrow	Kidney
1CK	8.7	2.6	2.4	2.1	4.4
2CS	9.8	2.7	1.9	1.8	3.5
3SP	14.6	2.7	1.6	2.5	5
4MC	10.1	4.2	2.1	3	5.7
5SH	6.2	3.5	2	2.3	5
6JB	13.8	4.7	3.8	2.4	6.9
7EB	6.3	2.9	2.1	2.5	3.9
8SS	7.6	Splenectomy	1.8	2.2	4.8
9LM	7.4	2.5	1.9	2.7	5.2
10MR	21	3.5	1.3	3	3.9
11LC	7.2	2.3	1.5	1.2	5.5
12BP	10.6	3.8	1.9	3.4	5.6
13DV	10.3	3.2	2	2.4	4.9
14MQ	4.3	0.8	0.6	0.6	1.3

Table 6.4 Percentage of uptake in different organs with ^{90}Y-lanreotide

6.2.2e Statistical analysis

Using a two-tailed paired student t test the difference in uptake was calculated for ^{111}In-pentetreotide and ^{90}Y-lanreotide in each of the different organs measured. Statistical significance was assumed when p<0.05 (Table 6.5, 6.6, 6.7). These statistics were calculated using SPSS v 6.0 (SPSS, Chicago, Il, USA).

6.2.3 Results

Whilst the distribution of the two agents was generally similar (Fig 6.1) there was a significant difference in uptake for ^{111}In-pentetreotide and ^{90}Y-lanreotide in some organs (Fig 6.4). For ^{111}In-pentetreotide the liver uptake was significantly higher than for ^{90}Y-lanreotide (p=0.004, Table 6.8). The ^{111}In-pentetreotide uptake in the kidneys showed a much higher uptake than for ^{90}Y-lanreotide (p = 0.000, Table 6.8) (Fig 6.5), with the mean renal uptake of ^{111}In-pentetreotide being more than double that seen with ^{90}Y-lanreotide. In the spleen and bone marrow there was no significant difference in the uptake of the two agents. The uptake in the heart, which represents remaining circulating activity of the radio-peptide at 24 hours, was higher with ^{90}Y-lanreotide than with ^{111}In-pentetreotide but this was not significant (Table 6.8).

		N	Correlation	Sig.
Pair 1	I_LIVER & Y_LIVER	14	.7	.005
Pair 2	I_SPLEEN & Y_SPLEEN	13	.1	.84
Pair 3	I_HEART & Y_HEART	14	.8	.001
Pair 4	I_MARROW & Y_MARROW	14	.1	.73
Pair 5	I_L_KID & Y_L_KID	14	.2	.45

Table 6.6 Paired Samples Correlations of ^{111}In-pentetreotide and ^{90}Y-lanreotid

	Mean	N	Std. Deviation	Std. Error Mean
Pair 1				
I_LIVER	23.4	14	17.3	4.6
Y_LIVER	9.8	14	4.3	1.1
Pair 2				
I_SPLEEN	6.2	13	5.4	1.5
Y_SPLEEN	3	13	.98	.3
Pair 3				
I_HEART	1.3	14	.5	.1
Y_HEART	1.9	14	.7	.9
Pair 4				
I_MARROW	2.5	14	1	.3
Y_MARROW	2.3	14	.7	.2
Pair 5				
I_L_KID	13.6	14	6.7	1.8
Y_L_KID	4.7	14	1.3	.3

Table 6.5 Paired sample statistics of ^{111}In-pentetreotide and ^{90}Y-lanreotide

		Paired Differences					t	df	Sig. (2-tailed)
		Mean	Std. Deviation	Std. Error Mean	95% Confidence Interval of the Difference				
					Lower	Upper			
Pair 1	I_LIVER - Y_LIVER	13.5	14.5	3.9	5.1	21.9	3.5	13	.004
Pair 2	I_SPLEEN - Y_SPLEEN	3.2	5.4	1.5	-6.7E-02	6.5	2.1	12	.054
Pair 3	I_HEART - Y_HEART	-.6	.4	.1	-.8	-.38	-5.6	13	.000
Pair 4	I_MARROW - Y_MARROW	.2	1.1	.3	-.4	.9	.7	13	.5
Pair 5	I_L_KID - Y_L_KID	8.9	6.9	1.7	5.1	12.7	5	13	.000

Table 6.7 Paired Samples test of ^{111}In-pentetreotide and ^{90}Y-lanreotide

Organs	p value
Liver (n=14)	0.004
Spleen (n=13)	0.054
Heart (n=14)	0.000
Bone marrow (n=14)	0.5
Kidneys (n=14)	0.000

Table 6.8 Shows the p values for each organ

Organs	p value
Liver (n=12)	0.000
Spleen (n=11)	0.05
Heart (n=12)	0.000
Bone marrow (n=12)	0.06
Kidneys (n=12)	0.000

Table 6.9 Shows the p values for each organ without patients 10 and 12
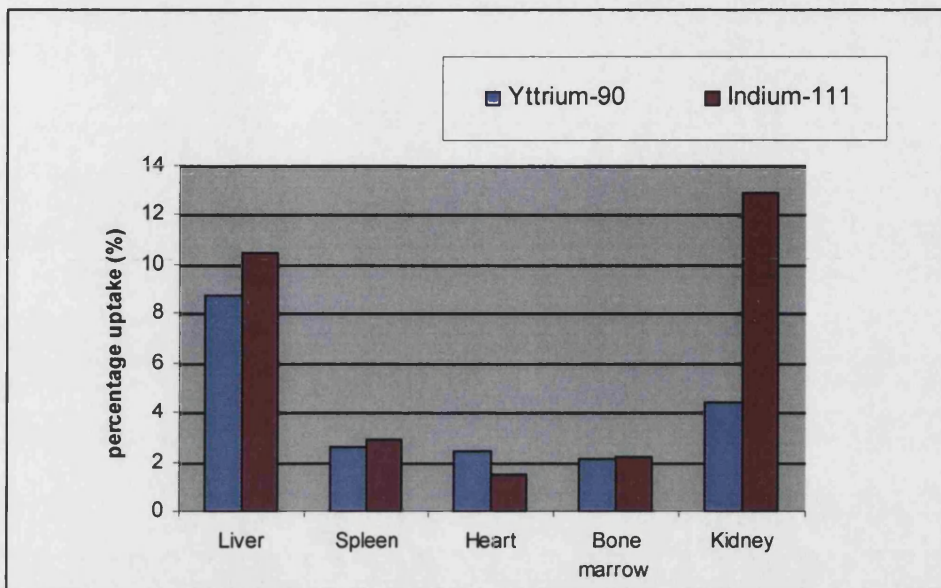
Fig 6.4 Example of Distribution of ^{90}Y-lanreotide and ^{111}In-pentetreotide in various organs
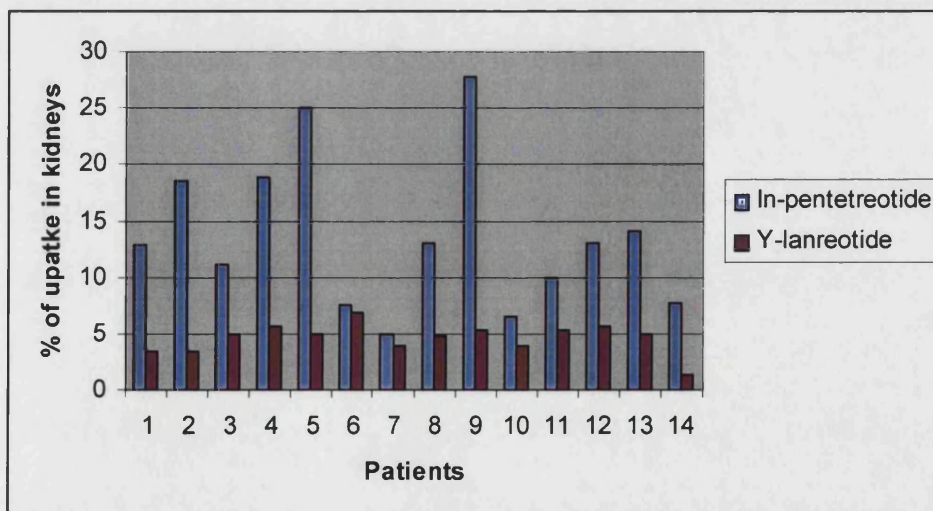
Fig 6.5 Percentage of uptake in the kidneys at 24 hours in all the 14 patients

6.3 Experiment 2

6.3.1 Aim

The aim of this study was to compare the biodistribution of ^{111}In-pentetreotide and ^{90}Y-SMT

6.3.2 Material and methods

6.3.2a Inclusion criteria

Five patients with somatostatin receptor-positive neuroendocrine tumours were included in this study, 3 males and 2 females (46-63 years) (Table 6.9). All the patients were referred to the Nuclear Medicine Department from the Neuroendocrine Tumour Clinic of Royal Free Hospital, London. 3 patients had carcinoid tumour and 2 patients had Insulinoma. All had been assessed as unsuitable for surgery, chemotherapy or ^{131}I-mIBG therapy and had been offered ^{90}Y-SMT therapy for symptom control or control of growing tumour.

Patient	Age in years	Sex	Diagnosis
1 RA	61	M	Insulinoma
2 MR	57	F	Secretory-carcinoid tumour
3 FN	46	M	Secretory-carcinoid tumour
4 LC	62	F	Secretory-carcinoid tumour
5 MA	63	M	Insulinoma

Table 6.10 Patients with somatostatin receptor-positive neuroendocrine tumours

6.3.2b Imaging

The patients were assessed for the presence of somatostatin receptors by the use of commercially available ^{111}In-pentetreotide (Octreoscan, Tyco Healthcare, Petten Netherlands). For analysis of the biodistribution of ^{111}In-pentetreotide, whole body imaging at 24 hours post injection of 120 MBq ^{111}In-pentetreotide was used (Fig 6.6)

(Table 6.10). Imaging was performed on a two headed gamma camera fitted with medium energy collimators (Phillips-Marconi Prism 2000, Cleveland, Ohio). Anterior and posterior views were obtained into a 256 X 256 matrix at a scanning rate of 20 minute/metre and peak energies of 170 and 250 keV with 15% window.

Within 8 weeks of this scan all 5 patients received 4 GBq ^{90}Y-SMT (amino acid infusion was administered before and during infusion) followed by whole-body brehmsstrahlung imaging 24 hours later. All the images were acquired using the same gamma camera fitted with high-energy collimators; with a 75 keV photo peak and 50% windows. The same matrix size and acquisition time were used as in the ^{111}In-pentetreotide imaging.

| Study	Whole body somatostatin imaging	^{90}Y brehmsstrahlung
Radiopharmaceutical	^{111}In-pentetreotide	^{90}Y-SMT
Activity administered	120 MBq	4 GBq
Patient preparation	None	None
Patient positioning	Supine, arms to side using the arm rest	Supine, arms to side Using the arm rest
Collimator /energy	Medium energy general purpose 170 + 250 keV with 15% window	High energy general Purpose 75 keV with 50% windows

Table 6.11 Whole body imaging protocol for^{111}In- pentetreotide and ^{90}Y-SMT

6.3.2c Biodistribution and dosimetry

The whole body ^{111}In-pentetreotide and the ^{90}Y-SMT (brehmsstrahlung) images were then used for the calculation of the bio-distribution of radiolabelled somatostatin (Fig 6.7) (Table 6.11 and 6.12). The biodistribution and statistical analysis were performed as done in study 6.2.

111-In	Liver	Spleen	Heart	Bone marrow	Kidneys
1 RA	20	4.5	0.7	4.3	17.8
2 MR	17	10	0.8	3	10
3 FN	24.8	7.2	0.5	2	10.7
4 LC	21	14	0.5	4.2	12
5 MA	35	1.1	0.5	1.8	8

Table 6.12 Percentage of uptake in different organs with ^{111}In-pentetreotide

90-Y	Liver	Spleen	Heart	Bone marrow	Kidneys
1 RA	20.3	2.4	1.4	2.8	4
2 MR	17.4	2.8	1.2	2.9	6
3 FN	13.3	8.6	1.1	4.6	8
4 LC	12	3.7	1.2	2.7	7
5 MA	10.5	4.2	1.2	4	6.6

Table 6.13 Percentage of uptake in different organs with [90]Yttrium-SMT

6.3.3 Results

Whilst the distribution of the two agents was generally similar (Fig 6.6) there was a difference in uptake for ^{111}In-pentetreotide and ^{90}Y-SMT in some organs (Fig 6.8). For ^{111}In-pentetreotide the liver uptake was higher than for ^{90}Y-SMT.
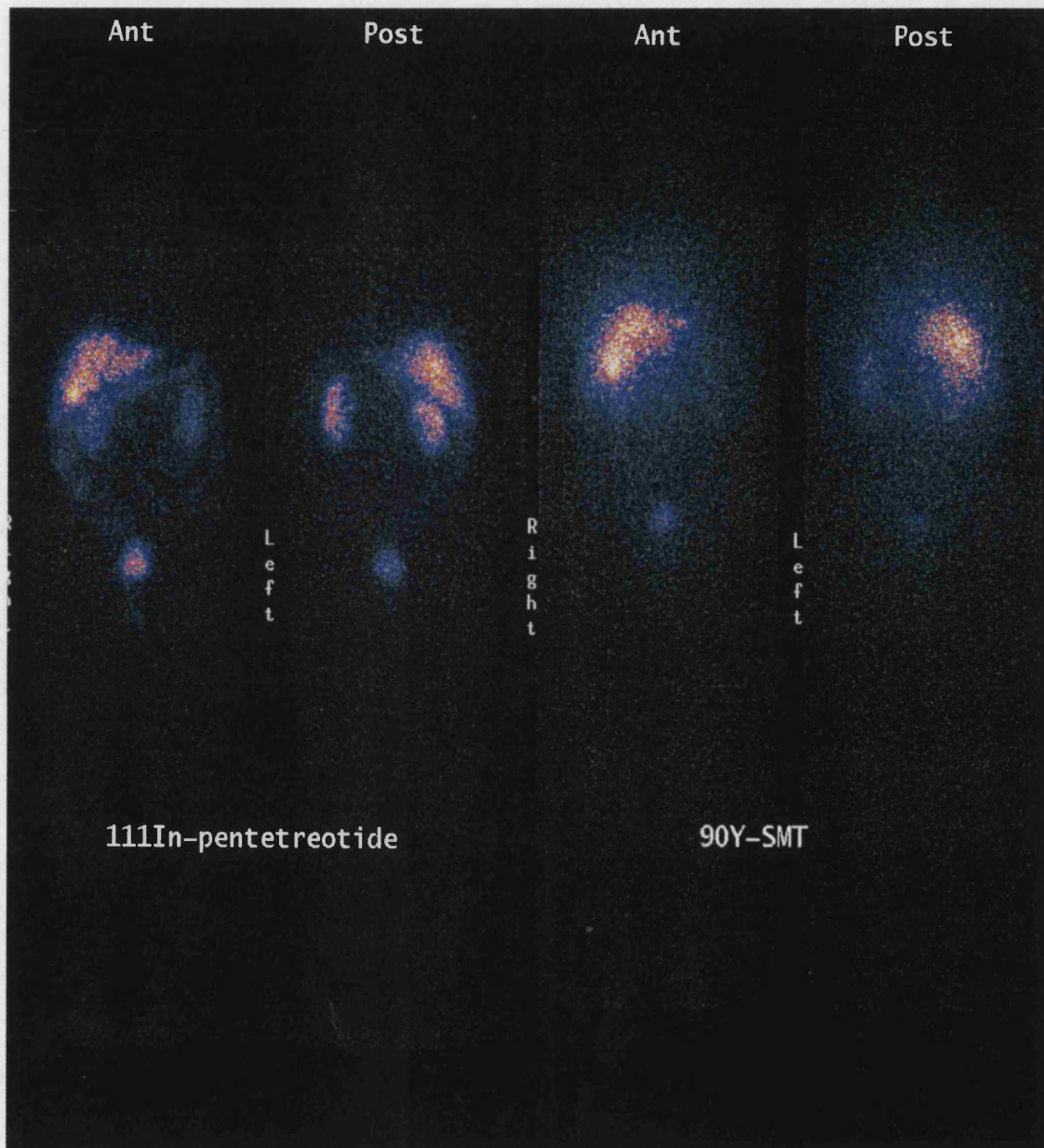
Fig 6.6 Demonstrates the distribution of ^{111}In-pentetreotide and ^{90}Y-SMT
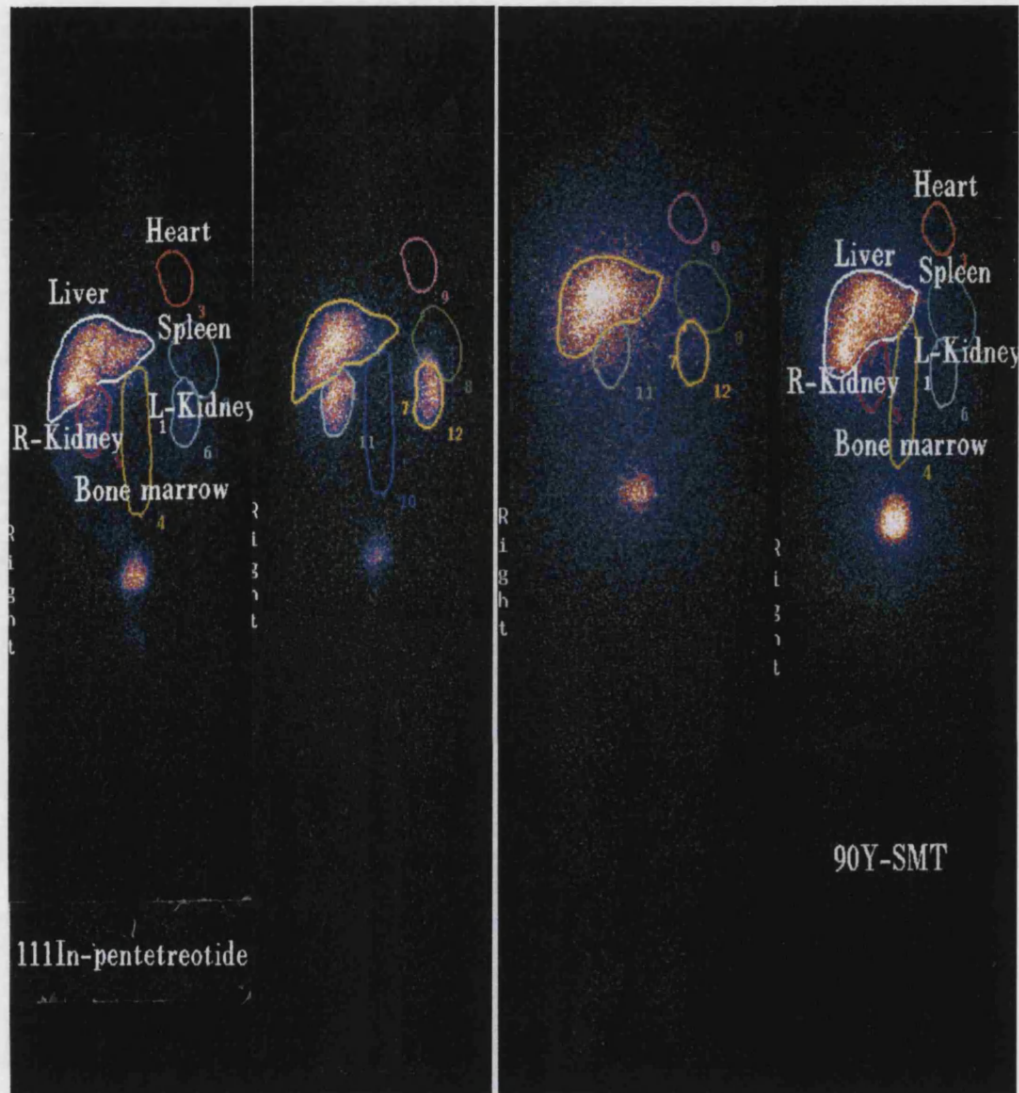
Fig 6.7 Anterior and posterior whole body image of ^{111}In pentetreotide and ^{90}Y-SMT image showing regions drawn for calculation of percentage of whole body uptake in various organs

The ^{111}In-pentetreotide activity in the kidneys showed a much higher uptake than for ^{90}Y-SMT p=0.041(Table 6.13) (Fig 6.8), with the mean renal uptake of ^{111}In-pentetreotide being more than double that seen with ^{90}Y-SMT. In the spleen and bone marrow there was no difference in the uptake of the two agents. The uptake in the heart, which represents remaining circulating activity of the radio-peptide at 24 hours, was higher with ^{90}Y-SMT than with ^{111}In-pentetreotide but this was not significant.
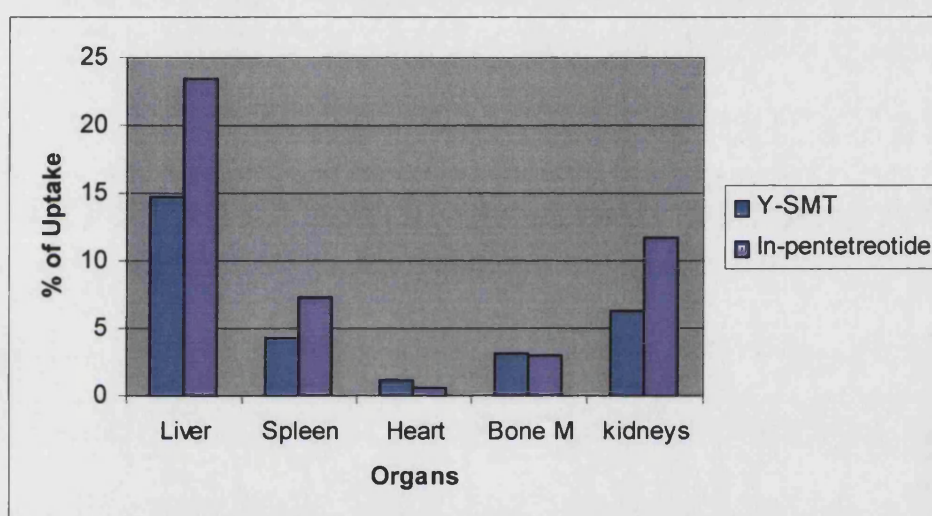
Fig 6.8 Distribution of ^{90}Y-SMT and ^{111}In-pentetreotide in various organs

----

Organs	p value
Liver (n=5)	0.004
Spleen (n=5)	0.095
Heart (n=5)	0.02
Bone marrow (n=5)	0.532
Kidneys (n=5)	0.041

Table 6.14 shows the p values in different organs

6.4 Experiment 3

6.4.1 Aim

The aim of this study was to compare the biodistribution of ^{90}Y-SMT at 4 hrs and 24 hours.

6.4.2 Material and methods

6.4.2a Inclusion criteria

Two patients (1male & 1 female) with Somatostatin receptor-positive neuroendocrine tumours were included in this study (Table 6.14). They had been offered ^{90}Y-SMT therapy for symptom control or control of growing tumour.

	Sex-age	Tumour type	Therapy
Patient 1	F/45	Carcinoid	^{90}Y-SMT
Patient 2	M/63	Insulinoma	^{90}Y-SMT

Table 6.15 Patients with somatostatin receptor-positive neuroendocrine tumours

6.4.2b Imaging

Both the patients received 4 GBq ^{90}Y-SMT (amino acid infusion was administered before and during infusion) followed by whole-body brehmsstrahlung imaging at 4 hour and 24 hours later (Table 6.10). All the images were acquired using the same gamma camera used in the previous studies (6.2 & 6.3) fitted with high-energy collimators; with a 75 keV photo peak and 50% windows.

6.4.2c Biodistribution and dosimetry

The whole body ^{90}Y-SMT (brehmsstrahlung) images at 4 hours and 24 hours were then used for the calculation of the bio-distribution of radiolabelled somatostatin. Irregular regions of interest (ROI) were drawn over the ^{90}Y-SMT images. The ROIs were drawn, manually, on the anterior whole body image over the liver, spleen heart, bone marrow (spine), and the kidneys. These regions were then stored and applied to the posterior image after "flipping" the images. The whole body activity was calculated using a geometric mean (Formula 6.1) and then the geometric mean uptake was calculated for the liver, spleen, heart, bone marrow, left kidney and the right kidney by counting the uptake from the anterior and posterior images (Formula 6.2).

6.4.3 Results

Whilst the distribution of the ^{90}Y-SMT was generally similar at 4 hours and 24 hours (Fig 6.9) there was a difference in uptake during these times. The initial 4-hour uptake of ^{90}Y-SMT in liver, spleen, bone marrow and kidney's was lower than the 24 hours uptake. The uptake in the heart did not change during 4 hours and 24 hours (Table 6.14) (Fig 6.15).
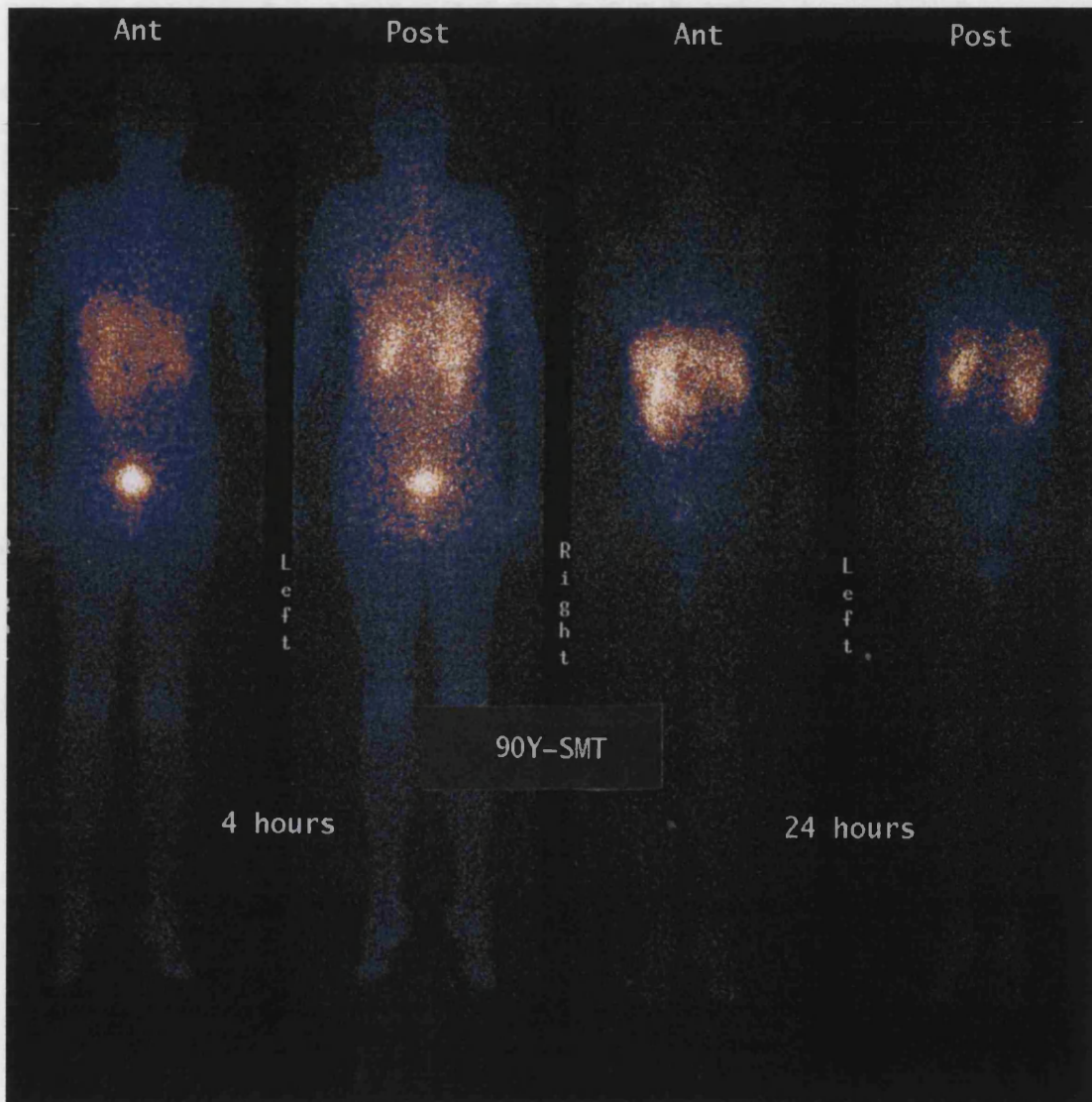
Fig 6.9 Whole body images showing distribution of ^{90}Y-SMT at 4 & 24 hours

		Liver	Spleen	Heart	BM	Kidney's
Patient 1	4 hours	4.9	1.7	1.3	2.7	1.8
	24 hours	8.3	4.02	1.6	5	3.8
Patient 2	4 hours	12.6	5.9	1	6.7	4.8
	24 hours	12.7	1.9	1.4	8.4	5.1

Table 6.16 Percentage of uptake in different organs with ^{90}Y-SMT at 4 & 24 hours
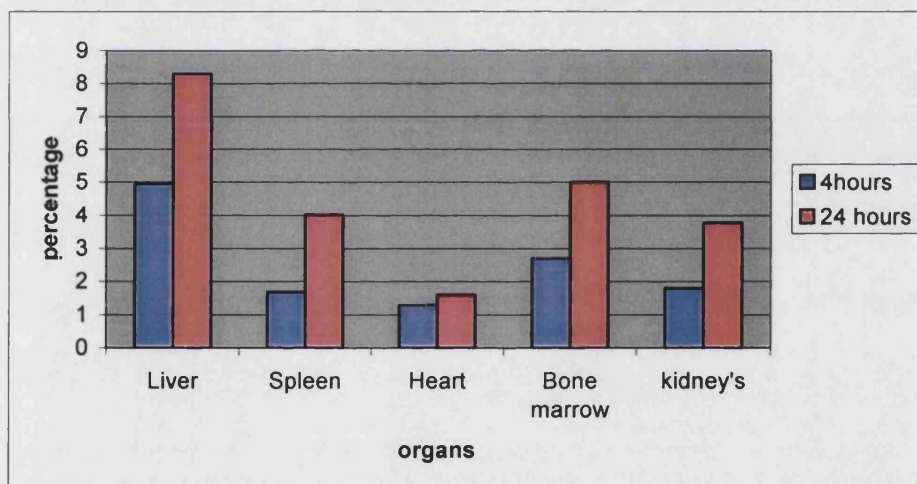
Fig 6.10 Shows Distribution of ^{90}Y-SMT at 4 & 24 hours in various organs

6.5 Experiment 4

6.5.1 Aim

The aim of our study was to determine if brehmsstrahlung imaging was useful in predicting bone marrow toxicity after ^{90}Y-lanreotide.

6.5.2 Material and methods

6.5.2a Inclusion criteria:

12 patients (6 males & 6 females) with biopsy proven neuroendocrine tumours were included in the study (Table 6.16). All the patients had serial blood tests for urea, creatinine, platelets, and at regular intervals pre and post treatment. 6 patients were suffering from grade 3 & 4 bone marrow toxicity was compared with 6 further patients in whom no toxicity occurred. The factors compared included; previous chemotherapy, known bone metastases of NET and the % spinal bone marrow at 24 hours post therapy as determined by brehmsstrahlung imaging.

Patient	Age	Sex	Diagnosis
BJ	77 years	Female	Carcinoid tumour ©
BE	62years	Female	Carcinoid tumour©
CK	67years	Female	Carcinoid tumour©
FB	65years	Male	Carcinoid tumour
HS	45years	Male	Carcinoid tumour©
SS	56years	Female	Carcinoid tumour©
HM	59years	Male	Carcinoid tumour©
ME	56years	Male	Carcinoid tumour©
LM	78years	Female	Medullary carcinoma thyroid
HR	62years	Male	Carcinoid tumour
VC	30years	Male	Carcinoid tumour
CS	54years	Female	Carcinoid tumour

Table 6.17 Patients with somatostatin receptor-positive neuroendocrine tumours (© patients with bone metastases)

6.5.2b Brehmsstrahlung imaging and analysis

All the patients had ^{90}Y-lanreotide whole-body brehmsstrahlung imaging 24 hours post therapy. All the images were acquired using the gamma camera, fitted with high-energy collimators, with a 75 keV photo-peak and 50% windows. The ^{90}Y-lanreotide (brehmsstrahlung) images were then used for the calculation of the bio-distribution of radiolabelled somatostatin in the bone marrow. Irregular regions of interest (ROI) were drawn manually, over the anterior whole body image over the bone marrow (spine). These regions were then stored and applied to the posterior image after "flipping" the images (Fig 6.11). The whole body activity was calculated using a geometric mean and then the geometric mean activity was calculated for the bone marrow, by counting the activity from the anterior and posterior images (Formula 6.1 and 6.2) (Table 6.17).

6.5.2a Blood tests

All the patients had regular blood tests for urea, creatinine, platelets and white blood cells (WBC) at 3months interval to assess their general well being and also to check their platelet counts prior therapy and post therapy. These laboratory values were obtained from March 2000 - December 2002.

6.5.3 Results

Urea: In the toxicity group 2 out of the 6 patients and in the non-toxicity group 2 out of the 6 patients had raised urea levels.

Serum creatinine: In the toxicity group 4 out of the 6 patients and in the non-toxicity group 1 out of the 6 patients had raised creatinine levels.

Platelets: In the toxicity group 6 out of the 6 patients had reduced platelet counts and in the non-toxicity group 1 out of the 6 patients had reduced platelet counts (Fig 6.12).

There was no difference in the mean % bone marrow activity at 24 hours (2.83% in toxicity versus 2.93% in control group). However 4 out 6 in the toxicity group had received prior chemotherapy compared with only 1 in the non-toxicity group. Likewise 5 out 6 with toxicity had bone metastases compared with 2 out 6 with no toxicity (Table 6.18)

Name	PLAT pre	PLAT post	Bone marrow counts % whole at 24 hours
BJ	369	18	2.5
BE	249	17	2.5
CK	84	84	2.2
FB	300	96	3.8
HS	236	77	2.3
SS	311	41	3.7
HM	228	134	2.2
ME	240	106	3.4
LM	290	191	2.5
HR	471	213	3.0
VC	398	402	3.3
CS	299	260	3.2

Table 6.18 Platelet count and the bone marrow activity of patients treated with ^{90}Y-lanreotide.
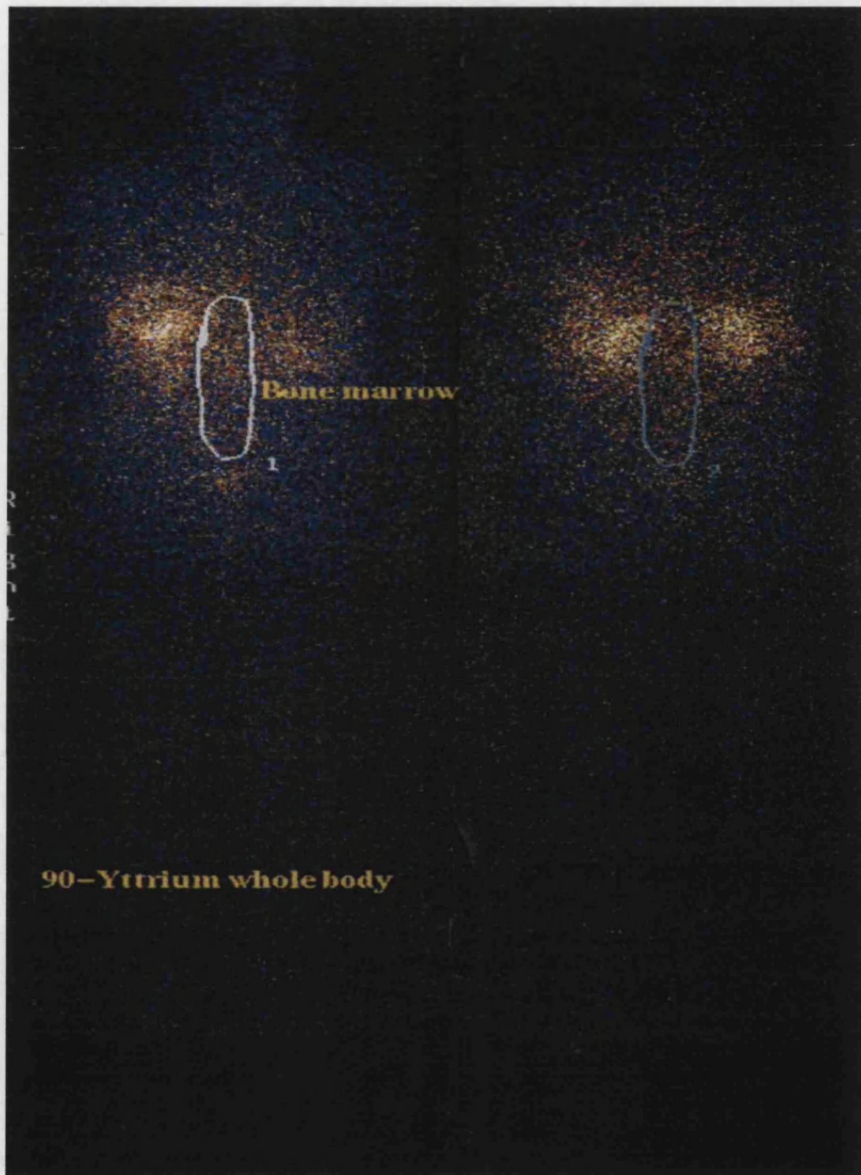
Fig 6.11 Bone marrow uptake was calculated by Geometric mean (by taking counts from the anterior and posterior images)
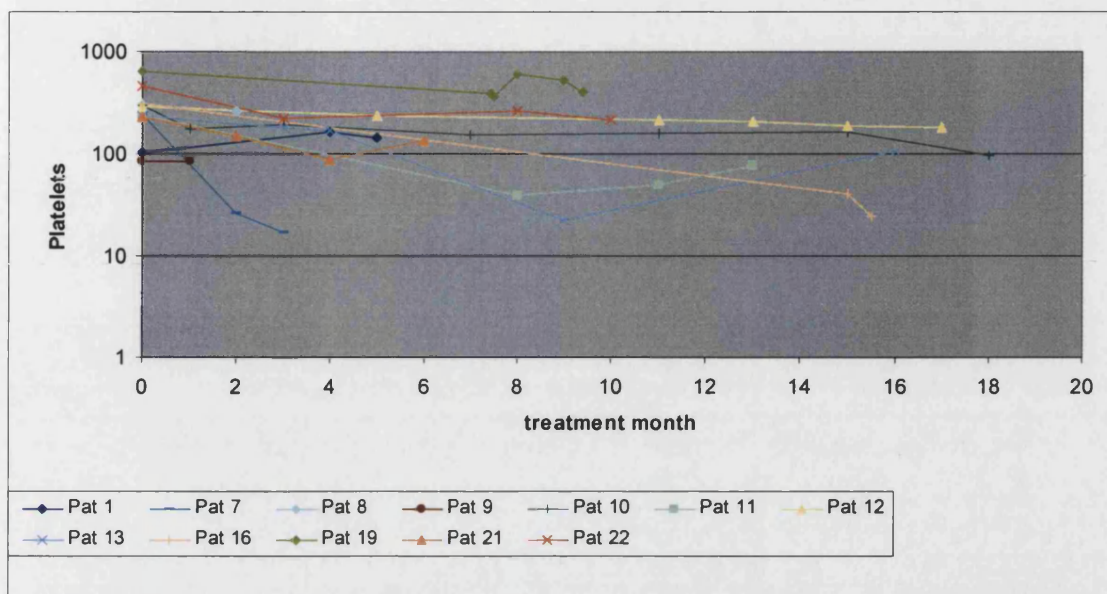
Fig 6.12 Graph showing the platelet counts for a period of 20 months in patients treated with ^{90}Y-lanreotide. [Patient 1(BJ), 7 (BE), 8 (CS), 9 (CK), 10 (FB), 11 (HS), 12 (LM), 13 (ME), 16 (SS), 19 (VC), 21 (HM), 22 (HR)].

6.6 Discussion

The results of this study show that there is a similar biodistribution of the three-Somatostatin analogues ^{111}In-pentetreotide, ^{90}Y-lanreotide and ^{90}Y-SMT. This is not surprising as the three molecules are similar with minor differences in their peptide chain. The differences, which were found, may however be clinically significant in that unlike ^{111}In-pentetreotide, ^{90}Y-lanreotide and ^{90}Y-SMT (with amino acid infusion) have much lower uptake in the kidneys. This is important, as the renal uptake of ^{90}Y labelled products is one of the dose-limiting factors (Virgolini *et al*, 2000; Waldherr *et al*, 2002; Virgolini *et al*, 2001; de Jong *et al*, 2002$_1$). For example it has been calculated that an activity of 4 GBq of ^{90}Y-DOTA octreotide, a ^{90}Y-labelled analogue of ^{111}In-pentetreotide, would give a radiation dose to the kidneys of about

30mSv, which is just below the accepted toxic dose. Despite this there has been evidence of toxicity in patients treated with this level of activity (Cybulla *et al*, 2001). Using a rough estimate of dosimetry based on the work of Cremonesi *et al* (1999) our data suggests that the radiation dose to the kidneys of 4 GBq of ^{90}Y-lanreotide would be about 40% of the radiation dose from ^{111}In-pentetreotide , (though this would have to be confirmed with more formal dosimetry). This would explain why, when using ^{90}Y-lanreotide for treatment, little toxicity has been seen in the kidneys and the dose limiting toxicity has tended to be within the bone marrow (Buscombe *et al*, 2001). Different somatostatin receptor subtypes have different affinities for the radioligand; variable tumour differentiation/receptor expression also influences biodistribution. Ideally one should have compared ^{111}In-lanreotide with 90Y-lanreotide, because biologically octreotide and lanreotide are different and the chelators used to label them are also different (Table 6.19).

It had been originally planned to use ^{111}In-labelled lanreotide to assess patients for therapy but it was found that the resulting product was highly unstable in-vitro resulting in rapid disassociation of the ^{111}In from the lanreotide (Croasdale, personal communication).

Octreotide	Lanreotide
Octreotide is a synthetic cyclic octapeptide, i. e. six of its eight amino acids are connected by a disulphide bond to form a ring	The structure of lanreotide is closely related to octreotide: having the same number of amino acids, but D-Phe is replaced by D-Naph, Phe by Tyr and Thr by Val.
Binds to somatostatin receptors 2 and 5 with high affinity, to receptor 2 with moderate affinity and does not bind to receptor 1 and 4	Binds to somatostatin receptors 2,3,4 and 5 with high affinity, to receptor 1 with lower affinity
Half-life of octreotide is approximately 1.7 hours. The effects of octreotide are variable but can last for up to 12 hours	Half-life of lanreotide is approximately 2.5 hours and mean residence time is around 0.68 hours.

Table 6.19 Difference between octreotide and lanreotide (Virgolini et al, 2002)

The group in Vienna and UK were able to label them (Virgolini *et al*, 1998, 2002, Britton *et al,* 2000).

Therefore, though not ideal, the role of the ^{111}In-pentetreotide was to demonstrate that a given tumour was receptor positive, allowing therapy. It would have been useful if this study had shown the same tumour uptake of ^{90}Y-lanreotide as seen in the ^{111}In-pentetreotide images, but the resolution of the brehmsstrahlung images was not sufficient for this to be achieved with present gamma camera systems and the activities which were used. We know that 40% of patients treated with ^{90}Y-lanreotide have some tumour response, implying that targeting not only occurs but also is sufficient to affect tumour outcome (Virgolini *et al*, 2002).

Another area of error in this experiment could be the use of manual region of interest (ROI) over the organs, which might introduce errors in the final values. The most common pitfall in drawing ROI are (a) Intra-observer variability (estimated position of the boundary of organs), (b) ROI could be over or underestimated as it is drawn over the brehmsstrahlung images where the images are not well defined, (c)When the organs are closely situated there is a possibility of overlapping of the ROI (example: ROI around Liver and the right kidney) , (d) Organ ROI over the brehmsstrahlung images are based on Indium-pentetreotide images, (e) Lighting arrangement in the processing/reconstruction room and (f) If we are taking two or three ROIs, in a similar region, the anatomical ROI may probably overlap the functional ROI.

Other areas of error in these calculations are that with brehmsstrahlung imaging several parameters are as yet unknown. The activity can be calculated from the counts recorded over the organ by drawing a region of interest (ROI), provided after correction for back ground and scatter attenuation have been applied. Finally if the

attenuation coefficients of the tissue traversed are known, an attenuation correction can be applied.

As the energies imaged in brehmsstrahlung imaging are so wide (unlike the discrete energies of the gamma emissions from isotopes such as ^{111}In), it is not possible accurately to identify a correction co-efficient for attenuation which could be used to obtain depth-corrected organ counts. Likewise, background subtraction may have a differing effect on the results for the two types of radiation. Due to all these difficulties quantitation was not performed as percentage of injected dose. Further phantom-based work is needed to determine how these issues may be resolved.

The main concern in ^{90}Y-labelled peptide therapy is renal toxicity. Traditionally methods to reduce renal radiation dose from ^{90}Y-labelled somatostatin analogues, such as ^{90}Y-SMT have included the use of amino-acid infusions before, during and after the infusion of the radiopeptide. In our experience this often causes severe nausea and vomiting which is resistant to most anti-nausea drugs. However, this strategy does reduce kidney radiation dose, allowing increased injected activities of ^{90}Y labelled somatostatin analogues to be used (Chinol et al, 2002). The expected reduction in renal activity of ^{90}Y labelled somatostatin analogues can be as great as 20-30% if such an amino acid infusion is used (Cremonesi et al, 1999; de Jong et al, 2002 [1]). To obtain this reduction nearly 60% of the patients had some unwanted symptoms such as severe nausea and vomiting. The results of this study with ^{90}Y-lanreotide suggest a different strategy which avoids the use of intravenous peptide infusions and that it may be possible to obtain a reduction in radiation dose to the kidneys with ^{90}Y labelled peptides by changing the design of the peptide and monitoring its biodistribution using techniques such as brehmsstrahlung imaging. For example, the bio-distribution results obtained from this study confirm the possibility

of delivering high doses of ^{90}Y-lantreotide for the treatment of neuroendocrine tumours with little or no renal toxicity.

In my study to determine if distribution of neuroendocrine tumours in the bone or of subsequent ^{90}Y-lanreotide predicts myelotoxicity, the principle finding is that patients with bone metastases or previous chemotherapy are prone to develop myelotoxicity, which was seen in all our 6 patients with bone metastases or previous chemotherapy.

Radionuclide therapy based on patient-specific dosimetry offers the potential for optimising the dose delivered to the target tumour through utilization of measured radiopharmaceutical kinetics specific to the individual. The administered activity may be tailored for the patient such that the highest possible radiation dose may be given to the tumour while limiting the dose to critical organs and tissues below any designated threshold for negative biological effects (Stabin et al, 1999). Usually pre-treatment quantitative dosimetry work-up using diagnostic ("tracer") activities of the therapy radiopharmaceutical serves to identify those cancer patients for whom the treatment is likely to be most effective while eliminating those for whom it would be unsuccessful. These considerations seem to be of particular importance in that the low uptake in tumour regions (low target to non-target uptake ratios) may constrain the treatment protocol (Erdi et al, 1996). For targeted radionuclide therapy, the level of activity to be administered is often determined from whole-body dosimetry performed on a pre-therapy tracer study. The largest potential source of error in this method is inconsistent or inaccurate activity retention measurements. It is also shown that any errors present in the dosimetry calculations following the tracer study will propagate to errors in predictions made for the therapy study according to the ratio of the respective effective half-lives (Stabin et al, 1999).

6.7 Conclusion

There is difference in biodistribution between ^{111}In-pentetreotide, ^{90}Y- lanreotide and ^{90}Y-SMT, as imaged with this method, especially in the kidneys, which may explain why there is minimal or no renal toxicity reported with ^{90} Y-lanreotide and ^{90}Y-SMT (with amino acid) therapies. Clinically, additional factors than just marrow dose (e.g., previous myelotoxic therapy, bone marrow involvement by metastatic malignancy) seem to affect the resulting myelotoxicity. If the use of brehmsstrahlung imaging can be refined, more truly quantitative measurements of uptake and retention may be possible leading to using these methods to determine dosimetry. However, even with these results it would appear possible to design radiolabeled peptides, which will have minimal renal activity and thus reduce the radiation dose to this critical organ.

Assessment of tumour volume in patients treated for Neuroendocrine Tumours

----

7.1 Introduction

Disseminated neuroendocrine tumours tend to present when there is disease within the liver, as this often leads to a characteristic and diagnostic endocrine syndrome such as carcinoid (Caplin *et al*, 1998). Patients with non-secreting neuroendocrine tumours may present with a mass effect of their tumour, resulting in symptoms such as portal vein blockage, ascites and liver failure. Chemotherapy generally is of little use in most of the neuroendocrine tumours with response rates of less than 15% (Kaltsas *et al*, 2002). There may, however, be better response rates in tumours of pancreatic and foregut origin where a combination of high dose 5FU and streptozocin can result in response rates of up to 50% (Cheng *et al*, 1999). As the diagnosis in most patients is only made after the disease has become advanced the aim of therapy becomes symptom control and not curative. Other forms of treatment are the use of radiotargeted therapy, for example with ^{131}I-mIBG or radiolabelled somatostatin analogues, which have been shown to improve symptoms in about 70-80% of patients (de Jong *et al*, 2002). However, only a small proportion of patients show any significant difference in tumour size as measured by CT (WHO or RECIST criteria) (Therasse *et al*, 2002). In addition to these systemic treatments, neuroendocrine tumours are generally hypervascular, so that trans-arterial embolisation can be used for the treatment of liver metastases. The effect of this can then be enhanced by the addition of chemotherapy or radionuclide agents (Schell *et al*, 2002). However, even when there is a clear reduction in symptoms, and endocrine markers such as 5-hydroxyindolacetic acid (5HIAA) production are reduced, CT imaging may fail to

show much change in tumour size (Schell *et al*, 2002). Therefore, though the size of the mass lesion remains unchanged, the amount of functional tumour may have decreased.

Tumour response following cancer therapy is traditionally evaluated with the help of clinical evaluation, tumour markers, conventional imaging (US, CT, MRI) (Fig 7.1) and also using nuclear medicine procedures (Planar, SPECT, PET) (Fig 7.2).

Tumour response assessment with conventional imaging modalities such as CT has its own problems. Tumour response after non-operative cancer therapy is usually evaluated by bi-dimensional measurement of maximum tumour diameters on computed tomography (CT) scans, based on the World Health Organization's (WHO) criteria (Miller *et al*, 1981) (Table 7.1). Assessment of response in irradiated tissue is sometimes assessed with difficulty, mostly due to the treatment-related fibrosis obscuring measured tumour and also due to displacement of tumour and normal structures caused by scarring (Table 7.2).

The recently proposed RECIST (Response Evaluation Criteria In Solid Tumours) (Therasse *et al*, 2000; Werner *et al*, 2001) raises the question whether a simple one-dimensional tumour measurement is equivalent to the more complicated bidimensional measurements with regard to tumour response assessment. RECIST is based on the assumption that "tumours are spherical and that responding patients have equivalent percentage reductions in the measures of length, width and depth of the tumour, which makes no difference in defining a partial response based on changes in largest dimension or the product of perpendicular diameters (Gehan *et al*, 2000).

An early non-invasive indicator of tumour response to therapy and the ability to predict clinical outcome may potentially enhance disease management. Currently, however, tumour response to therapy is often delayed, potentially compromising

disease management. Tumour response will be governed by repair, repopulation, reoxygenation and redistribution, as well as by mechanisms peculiar to targeted radiotherapy (Wessels *et al*, 2000). Tumour response assessment is very important because early change of treatment protocol to a more effective one may increase the period of failure-free survival and eventually cure. Early tumour response will also help us to change or modify the treatment before resistant or partially resistant clones become dominant.

Fortunately the majority of neuroendocrine tumours show uptake of [111]Indium (^{111}In) pentetreotide. Therefore it should be possible to assess the functional response to treatment by sequential ^{111}In-pentetreotide imaging.

	WHO	RECIST
Complete response (CR)	**Complete disappearance of whole disease**	**Complete resolution of all target lesions**
Partial response (PR)	**At least 50% reduction in tumour size**	**At least 30% reduction in tumour size**
No change (NC)	**Neither (PR) nor (PD)**	**Neither (PR) nor (PD)**
Progressive disease (PD)	**Greater than 25% increase in size of at least one lesion (or new lesion)**	**Greater than 20 % increase in size**

Table 7.1 CT criteria for tumour response (Miller *et al*, 1981; Therasse *et al*, 2000; Sohaib *et al*, 2000)

1. CT is not suitable for tumour response evaluation because it does not establish, the presence or absence of viable tumour in a mass

2. Even if CT shows that mass has regressed, it does not provide information about the presence of tumour cells that can cause relapse

3. Using the size of a mass as a criterion for response is questionable

4. Limited accuracy and reproducibility for small tumours (due to a combination of partial volume effect and measurement error)

5. 3D measurements are time consuming to perform

Table 7.2 Limitations of Tumour response assessment using CT scan (Sohaib *et al*, 2000)
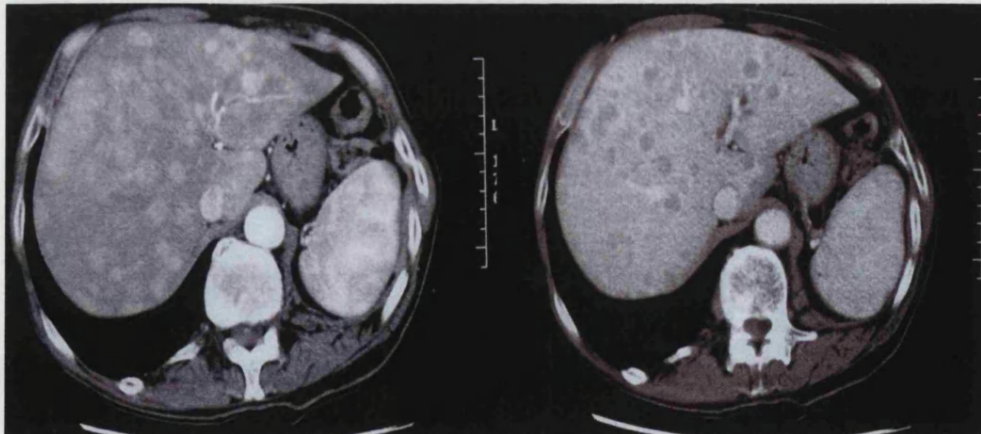
Fig 7.1 CT scan of abdomen in arterial phase (left), showing metastases in liver (paler areas) and CT scan of abdomen in venous phase, showing metastases in liver (darker areas) (Picture from Bax NDS *et al*)
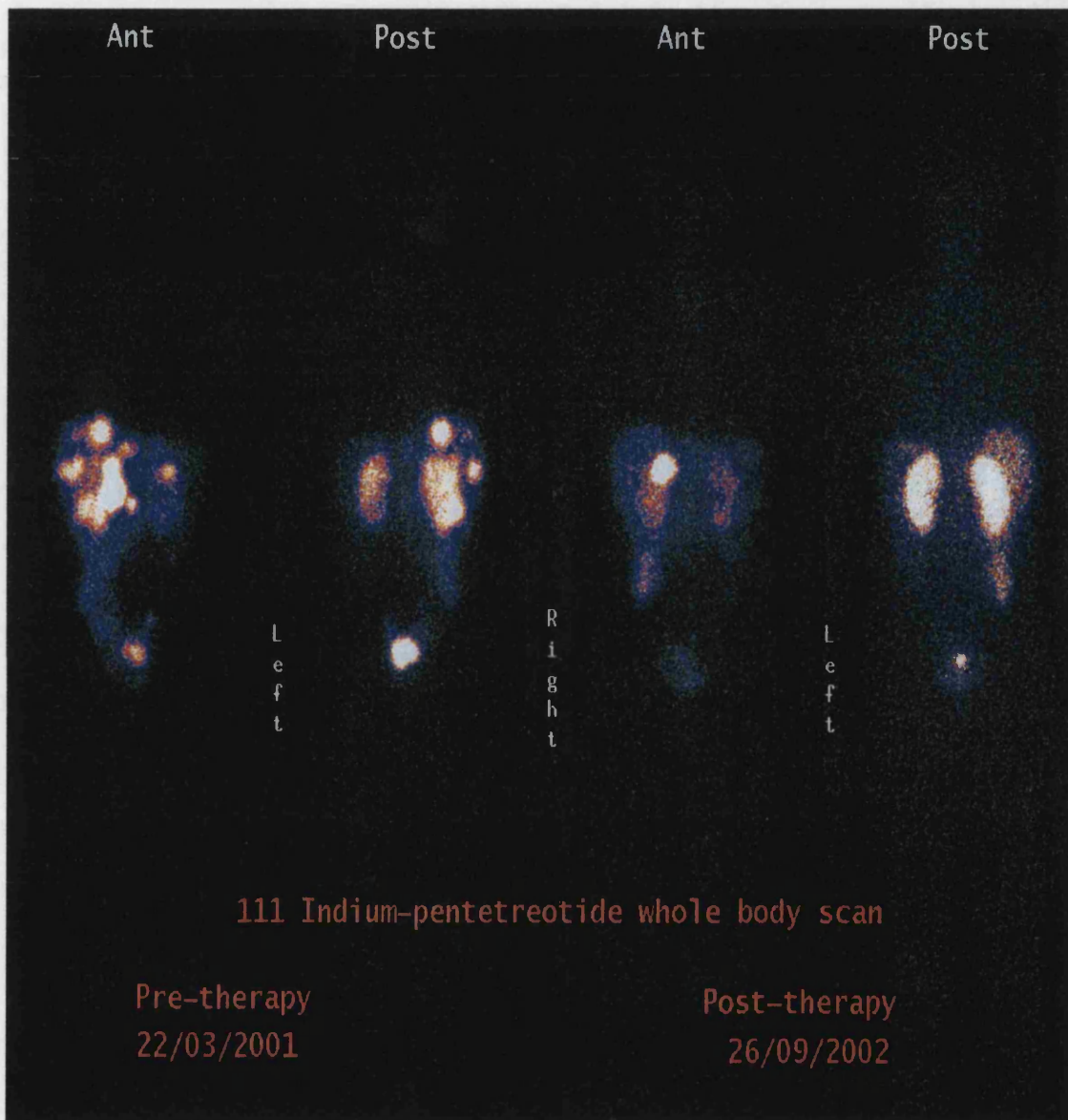
Fig 7.2 Example of use of ^{111}In-pentetreotide whole body images for tumour response assessment.

7.2 Experiment 1

7.2.1 Aim

The aim of this study was to develop a semi-quantitative method using ^{111}In-pentetreotide SPECT liver imaging to monitor change in functional activity using SPECT Tumour Volume (STV) and determine how this correlates with clinical response.

7.2.2 Material and methods

7.2.2a Inclusion criteria

A retrospective analysis was performed of the ^{111}In-pentetreotide imaging performed in 42 patients, 18 males and 24 females (Age: 30-80 years) with biopsy-proven neuroendocrine tumours in the liver. Imaging was performed within the 13 weeks prior to commencement of therapy and 13 months after the termination of that particular therapy usually after 6 cycles of chemotherapy or 3 cycles of radiotargeted therapy. The type of treatments used and tumour type are tabulated in Table 7.3. All patients had assessment of symptoms using a 10-point questionnaire, developed in-house and designed specifically for neuroendocrine tumours. This would include questions such as flushing, bowel function, wheezing and other neuroendocrine tumour related symptoms. General health was assessed using direct questioning and a self-administered symptom-grading questionnaire.

	Age in years /Sex	Tumour type	Treatment
WM	M/62	Carcinoid	Chemotherapy
RM	F/53	Carcinoid	Embolisation
WG	M/33	Carcinoid	Embolisation
JJ	F/47	Carcinoid	Embolisation
HC	M/75	Glucogonoma	Embolisation
CH	F/51	Carcinoid	Embolisation
HR	F/62	Carcinoid	Embolisation
DR	F/53	Carcinoid	Embolisation
SN	F/45	Carcinoid	Embolisation
CP	F/37	Carcinoid	Chemotherapy
FA	F/60	Carcinoid	Y-90 therapy
MH	M/55	Carcinoid	Chemotherapy
BB	F/51	Carcinoid	Embolisation
RC	M/58	Carcinoid	Embolisation
KM	F/72	Carcinoid	Y-90 therapy
SP	M/52	NET of unknown type	Chemotherapy
LE	F/65	Carcinoid	Chemotherapy
NR	M/47	Carcinoid	Chemotherapy
LP	F/67	Carcinoid	Chemotherapy
TW	F/53	Carcinoid	Chemotherapy
TA	M/73	Carcinoid	Chemotherapy
PM	F/48	Carcinoid	Chemotherapy
AS	M/71	NET of unknown type	Embolisation
LH	M/68	Carcinoid	Embolisation
BP	M/62	Carcinoid	Embolisation
GC	F/49	Carcinoid	Embolisation
PB	M/63	Carcinoid	Embolisation
SO	M/40	NET of unknown type	Embolisation
EK	F/45	Carcinoid	Chemotherapy
SS	M/78	Carcinoid	Chemotherapy
DE	F/59	Gastrinoma	Chemotherapy
CC	F/30	NET of unknown type	Chemotherapy
PT	F/63	Carcinoid	Chemotherapy
BH	F/69	Carcinoid	Chemotherapy
PH	M/80	Carcinoid	Chemotherapy
AR	M/60	Insulinoma	Chemotherapy
WD	F/41	Carcinoid	Embolisation
BS	F/43	Carcinoid	Chemotherapy
CS	M/38	Carcinoid	Chemotherapy
RL	F/40	Gastrinoma	Chemotherapy
PY	M/53	Carcinoid	Chemotherapy
LN	F/42	Carcinoid	Chemotherapy

Table 7.3 List of patients with tumour type and the type of treatments used.

7.2.2b ^{111}Indium pentetreotide imaging

The ^{111}In-pentetreotide images were acquired on a Prism 2000XP gamma camera (Picker International, Inc. Cleveland Ohio, USA), interfaced to a Odyssey FX computer. The liver SPECT images were acquired 24 hours after intravenous injection of 120 MBq ^{111}In- pentetreotide (Tyco Healthcare, Gosport UK), using a two headed gamma camera equipped with medium-energy general- purpose collimators (MEGP) (Table 7.4). The ^{111}In pentetreotide SPECT images of the liver were obtained with a 360 degrees circular orbit, 64 projections, 64 x 64 matrix, and peak energies of 170 + 250 keV with 15% windows. Attenuation correction was not applied. The functional STV was calculated from the transverse SPECT images (Fig 7.3). Each SPECT slice was displayed using a 10-point scale (Fig 7.4). When drawing tumour regions of interest, care was taken to exclude activity in normal structures such as spleen, kidneys and large bowel. The area of the neuroendocrine tumour with maximum activity was set at 100% and then irregular regions of interest drawn around all the tumours in every size expressing 50% or more of the maximum tumour activity as assessed using the 10-point colour scale. The total functional STV was then calculated by summing the number of pixels within the regions of interest drawn around tumour in each of the slices in which tumour occurred and multiplying this total by the slice thickness of 0.93cm (resulting in each voxel having a volume of 0.93cm x 0.93cm x 0.93cm = 0.804cm^3).

Study	SPECT imaging
Radiopharmaceutical	[111] In- pentetreotide
Activity administered	120 MBq
Patient preparation	None
Patient positioning	Supine, arms to side using the arm rest
Collimator	Medium energy general purpose
Peak energies	170 + 250 keV with 15% window
Orbit, Projection and Matrix	360^0 cicular, 64 projections, 64 x 64 matrix

----

Table 7.4 SPECT imaging protocol at the Royal Free Hospital
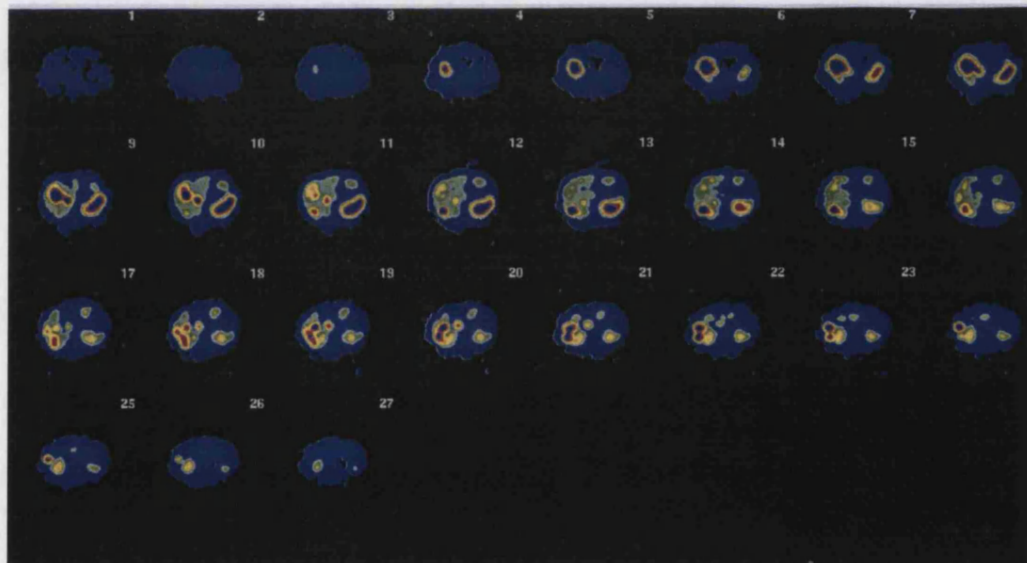
Fig 7.3 Transverse SPECT slices of liver display the tumour activity
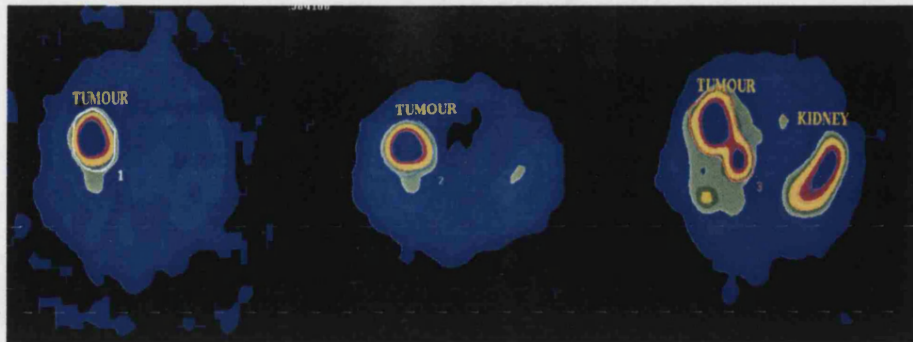
Fig 7.4 Three consecutive SPECT slices in phase display the regions of interest (ROI) s are drawn around the uptake outside of normal physiological uptake with is >50% maximum tumour activity

7.2.2c CT scan

Triple phase spiral CT scans with 5mm slicing of liver and upper abdomen were acquired after rapid intravenous administration of a low-ionic contrast medium. CT scans were performed in all the patients within 3 months pre-treatment and within 6 months post-treatment. CT scans were read by experienced cross-sectional radiologists and reported as regression, stable or progressive disease using RECIST criteria of response (Tsuchida *et al*, 2001; Padhani *et al*, 2001).

7.2.2d Clinical Evaluation

The clinical outcome of the patients was assessed in terms of symptomatic improvement, using the questionnaires described shown in appendix 1. Also any change in analgesia usage was assessed. Regular (4-6 week) physical examination was also performed to determine if there was any change of liver size on palpation and the presence, absence or change in volume of ascites was noted. A significant change in the patient's symptoms was taken as the prime determinant of response, with the other data providing secondary support data. When there was a disagreement

between symptomatology and other data the patient's own assessment of their well-being was paramount.

7.2.3 Results

There was a good correlation when the total functional STV was compared with clinical response (Table 7.5). In total, 22 patients had a good clinical response, including 11 patients who received chemotherapy, 9 who had embolisation and 2 patients received ^{90}Y-lanreotide infusions. The smallest change in total functional STV in this group of responders was a 1% reduction; the largest measured was a drop of 126%. The mean fall was 37%; of those with symptomatic relief, a drop of 10% or more was seen in 18 patients and a fall of 25% or greater in 12 patients. Of the 20 patients with no clinical response, 12 had received chemotherapy and 8 embolisation. All patients with a worsening clinical evaluation had an increase in total functional STV of between 3 % - 254% with a mean increase in total functional volume of 72 %. A change of 25% or greater increase in total functional STV was seen in 12 of these patients, and an increase of 10% or more was seen in all 16 of the patients.

Changes in CT, as assessed by the RECIST criteria, did not correlate well with changes in clinical outcome. Of the 22 patients with good response, CT showed a significant size reduction in 8 patients, no change in the remaining 13 patients and increased in one patient. In 4 of these patients there was also no change in total functional STV. In the 20 patients in whom there was no clinical response or in whom clinical symptoms worsened, the CT showed an increase in tumour size in 7 patients, no change in 12 and it was reduced in one, though in this patient the total functional STV increased by 61%. In total the CT was able to predict response in only 21 (50%) patients (Fig 7.5a, 7.5b, 7.6).

Patient	Treatment	Tumour volume	CT scans	Clinical evaluation	CT/STV Concordance	Symptoms/ STV Concordance	CT/ symptoms Concordance
1 WM	Chemotherapy	⟺ 8%	No change	Better	YES	NO	NO
2 RM	Embolisation	⇑ 61%	Reduction	Worse	NO	YES	NO
3 WG	Embolisation	⇑ 65%	Increased	Worse	YES	YES	YES
4 JJ	Embolisation	⇓ 13%	Reduction	Better	YES	YES	YES
5 HC	Embolisation	⟺ 1%	No change	Better	YES	NO	NO
6 CH	Embolisation	⇑ 13%	No change	Worse*	NO	YES	NO
7 HR	Embolisation	⇓ 10%	Reduction	Better	YES	YES	YES
8 DR	Embolisation	⇓ 52%	Reduction	Better	YES	YES	YES
9 SN	Embolisation	⟺ 7%	No change	Better	YES	NO	NO
10 CP	Chemotherapy	⇑ 77%	Increased	Worse	YES	YES	YES
11 FA	Y-90 therapy	⇓ 52%	No change	Better	NO	YES	NO
12 MH	Chemotherapy	⇓ 48%	Reduction	Better	YES	YES	YES
13 BB	Embolisation	⇓ 39%	No change	Better	NO	YES	NO
14 RC	Embolisation	⇑ 58%	No change	Worse	NO	YES	NO
15 KM	Y-90 therapy	⟺ 8%	No change	Better	YES	NO	NO
16 SP	Chemotherapy	⇑ 145%	Increased	Worse	YES	YES	YES
17 LE	Chemotherapy	⇓ 39%	Reduction	Better	YES	YES	YES
18 NR	Chemotherapy	⇑ 103%	No change	Worse	NO	YES	NO
19 LP	Chemotherapy	⇑ 254%	No change	Worse	NO	YES	NO
20 TO	Chemotherapy	⇓ 18%	No change	Better	NO	YES	NO
21 TA	Chemotherapy	⇓ 46%	Reduction	Better	YES	YES	YES
22 PM	Chemotherapy	⇓ 16%	No change	Better	NO	YES	NO
23 AS	Embolisation	⇓60%	No change	Better	NO	YES	NO
24 LH	Embolisation	⇑41%	No change	Worse	NO	YES	NO
25 BP	Embolisation	⇑45%	Increased	Worse	YES	YES	YES
26 GC	Embolisation	⇑22%	No change	No change	NO	NO	YES
27 PB	Embolisation	⇓35%	No change	Better	NO	YES	NO
28 SO	Embolisation	⟺3%	No change	No change	YES	YES	YES
29 EK	Chemotherapy	⇓17%	Increased	Better	NO	YES	NO
30 SS	Chemotherapy	⇑209%	Increased	worse	YES	YES	YES
31 DE	Chemotherapy	⇓22%	No change	Better	NO	YES	NO
32 CC	Chemotherapy	⟺10%	No change	No change	YES	YES	YES
33 PT	Chemotherapy	⇑50%	Increased	Worse	YES	YES	YES
34 BH	Chemotherapy	⇓80%	Reduction	Better	YES	YES	YES
35 PH	Chemotherapy	⇑22%	No change	No change	YES	NO	YES
36 AR	Chemotherapy	⇓43%	Reduction	Better	YES	YES	YES
37 WD	Embolisation	⇓126%	No change	Better	NO	YES	NO
38 BS	Chemotherapy	⇓25%	No change	No change	NO	NO	YES
39 CS	Chemotherapy	⇓85%	No change	Better	NO	YES	NO
40 RL	Chemotherapy	⇑185%	Increased	Worse	NO	YES	NO
41 PY	Chemotherapy	⇓46%	No change	No change	NO	NO	YES
42 LN	Chemotherapy	⟺3%	No change	No change	YES	YES	YES

Table7.5 Summary of results of CT, ^{111}In pentetreotide SPECT and clinical response in patients treated for disseminated neuroendocrine tumour (⇓=reduced, ⇑=increased, ⟺=stable/no change) *Died.
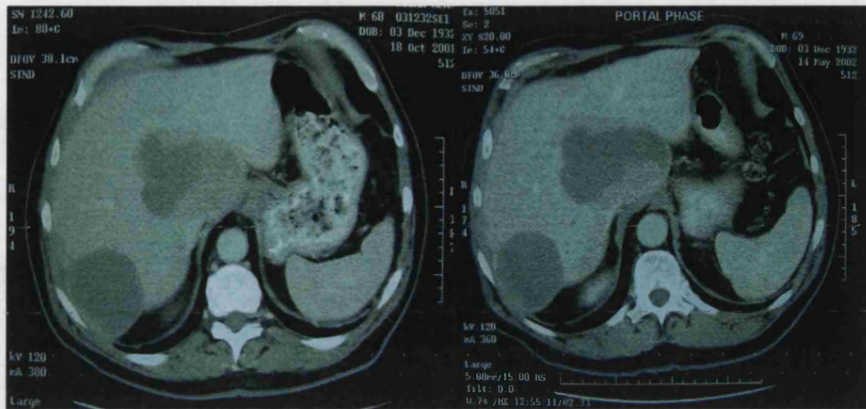
Fig 7.5a CT image of patient pre chemo-embolisation, note the dark areas are necrotic tissue and not tumour, which cannot be clearly seen. Post therapy (Fig 7.5b) there appears to be an extension of the necrotic area but it is still difficult to see the tumour
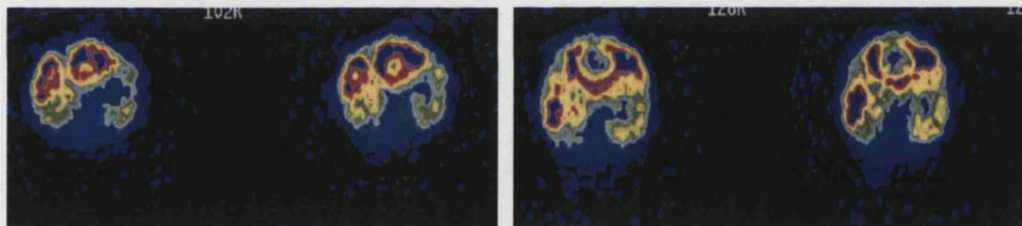
7.6a   **7.6b**

Fig 7.6a ^{111}In-pentetreotide SPECT image of the same patient with the liver tumour delineated in both lobes of the liver (before therapy), (Fig 7.6b) after therapy there has been significant reduction in the functioning tissue.

7.3 Experiment 2

7.3.1 Aim

The aim of this study was to assess the change in functional SPECT tumour volume (STV) using ^{111}In-pentetreotide SPECT in foregut neuroendocrine patients treated with chemotherapy or chemoembolisation.

7.3.2 Material and methods

7.3.2a Inclusion criteria

30 patients with liver tumours in the liver were treated with chemoembolisation (15 patients) and chemotherapy with Streptozocin (15 patients). Patients from both the groups had ^{111}In-pentereotide SPECT pre and post treatment. The type of treatments used is tabulated in Table 7.6

Name	Chemotherapy	Name	Chemoembolisation
MH	Chemotherapy	GW	Chemoembolisation
SS	Chemotherapy	LH	Chemoembolisation
PC	Chemotherapy	HC	Chemoembolisation
PT	Chemotherapy	HC	Chemoembolisation
PH	Chemotherapy	HR	Chemoembolisation
DE	Chemotherapy	SN	Chemoembolisation
EK	Chemotherapy	RH	Chemoembolisation
CM	Chemotherapy	GC	Chemoembolisation
CC	Chemotherapy	JJ	Chemoembolisation
AR	Chemotherapy	BP	Chemoembolisation
MW	Chemotherapy	BB	Chemoembolisation
WM	Chemotherapy	DR	Chemoembolisation
BH	Chemotherapy	RD	Chemoembolisation
PY	Chemotherapy	RC	Chemoembolisation
WG	Chemotherapy	AS	Chemoembolisation

Table 7.6 Type of treatments used in the 30 patients

7.3.2b ^{111}Indium pentetreotide imaging

The ^{111}In-pentetreotide images were acquired on a Prism 2000XP gamma camera (Picker International, Inc. Cleveland Ohio, USA), interfaced to Odyssey FX computer. The liver SPECT images were acquired 24 hours after intravenous injection of 120 MBq ^{111}In- pentetreotide (Tyco Healthcare, Gosport UK), using a two headed gamma camera equipped with medium-energy general- purpose collimators (MEGP) (Table 7.7). The ^{111}In pentetreotide SPECT images of the liver were obtained with a 360 degrees circular orbit, 64 projections, 64 x 64 matrix, and peak energies of 170 + 250 keV with 15% window. Attenuation correction was not applied. The functional STV was calculated from the transverse SPECT images (Fig 7.3). Each SPECT slice was displayed using a 10-point display. When drawing tumour regions of interest, care was taken to exclude activity in normal structures such as spleen, kidneys and large bowel. The area of the neuroendocrine tumour with the maximum activity was set at 100% and then irregular regions of interest drawn around all the tumours in every size expressing 50% or more of the maximum tumour activity as assessed using the 10-point colour display. The total functional STV was then calculated by adding the number of pixels within the regions of interest drawn around the tumour seen in each of the slices in which tumour occurred and multiplying this total by the slice thickness of 0.93cm (resulting in each voxel having a volume of 0.93cm x 0.93cm x 0.93cm = 0.804cm^3).

Study	SPECT imaging
Radiopharmaceutical	^{111}In-pentetreotide
Activity administered	120 MBq
Patient preparation	None
Patient positioning	Supine, arms to side using the arm rest
Collimator	Medium energy general purpose
Peak energies	170 + 250 keV with 15% window
Orbit, Projection and Matrix	360^{0} circular, 64 projections, 64 x 64 matrix

Table 7.7 SPECT imaging protocol at the Royal Free Hospital

7.3.3 Results

In patients who had chemotherapy, functional STV increased in 7 patients (mean increase 141%), it decreased in 6 patients (mean decrease 71%) and remained unchanged in 2 patients. In patients who had chemoembolisation, functional STV increased in 3 patients (mean increase 40%), decreased in 7 patients (mean decrease 42%) (Fig 7.7) and remained unchanged in 5 patients. The percentages difference in increase and decrease between the two groups was 84% and 37% respectively. Patients treated with chemoembolisation had better response rates than those treated with chemotherapy ($p<0.05$) (Fig 7.8 and Table 7.8).
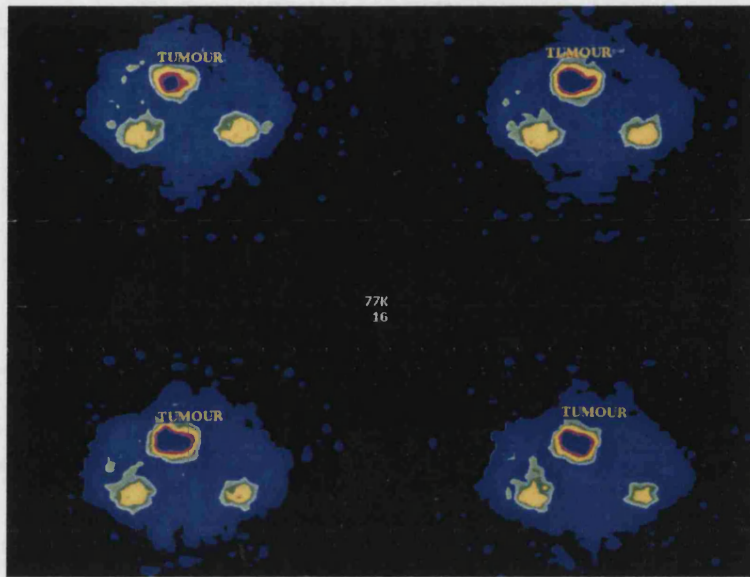
A. Pre-treatment (tumour in the liver)
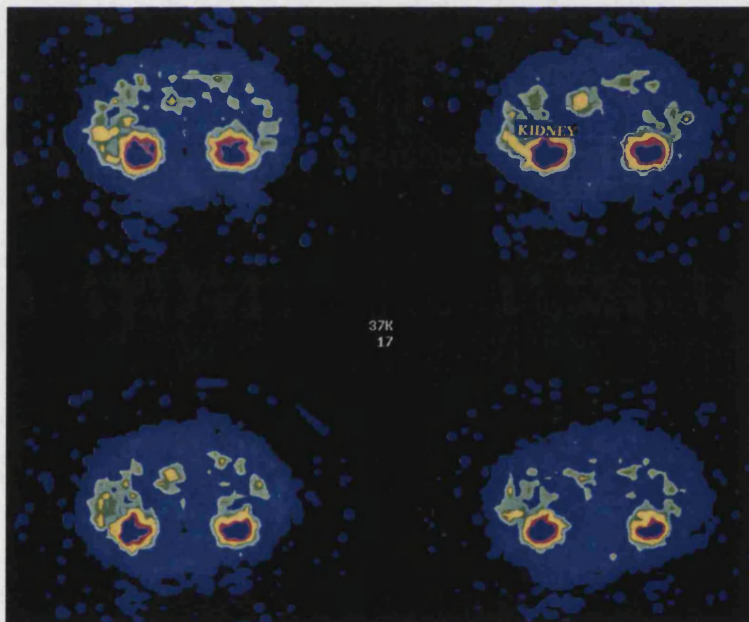
B. Post treatment (absence of tumour)

Fig 7.7A and B Transverse SPECT images showing a patient with tumour in the liver pre chemoembolisation and absence of tumour post chemoembolisation.

Name	Chemo	Name	C-embo
MH	481%	GW	65%
SS	209%	LH	41%
PC	189%	HC	13%
PT	50%	HR	<10%
PH	22%	CH	<10%
DE	22%	SN	<10%
EK	17%	RH	<10%
CM	<10%	GC	<10%
CC	<10%	JJ	-13%
AR	-43%	BP	-20%
MW	-53%	BB	-39%
WM	-71%	DR	-51%
BH	-80%	RD	-52%
PY	-82%	RC	-58%
WG	-95%	AS	-60%

Table 7.8 Change in functional SPECT tumour volume in patients treated with chemotherapy and chemoembolisation.
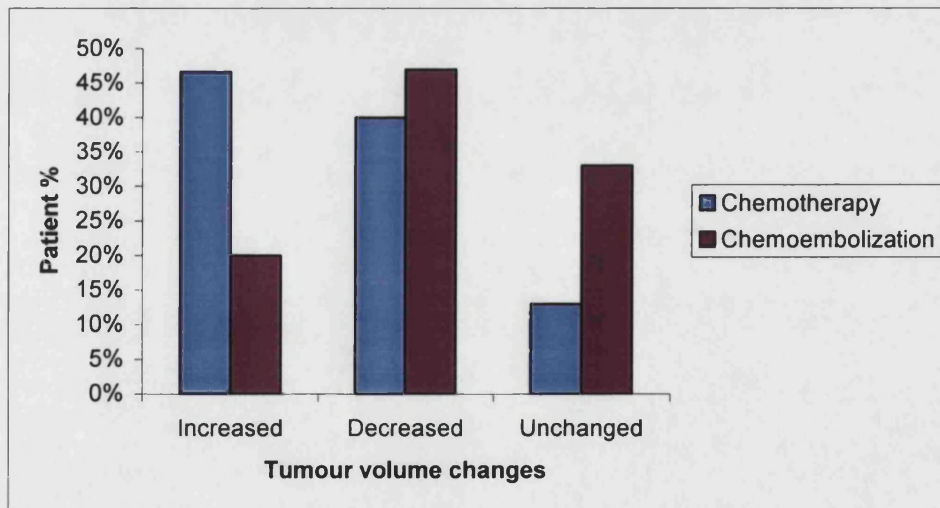
Fig 7.8 Percentage change in functional STV in patients with foregut neuroendocrine tumour treated with chemotherapy and chemoembolisation.

7.4 Discussion

In this study we could see a correlation between changes in functional STV and clinical response. However, we must accept that much of the data used to determine whether clinical response had occurred depended on the subjective reporting of the patient, which leaves the results open to a degree of bias. However, as the aim of treatment was tumour control and palliation, there is some validity in using the patient's assessment of their own disease as the prime assessment of clinical response. There is some evidence for this in that 9 patients, who had no change in CT, reported an improvement in symptoms and showed a fall in total functional STV. It appears, therefore, that the anatomical measurement of lesions using CT is a very poor predictor of clinical response. This is not unknown in patients with advanced disease where changes in CT have not reflected clinical response (Kimura *et al*, 2002). It may also be argued that we should only have assessed patients who received a single type of treatment (for example chemotherapy). However, this did not reflect our clinical practice and we felt it was important to test response to a variety of treatments. Further studies can be performed to assess the utility of functional volumes for a particular treatment modality, but early examination of this data suggest that treatment type was not a factor in deciding response in the clinical evaluation or total functional STV. It was also felt that we needed to have an approach that would be robust enough to be used without reference to the patient's treatment. We did note, however, that there was some discordance in patients receiving chemotherapy in that functional STV reduction was not followed by a clinical improvement. This could be due to the high levels of morbidity associated with this form of therapy (Rougier *et al*, 2000). The idea of functional response is not new and has been used widely in PET in a series of tumours (Sakamoto *et al*, 1998). This, however, is a first attempt to devise a

simplified but reproducible method that can be used with SPECT. Possible errors include the use of 50% of highest activity of the tumour, which may change between scans, and the effect of the non-homogenous uptake of ^{111}In-pentetreotide in normal liver. It would be difficult to determine a more accurate method as the use of a reference area such as the kidney or spleen might be affected by chemotherapy. To obtain more accurate results, it would be necessary to use an approach based on methods of absolute quantification or some measures of relative uptake (Sakamoto *et al*, 1998). Unfortunately, many of these tumours do not take up ^{18}F-FDG and alternative tracers need be sought (Orlefors *et al*, 1998). The optimal time interval between completion of therapy and performance of such measurements is not well defined. Finally even if we are using the commonly used Standardised uptake value (SUV) to assess the tumour response, there are numerous factors affecting the quantitative PET scan SUV like body composition, length of uptake period, recent physical activity, plasma glucose and insulin levels, renal function. These factors are also important for precise and accurate comparison of serial SUV's (Hunter *et al*, 1996; Hamberg *et al*, 1994).

Despite these shortcomings, this simplified method of measuring the functional STV has a better correlation with clinical symptomology in patients with neuroendocrine tumours than traditional dependence on CT measures alone.

What is clear is that an increase in functional STV which may be as great as 254% had a close correlation with a worsening clinical picture even though only 7/20 (35%) of these patients had an increase in tumour size on CT suggesting that tumour function may be the deciding factor in well being and symptomology in these patients.

The validation of the functional volume of the tumour was difficult as the study was performed within a tertiary referral centre. It was not possible to review CT scans performed on different machines with different protocols in a consistent way. It may be possible to consider this at a later stage where a standard CT protocol is used at a single centre.

In our second study, using only the functional STV, we compared the outcome in patients treated with chemotherapy and chemoembolisation for foregut neuroendocrine tumours.

Traditionally, patients with foregut neuroendocrine tumours seem to have good response to chemotherapy. However in our study we noted that those treated with chemoembolisation responded better (stable/improvement), in comparison to chemotherapy. To compare and confirm the clinical outcome in patients treated with chemotherapy and chemoembolisation more number of foregut tumour patients should be assessed.

7.5 Conclusion

Quantitative analysis is important in tumour imaging and treatment. The assessment of functional STV is more useful in monitoring the tumour response after treatment than CT. The changes in functional volumes after therapy correlate well with clinical response. It is a simplified technique which is clinically feasible and requires no extra effort or cost. Semi quantitative STV appears to provide information on treatment in a more reliable way than CT and this simplified method have a promising role in clinical use.

Chapter 8

Discussion

During the last decade our knowledge and understanding of neuroendocrine tumours has increased. There has been a considerable advance in the treatment of neuroendocrine tumours. The contribution of nuclear medicine towards diagnosis and treatment is commendable. One of the key challenges in targeted radionuclide therapy is to optimise drug administration and determine in advance which patients will benefit most. The assessment of biodistribution of the radiopharmaceutical could help us to characterise its distribution to the tumour and normal organs.

In my experiments there was no optimal window/photo peak for images; however in terms of uniformity of response, imaging using a HEGP collimator with an energy window centred at 75keV and a 60% window appears to be optimal. There is an argument for using a phantom with hot lesions instead of cold lesions to assess uniformity and contrast. However during my initial experiments (Gnanasegaran, 2001), I was unclear about the discharging structure of the scatter; therefore I wanted to eliminate the sources of scatter within the lesion.

In practice lesion detectability depends on spatial resolution, uniformity and the relative distribution of target and the background. It could be argued that it is irrelevant whether the relative distribution is positive (hot lesions) or negative (cold lesions). In general the spatial resolution, uniformity and the relative distribution of target to background is adequate, then it should be able to detect positive and negative distribution. However in nuclear medicine as we commonly perform hot-spot imaging, further phantom experiments with positive (hot) lesions could be performed.

To apply these methods clinically, a more realistic model for localised variations of brehmsstrahlung generation in tissue and for related photon transport mechanisms is required. Even then evaluation of radiation dosimetry could be difficult as it lacks a primary photon emission.

The results of the study in Chapter 6 show that there is a similar biodistribution of the three-Somatostatin analogues ^{111}In-pentetreotide, ^{90}Y-lanreotide and ^{90}Y-SMT. ^{90}Y brehmsstrahlung imaging detected lower uptake of lanreotide and ^{90}Y-lanreotide and ^{90}Y-SMT (with amino acid infusion) in the kidneys. This is interesting and important because renal activity of ^{90}Y labelled products is one of the dose-limiting factors (Virgolini *et al*, 2000; Waldherr *et al* 2002; Virgolini *et al*, 2001). This would explain why, when using ^{90}Y-lanreotide for treatment, little toxicity has been seen in the kidneys and the dose limiting toxicity has tended to be within the bone marrow (Buscombe *et al*, 2001).

Even though I was unable to perform formal dosimetry of these three compounds. I could satisfactorily determine the targeting (localisation) of the radioloabelled somatostatin analogues at the tumour sites, which gave us the confidence and proof that we are targeting the right organ or site. The results could have been more realistic if I had performed the experiments comparing ^{111}In-lanreotide with 90Y-lanreotide, because biologically octreotide and lanreotide are different and the chelators used to label them are also different.

In my study to determine bone marrow toxicity using brehmsstrahlung images. The patients with bone metastases or previous chemotherapy are at risk for myelotoxicity, which was seen in all 6 patients in this category, but I was unable to predict the bone marrow toxicity using brehmsstrahlung images. There may be other areas of error in

these calculations, as with brehmsstrahlung imaging several parameters are as yet less

understood and unknown or it may not be related only to bone marrow radiation dose.

An early non-invasive indicator of tumour response to therapy and the ability to

predict clinical outcome may potentially enhance disease management. Accurate and

reproducible measurements on images are needed for evaluating tumour response to

therapy in clinical practice. The idea of functional response is not new and has been

used widely with PET in a series of tumours (Sakamoto *et al*, 1998). Currently,

however, tumour response to therapy is often delayed, potentially compromising

disease management. In this study (chapter 7) I devised a simplified, reproducible and

cost-effective technique to assess the tumour response using the functional SPECT

tumour volume (STV). There was a good correlation when the total functional STV

was compared with clinical response. STV predicted the clinical outcome in 34/42

patients (81%) and CT predicted the outcome in 21/42 (50%) patients.

I proceeded to assess patients with foregut neuroendocrine tumours who were treated

with chemotherapy and chemoembolisation, and my results showed that people

treated with chemoembolisation fared better than the chemotherapy group. Presently

this technique can be applied to assess treatment responses and it is less time-

consuming and easy to perform compared to the existing modalities like CT which

has many limitations.

Significant technological advances have taken place in CT. Hypervascular neoplasm's

like carcinoids and other tumours are difficult to image by conventional CT because

they are iso-dense to the liver during peak hepatic enhancement. The liver normally

receives approximately 80% of its blood supply from the portal venous circulation.

After rapid administration of intravenous contrast material, the major abdominal

arteries (including the celiac axis and its branches) enhance rapidly, after

approximately 20 seconds. Subsequently, at approximately 40 seconds, the portal venous system becomes opacified, and peak liver enhancement occurs at 60 to 100 seconds (Baron, 1994 [1, 2]; Krasny et al, 1996), later than most other visceral organs because of the slower portal venous circulation. Most hepatic neoplasm's, being fed by the hepatic arterial blood supply, appear hypo-dense to the liver after contrast administration, and are most conspicuous during peak liver enhancement, at 60 to 100 seconds. Within a few minutes after contrast material infusion, most hepatic lesions have reached an equilibrium state of contrast enhancement with the surrounding liver and may be rendered invisible. Conventional CT therefore, because it requires 90 to 120 seconds to cover the entire liver, is suboptimal for lesion detection (Krasny et al, 1996). With the advent of rapid Helical CT, volumetric acquisition of image can be performed. There are several reports that structures with different peak contrast enhancement, such as liver and pancreas may be imaged more accurately during their optimal enhancement time windows (Krasny et al, 1996). Helical CT may be more useful for their detection with a two-phase scanning protocol, where an additional set of images is acquired through the liver during the early arterial phase. This technique allows visualization of tumour arterial enhancement before the liver itself is significantly enhanced (Baron, 1994). Despite the technologic advances of helical CT, it is important to understand that not all clinical applications can take advantage of the additional capability the technique offers. Current limitations of spiral technology include x-ray tube heating constraints, markedly increased demand on computing power and memory capacity, and the absolute dependence on a patient's ability to breath hold in order to take full advantage of the helical data (Krasny et al, 1996). Functional SPECT tumour volume (STV) does not face all these dilemmas, with respect to contrast and organ enhancement time etc. However possible errors include

the use of 50% of highest activity of the tumour, which may change between scans, the effect of the non-homogenous uptake of ^{111}In-penetetreotide in normal liver. It would be difficult to determine a more accurate method, as the use of a reference area such as the kidney or spleen might be affected by chemotherapy.

Although assessment of tumour response is extremely helpful in determining the best form of treatment, the responsibility for critical judgment and execution rests with the clinician in-charge to treat patients effectively, No computer software can correct the clinician's errors of clinical judgment, misunderstanding of physical concepts, or inadequate treatment delivery.

In the past and present there have been misconceptions about the role of nuclear medicine in neuroendocrine tumours, but despite all these challenges, radionuclide imaging and targeted radionuclide therapy in nuclear medicine is still a useful option. We should refocus to use the simpler available techniques more effectively to make the benefits noticeable. What we clearly need is newer techniques with increasing specificity without loosing sensitivity. These newer modalities should contribute not only towards diagnosis but also in staging, follow up and assessing tumour response at a very early stage. Because of the relative rarity of neuroendocrine tumours it is important to conduct prospective trials for the various forms of treatment.

Conclusion

- ^{90}Y brehmsstrahlung imaging is a useful technique for assessing the biodistribution of ^{90}Y labelled somatostatin analogues. The ^{90}Y brehmsstrahlung imaging was not precise enough for accurate dosimetry and also in determining toxicity on a patient by patient basis.

- Functional SPECT tumour volume (STV) is a useful technique to monitor and evaluate the treatment response in patients with neuroendocrine tumours. The assessment does not involve an extra scan, radiation burden or cost. Presently this technique is limited to the neuroendocrine tumour metastases in liver.

- Functional SPECT tumour volume (STV) is useful in the assessment of efficacy of various treatment modalities.

Finally, the effective treatment of patient with neuroendocrine tumours involves an integrated approach from clinicians, laboratory and imaging results (Fig 9.1). This in turn will help us in selecting effective treatment strategies. The treating team should not only have clear insights into the benefits and limitations of all the available therapeutic modalities, but must also have a clear understanding of the molecular or sub-cellular aspects of the disease process. Using brehmsstrahlung imaging for the assessment of biodistribution of radiolabelled somatostatin analogues and using ^{111}In-pentetreotide imaging to assess the functional SPECT tumour volume will help us in better understanding of conventional and targeted radionuclide therapy in neuroendocrine tumours.
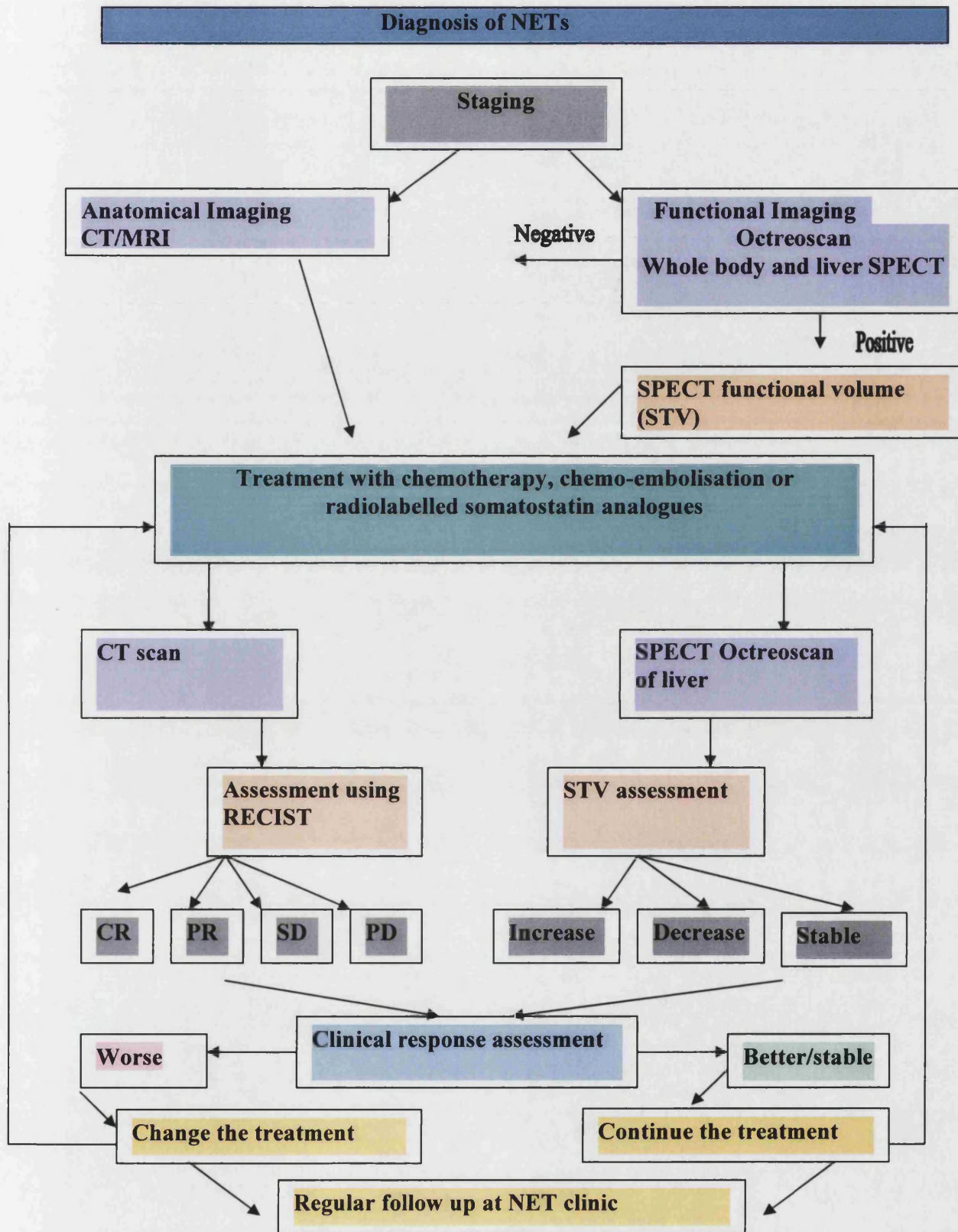
Figure 9.1 Neuroendocrine tumour management

- Experiments to find the optimal collimator, central energy and window width, uniformity and resolution needs to done with phantoms having hot lesions.

- To acquire planar and SPECT images under the proposed imaging protocol and test the accuracy as to whether it is possible to quantify the injected ^{90}Y activity. Initial experiments are presently in progress using an anthropometric phantom

- To acquire planar images using wider windows with increasing energy following the preliminary experiments conducted by (Gandon, 2003).

- The resolution of the brehmsstrahlung images was not sufficient so it was not possible to show the same tumour uptake of ^{90}Y-lanreotide as seen in the ^{111}In-pentetreotide images with present gamma camera systems. Assessment of biodistribution using positron emission tomography (PET) tracer ^{86}Y-DOTATOC, which is chemically identical to the therapeutic agent, would be helpful.

- Assessment of biodistribution by using same analogue (^{111}In-lanreotide and ^{90}Y-lanreotide.

- Functional SPECT tumour volume (STV) results will be compared with tumours markers and clinical response.

- Functional SPECT tumour volume (STV) will be used in the assessment of efficacy of individual treatment modalities and follow-up of patients.

References

Abrams MJ, Juweid M, Kate CI, Schwartz DA, Hauser MM, Gaul FE, Fuccello AJ, Rubin RH, Strauss HW and Fischman AJ. Technetium-99m.-human polyclonal IgG radiolabeled via the hydrazino nicotinamide derivative for imaging focal sites of infection in rats. J. Nucl. Med 1990; 31, 2022-2028.

Ackery D. Principles of radionuclide therapy, Chapter 78, Nuclear medicine in clinical diagnosis and treatment (Murray IPC, Ell PJ), Churchill Livingstone, second edition 1998, Volume 2, 1039-1042.

Akerstrom G. Management of carcinoid tumours of the stomach, duodenumand pancreas World J Surg 1996; 20,173-82.

Anderson CJ and Welch M J. Radiometal-labeled agents (non-technetium)
for diagnostic imaging. Chem. Rev 1999; 99, 2219-2234.

Anderson CJ, Dehdashti F, Cutler PD, Schwarz SW, Laforest R, Bass LA, Lewis JS and McCarthy DW. 64Cu-TETA-octreotide as a PET imaging agent for patients with neuroendocrine tumors. J. Nucl. Med 2001; 42, 213-221.

Andersson P, Forssell-Aronsson E, Johanson V, et al. Internalization of indium-111 into human neuroendocrine tumor cells after incubation with indium-111 DTPA-D-Phe1-octreotide J Nucl Med 1996; 37, 2002–2006.

Andersson T, Wilander E, Eriksson B, Lindgren PG et al. Effects of interferon on tumour tissue content in liver metastases of carcinoid tumours.Cancer Res 1990;50, 3413-3415.

Anon. SomatulineÒ LA. Summary of Product Characteristics. Ipsen. May 1998.

Anthony LB. Long-acting formulations of somatostatin analogues. Ital J Gastroenterol Hepatol 1999; 31 Suppl 2, S216-8.

Arnold R, Frank M and Kajdan U, Management of gastroenteropancreatic endocrine tumours the place of somatostatin analogues. Digestion 1995; 55,107–113.

Arnold R, Trautmann ME, Creutzfeldt W et al. Somatostatin analogue octreotide and inhibition of tumour growth in metastatic endocrine gastroenteropancreatic tumours. Gut 1996; 38, 430–438.

Arnold R, Simon B, Wied M. Treatment of neuroendocrine GEP tumours with somatostatin analogues. Digestion 2000, 62 (Suppl. 1), 84-91.

Arslan N, Ilgan S, Yuksel D, Serdengecti M, Bulakbasi N, Ugur O, Ozguven MA. Comparison of In-111 octreotide and Tc-99m (V) DMSA scintigraphy in the detection of medullary Thyroid tumor foci in patients with elevated levels of tumor markers after surgery. Clin Nucl Med 2001; 26(8), 683-8.

Aspestrand F, Kolmannskog Fand MCT Jacobsen, MR imaging and angiography in pancreatic apudomas. Acta Radiol 1993; 34, 468–473.

Babich JW, Solomon H, Pike MC, Kroon D, Graham W, Abrams MJ, Tompkins R G, Rubin R H, and Fischman A J. Technetium-99m-labeled hydrazino nicotinamide derivatized chemotactic peptide analogues for imaging focal sites of bacterial infection. J Nucl. Med 1993; 34, 1964-1974.

Babich JW and Fischman AJ. Effect of "co-ligand" on the biodistribution of 99mTc-labeled hydrazino nicotinic acid derivatized chemotactic peptides. Nucl Med Biol 1995; 22, 25-30.

Baidoo KE, Scheffel U, and Stathis M. High-affinity no-carrier-added ^{99m}Tc-labeled chemotactic peptides for studies of inflammation in vivo. Bioconjugate Chem1998; 9, 208-217.

Bajetta E, Ferrari L, Merlonetti A, Celio L, Procopio G, Artale S, Zilembo N, Di Bartholomeo M, Serregni E and Bombardieri E. Chromogranin A, neuron-specific enolase, carcinoembryonic antigen and hydroxyindole acetic acid evaluation in patients with neuroendocrimne tumors. Cancer 1999; 86, 858–865.

Bakker WH, Krenning EP, and Breeman WA. Receptor scintographywith a radiolabeled somatostatin analog: radiolabeling, purification, biological activity and in vivo application in animals. J. Nucl. Med 1990; 31, 1501-1509.

Bakker WH, Albert R, Bruns C, Breeman WAP, Hofland LJ, Marbach P, Pless J, Pralet D, Stolz B, Koper JW, Lamberts SWJ, Visser TJ, and Krenning EP. [^{111}In-DTPA-D-Phe]-octreotide, a potential radiopharmaceutical for imaging of somatostatin receptor-positive tumors: synthesis, radiolabeling and in vitro validation. Life Sci 1991; 49, 1583-1591.

Bale S, Bale AE, Stewart S. Linkage analysis of multiple endocrine neoplasia type 1 with INT2 and other markers on chromosome 11. Genomics 1989; 4, 320–322.

Bangard M, Behe M, Guhlke S, Otte R, Bender H, Maecke H, and Biersack H-J. Detection of somatostatin receptor -positive tumours using the new 99m-Tc-tricine-HYNIC-d-Phe1-Tyr3-octreotide: first results in patients and comparison with 111In-DTPA-d-Phe1-octreotide. Eur J Nucl Med 1998; 27, 628-637.

Baron RL. Understanding and optimizing use of contrast material for CT of the liver. A J R Am J Roentgenol 1994 $_1$; 163, 323.

Baron RL. Detection of liver neoplasms: techniques and outcomes. Abdom Imaging 1994 $_2$; 19(4):320-4.

Bauer W, Briner U, Doepfner W, Haller R, Huguenin R, Marbach P et al. SMS 201-995: a very potent and selective octapeptide analog of somatostatin with prolonged action. Life Sciences 1982; 31, 1133–1140.

Bax NDS et al. Carcinoid tumours, A guide to the epidedemilogy, clinical presentation, investigation, diagnosis, treatment and prognosis, IPSEN Ltd 2000.

Beierwaltes WH. Endocrine imaging; parathyroid, adrenal cortex and medulla, and other endocrine tumours. PartII. J Nucl Med 1991; 32, 1627-1639.

Benezra R, Rafii S, Lyden D. The Id proteins and angiogenesis. Oncogene 2001; 20, 8334-8341.

Bernard BF, Krenning EP, Breeman WA, Rolleman EJ, Bakker WH, Visser TJ, Macke H, de Jong M. D-lysine reduction of indium-111 octreotide and yttrium-90 octreotide renal uptake. J Nucl Med 1997; 38(12), 1929-33.

Bernhard N Kiming. Radiotherapy for gastroenteropancratic neuroendocrine tumours Molecular and cell biological aspects of gastroenteropancraetic neuroendocrine tumour disease. Annals of the New York academy of sciences 1994, vol 733, 488-495.

Black WC. Enterochromaffin cell types and corresponding carcinoid tumours. Lab Invest 1968; 19, 473–476.

Blakey DC, Westwood FR, Walker M, Hughes GD, Davis PD, Ashton SE, Ryan AJ. Antitumor activity of the novel vascular targeting agent ZD6126 in a panel of tumor models. Clin. Cancer Res 2002; 8, 1974-1983.

Blok D, Feitsma RIJ, Vermeij P and Pauwels EJK. Peptide radiopharmaceuticals in nuclear medicine. Eur. J. Nucl. Med 1999; 26, 1511-1519.

Blum J, Handmaker H, Lister-James J, Rinne NA multicenter trial with a somatostatin analog (99m)Tc depreotide in the evaluation of solitary pulmonary nodules. Chest 2000; 117 (5), 1232-8.

Blum J, Handmaker H, Rinne NA. Technetium labeled small peptide radiopharmaceuticals in the identification of lung cancer. Curr Pharm Des 2002; 8(20), 1827-36.

Brazeau P, Vale W, Burgus R, Ling N, Butcher M, Rivier J et al. Hypothalamic polypeptide that inhibits the secretion of immunoreactive pituitary growth hormone. Science 1973; 179, 77-9.

Brechbiel MW and Gansow OA. Backbone-substituted DTPA ligands for 90Y radioimmunotherapy. Bioconjugate Chem 1991; 2, 187-194.

Britton K E, Foley R R, Barlow R et al. Neuroendocrine tumour patients evaluated with In-11 Lanreotide for Y-90 Lanreotide therapy. Eur J Nucl Med 2000; 27: 962.

Brown JM, Giaccia AJ. The unique physiology of solid tumors: opportunities (and problems) for cancer therapy. Cancer Res 1998; 199, 58, 1408-1416,

Brown KT, Koh BY, Brody LA, et al. Particle embolizationof hepatic neuroendocrine metastases for control of painand hormonal symptoms. J. Vasc. Interv. Radiol 1999; 10, 397.

Bruns C, Raulf F, Hoyer D, Schloos J, Luebbert H & Weckbecker G.Binding properties of somatostatin receptor subtypes. Metabolism: Clinical and Experimental 1996; 45, 17–20.

Bruns C, Lewis I, Briner U, Meno-Tetang G, Weckbecker G. SOM230: a novel somatostatin peptidomimetic with broad somatotropin release inhibiting factor (SRIF) receptor binding and a unique antisecretory profile. Eur J Endocrinol 2002; 146(5), 707-16

Buscombe JR, Caplin ME, Chao D, Hochhauser D, Hipplewhite J, Johnson G, Croasdale PL Yong TA, IVirgolini I, Hilson AJW Early results of radiolabelled lanreotide in disseminated NETs .Nucl Med Commun 2001; 22, 445.

Buscombe JR. Interventional nuclear medicine in hepatocellular carcinoma and other tumours. Nucl Med Commun 2002; 23(9):837-41.

Buscombe JR, Caplin ME, Hilson AJ. Long-term efficacy of high-activity 111in-pentetreotide therapy in patients with disseminated neuroendocrine tumors. J Nucl Med 2003; 44(1), 1-6

Capella C, Heitz PU, Ho"fler H, Solcia E, Klo"ppel, G. Revised classification of neuroendocrine tumors of the lung, pancreas and gut. Digestion 1994; 50(Suppl. 3), 11.

Caplin ME, Buscombe JR, Hilson AJ, Jones AL, Watkinson AF, Burroughs AK. Carcinoid tumour. Lancet. 1998 $_1$; 352, 799-805.

Caplin ME, Hodgson HJ, Dhillon AP, Begent R, Buscombe J, Dick R, Rolles K, Burroughs AK. Multimodality treatment for gastric carcinoid tumour with liver metastases. Am J Gastroenterol 1998 $_2$; 93(10), 1945-8.

Caplin ME, Mielcarek W, Buscombe JR, Jones AL, Croasdale PL, Cooper MS, Burroughs AK, Hilson AJW. Toxicity of high-activity ^{111}In-Octreotide therapy in patients with disseminated neuroendocrine tumours. Nucl Med Commun 2000; 21, 97-102.

Carmeliet P, Jain RK. Angiogenesis in cancer and other diseases. Nature 2000; 407, 249-257.

CCO Formulary Revised Feb 2000.

Chandrasekharappa SC, Guru SC, Manickam P et al. Positional cloning of thegene for multiple endocrine neoplasia-type 1. Science 1997; 276; 404–407.

Chaplin DJ, Dougherty GJ. Tumour vasculature as a target for cancer therapy.Br. J. Cancer 1999; 80 (Suppl 1), 57-64.

Chatal JF, Hoefnagel CA. Radionuclide therapy.Lancet 1999; 11; 354(9182), 931-5.

Chaudhry A, Papanicolau V, Öberg K, et al. Expression of platelet-derived growth factor and its receptors in neuroendocrine tumors of the digestive system, Cancer Res 1992 $_1$; 52,1006–1012.

Chaudhry A, Öberg K, Wilander E. A study of biological behavior based on the expression of a proliferating antigen in neuroendocrine tumors of the digestive system. Tumor Biol 1992 $_2$; 13, 27–35.

Chaudhry A, Funa K, Öberg K, et al. Expression of growth factor peptides and their receptors in neuroendocrine tumors of the digestive system. Acta Oncol 1993; 32,107–114.

Cheng PN, Saltz LB. Failure to confirm major objective antitumor activity for streptozocin and doxorubicin in the treatment of patients with advanced islet cell carcinoma. Cancer 1999; 15, 86:944-8

Chezmar JL, Nelson RC, Small WC, Bernardino ME. Magntic resonance imaging of the pancreas with gadolinium-DTPA. Gastrointest Radiol 1991; 16:139–42.

Chinol M, Brodei L, Cremonesi M, Paganelli Receptor-mediated radiotherapy with Y-90 DOTA-D-Phe-1-Tyr-3-octreotide. The experience of the European Institute of Oncology. Semin Nucl Med 2002, 32: 141-147.

Chott AG, Kloppel G, Baxbaum P et al. Neuron specific enolase demonstration in the dignosis of a solid cystic tumour of pancreas, Virchow Arch 1987; 410, 397-402.

Clarke LP, Cullom SJ, Shaw R, Reece C, Penney BC, King MA, Silbiger M.Bremsstrahlung imaging using the gamma camera: factors affecting attenuation. J Nucl Med 1992; 33(1), 161-6.

Clouse ME, Perry L, Stuart K, and Stokes K R. Hepatic arterial chemoembolization for metastatic neuroendocrine tumors. Digestion 1994; 55, 92.

Cremonesi M, Ferrari M, Zoboli S, Chinol M, Stabin MG, Orsi F, Maecke HR, Jermann ,Robertson C, Fiorenza M, Tosi G, Paganelli G Biokinetics and dosimetry in patients administered with (111)In-DOTA-Tyr(3)-octreotide: implications for internal radiotherapy with (90)Y-DOTATOC. Eur J Nucl Med 1999; 26, 877-86.

Croasdale J, Chief Radiopharmacist, Department of Nuclear Medicine, Royal Free Hospital, London NW3 2QG, UK.

Creutzfeldt W, Carcinoids tumours. Development of our knowledge. World J Surg 1996; 20,126-131.

Curley SA, Izzo F, Delrio P et al. Radiofrequency ablation of unresectable primary and metastatic hepatic malignancies: Results in 123 patients. Ann Surg 1999; 230,1, 1–8.

Cybulla M, Weiner SM, Otte A. End-stage renal disease after treatment with 90Y-DOTATOC. Eur J Nucl Med 2001; 28, 1552-4.

Decristoforo C, Mather SJ. 99m-Technetium-labelled peptide-HYNIC conjugates: effects of lipophilicity and stability on biodistribution. Nucl Med Biol 1999[1]; 26(4):389-96

Decristoforo C and Mather SJ. Technetium-99m somatostatin analogues: effect of labeling methods and peptide sequence. Eur J Nucl Med 1999 [2]; 26, 869-876.

Decristoforo C, Melandez-Alafort L, Sosabowski JK., and Mather S J. 99mTc-HYNIC-[Tyr3]-octreotide for imaging somatostatin-receptor-positive tumors: preclinical evaluation and comparison with 111In-octreotide. J. Nucl. Med 2000; 41, 1114-1119.

de Herder WW, Lamberts SW. Somatostatin and somatostatin analogues: diagnostic and therapeutic uses, Curr Opin Oncol 2002; 14(1), 53-7.

de Jong M, Bakker WH, Krenning EP, Breeman WAP, van der Pluijm ME, Bernard BF, Visser TJ, Jermann E, Behe M, Powell P and Maecke HR. Yttrium-90 and indium-111 labeling, receptor binding and biodistribution of [DOTA^0, D-Phe^1, Tyr3] octreotide, a promising somatostatin analogue for radionuclide therapy, Eur J Nucl. Med 1997; 24, 368-371.

de Jong M, Breeman WA, Bakker WH, et al. Comparison of (111)In-labeledsomatostatin analogues for tumor scintigraphy and radionuclide therapy. Cancer Res 1998; 58, 437–441.

de Jong M, Breeman WA, Bernard HF, et al. Therapy of neuroendocrine tumor with radiolabeled somatostatin analogues. Quart J Nucl Med. 1999; 43, 356–366.

de Jong M, Breeman WA, Bernard BF, Bakker WH, Schaar M, van Gameren A, Bugaj JE, [177Lu-DOTA(0),Tyr3] octreotate for somatostatin receptor-targeted radionuclide therapy. Int J Cancer 2001 Jun 1; 92(5), 628-33.

de Jong M, Krenning E, New Advances in Peptide Receptor Radionuclide Therapy. Journal of Nuclear Medicine 2002 $_1$; 43, 5, 617-620.

de Jong M, Valkema R, Jamar F, Kvols LK, Kwekkeboom DJ, Breeman WA, Bakker WH, Smith C, Pauwels S, Krenning EP. Somatostatin receptor-targeted radionuclide therapy of tumors: preclinical and clinical findings. Semin Nucl Med 2002 $_2$; 32, 133-40.

Delacroix D, Guerre JP, Leblanc P, Hickman C, Radiation protection dosimetry, Radionuclide and radiation protection data handbook 1998; Vol 76 Nos.1-2,

DeLellis RA, Dayal Y and Wolfe HJ, Carcinoid tumours: changing concepts and new perspectives. Am J Surg Pathol 1984; 8, 295–300.

DeNardo SJ, Zhong GR, Salako Q, Li M, DeNardo GL, and Meares CF. Pharmacokinetics of chimeric L6 conjugated to indium-111- and yttrium-90-DOTA-peptide in tumor-bearing mice. J Nucl Med 1995; 36, 829-836.

DeNardo SJ, Kukis DL, Miers L, Winthrop MD, Kroger LA, Salako Q, Shen S, Lamborn KR, Gumerlock PH, Meares CF, and DeNardo G L. Yttrium-90-DOTA-peptide-chimeric L6 radioimmunoconjugate: efficacy and toxicity in mice bearing p53 mutant human breast cancer xenografts. J. Nucl. Med 1998; 39, 842-849.

Dietrich WF, Radany EH, Smith JS, Bishop JM, Hanahan D and Lander ES. Genome-wide search for loss of heterozygosity in transgenic mouse tumors reveals candidate tumor supressor genes on chromosomes 9 and 16. Proceedings of the National Academy of Sciences (USA) 1994; 91, 9451–9455.

Dogliotti L, Tampellini M, Stivanello M, Gorzegno G, Fabiani L. The clinical management of neuroendocrine tumors with long-acting repeatable (LAR) octreotide: comparison with standard subcutaneous octreotide therapy. Ann Oncol 2001; 12 Suppl 2:S105-9.

Doppman JL, Jensen RT. Localization of gastroenteropancreatic tumours by angiography. Ital J Gastroenterol Hepatol. 1999; 31 Suppl 2, S163-6.

Dousset B, Houssin D, Soubrane O, Boillot O, Baudin F, Chapuis Y. Metastatic endocrine tumors: is there a place for liver transplantation? Liver Transpl Surg 1995; 1(2), 111-7.

Dousset B, Saint-Marc O, Pitre J et al., Metastatic endocrine tumors: Medical treatment, surgical resection, or liver transplantation. World J Surg 1996; 20, 7, 908–915.

Ducreux M, Baudin E, Schlumberger M. Treatment strategy of neuroendocrine tumors, Rev Prat 2002; 1; 52(3), 290-6.

Duncan JR, Stephenson MI, Wu HP, Anderson CJ. Indium-111-diethylenetriaminepentaacetic acid-octreotide is delivered in vivo to pancreatic, tumor cell, renal, and hepatocyte lysosomes. Cancer Res 1997; 57,659–671.

Dusmet ME and McKneally MF. Pulmonary and thymic carcinoid tumours, World J Surg 1996; 20, 189–195.

EANM Radionuclide Therapy Committee guidelines- www.eanm.org

Edwards DS, Liu S, Barrett JA, Harris AR, Looby RJ, Ziegler MC, Heminway SJ, and Carroll TR. New and versatile ternary ligand system for technetium radiopharmaceuticals: water soluble phosphines and tricine as coligands in labeling a hydrazinonicotinamide-modified cyclic glycoprotein IIb/IIIa receptor antagonist with ^{99m}Tc. Bioconjugate Chem 1997; 8, 146-154.

Eisenwiener KP, Powell P, and Maecke HR. A convienent synthesis of novel bifunctional prochelators for coupling to bioactive peptides for radionuclidelabeling. Bioorg Med Chem Lett 2000; 10, 2133-2135.

Elgazzer AH, Gelfand MJ, Wahburn LC et al. I-123MIBG scintigraphy in mIBG adults. A report of clinical experience. Clin Nucl Med 1995; 20,147-152.

Erasmus JJ, McAdams HP, Patz Jr. EF, Coleman RE, Ahuja V, Goodman PC. Evaluation of primary pulmonary carcinoid tumors using FDC PET. American Journal of Roentgenology 1998; 170, 1369–73.

Erdi AK, Erdi YE, Yorke ED, Wessels BW. Treatment planning for radio-immunotherapy.Phys Med Biol 1996; 41(10), 2009-26.

Eriksson B, Bergström M, Lilja A et al. Positron emission tomography (PET) in neuroendocrine gastrointestinal tumors. Acta Oncol 1993; 32:189-196.

Eriksson B & Oberg K. Summing up 15 years of somatostatin analog therapy in neuroendocrine tumors: future outlook. Annals Oncology 1999; 10 S31-S38.

Eriksson B, Bergstrom M, Orlefors H, Sundin A, Oberg K, Langstrom B.Use of PET in neuroendocrine tumors. In vivo applications and in vitro studies. Q J Nucl Med. 2000$_1$; 44(1), 68-76.

Eriksson B, Oberg K and Stridsberg M. Tumor markers in neuroendocrine tumors. Digestion 2000 2, 62 suppl 1, 33–38.

Eriksson B, Bergstrom M, Sundin A, Juhlin C, Orlefors H, Oberg K, Langstrom B. The role of PET in localization of neuroendocrine and adrenocortical tumors. Ann N Y Acad Sci 2002; 970, 159-69.

Faiss S, Scherbubl H, Riecken EO, Wiedenmann B. Drug therapy in metastatic neuroendocrine tumours of the gastrointestinal system. Recent Results in Cancer Research 1996; 142, 193-207.

Feldman JM and TM O'Dorisio. The role of neuropeptides and seretonin in the diagnosis of carcinoid tumors. American Journal of Medicine 1986; 81, 41.

Feyrter F. Uber diffuse endocrine epitheliale Organe J A Barth Leipzig 1938.

Fichna J, Janecka A. Synthesis of target-specific radiolabeled peptides for diagnostic imaging. Bioconjug Chem 2003; 14(1), 3-17.

Firestone RB. Table of isotopes (Shirley, W. S., Ed.), Horizon Pubs & Distributors Inc 1996.

Fischman AJ, Babich JW, and Strauss W. A ticket to ride: Peptide radiopharmaceuticals. J Nucl Med 1993; 34, 2253-2263.

Flower MA, Dosimetric considerations, Chapter 79 Nuclear medicine in clinical diagnosis and treatment (Murray IPC, Ell PJ), Churchill Livingstone, second edition1998, Volume2, 1043-1048.

Flux GD, Guy MJ, Beddows R, Pryor M, Flower MA.Estimation and implications of random errors in whole-body dosimetry for targeted radionuclide therapy. Phys Med Biol 2002; 7; 47(17), 3211-23.

Forster GJ, Engelbach MJ, Brockmann JJ, Reber HJ, Buchholz HG, Macke HR, Rosch FR, Herzog HR, Bartenstein PR Preliminary data on biodistribution and dosimetry for therapy planning of somatostatin receptor positive tumours: comparison of (86)Y-DOTATOC and (111)In-DTPA-octreotide. Eur J Nucl Med 2001; 28(12), 1743.

Froidevaux S, Eberle AN. Somatostatin analogs and radiopeptides in cancer therapy. Biopolymers 2002; 66 (3), 161-183.

Fujita, T. Concept of Paraneurons, Arch.Histol Jn 1977; 40 (suppl) 1-12.

Gandon L, Quantitative imaging of Y-90 Brehmsstrahlung, MSc Thesis 2003 London University.

Ganim RB, Norton JA. Recent advances in carcinoid pathogenesis, diagnosis and management. Surg Oncol 2000; 9(4), 173-9

Gates J, Hartnell GG, Stuart KE, and Clouse ME. Chemoembolization of hepatic neoplasms: Safety, complications, and when to worry. Radiographics 1999; 19, 399.

Gehan EA and Tefft MC. Will there be resistance to the RECIST (Response Evaluation Criteria in Solid Tumors)? J Natl Cancer Inst 2000; 92, 179-181.

Gerdes J, Schwab H, Lenke H, et al: Production of mouse monoclonal antibody reacting with a human nuclear antigen associated with proliferation. Int J Cancer 1983 31, 13-20.

Giap HB, Macey DJ, Podoloff DA. Development of a SPECT–based three-dimensional treatment planning system for radioimmunotherapy. J Nucl Med 1995; 36, 1885-1894.

Gibril F, Doppman JL, Reynolds JC, Chen CC, Sutliff VE, Yu F, Serrano J, Venzon DJ, Jensen RT. Bone metastases in patients with gastrinomas: a prospective study of bone scanning, somatostatin receptor scanning, and magnetic resonance image in their

detection, frequency, location, and effect of their detection on management.J Clin Oncol 1998; 16(3), 1040-53.

Gibril F, Reynolds JC, Chen CC, et al. Specificity of somatostatin receptor scintigraphy: a prospective study and effects of false-positive localizations on management in patients with gastrinomas. J Nucl Med 1999; 40, 539–553.

Gilligan, CJ, GP Lawton, LH Tang, AB West and IM Modlin, Gastric carcinoid tumors: the biology and therapy of an enigmatic and controversial lesion. Am J Gastroentrol 1995; 90,338–353.

Giovanni M, Seitz JF, Thomas P et al. Electronic sectorial ultrasound endoscopy in benign and malignant tumoral pathology of the stomach: results in 30 patients. Gastroenterol Clin Biol 1993; 17, 26–32.

Glover JR, Shorvon PJ, Lees WR.Endoscopic ultrasound for localisation of islet cell tumours.Gut 1992; 33,108-110.

Gnanasegaran G. Biodistribution of radiolabelled analogues MSc Thesis University of London 2001; 53-54.

Godwin JD. Carcinoid tumours.An analysis of 2,837 cases. Cancer 1975; 36(2), 560-9.

Gores GJ. Liver transplantation for malignant disease.Gastroenterol. Clin.North Am 1993; 22, 285-299.
Grewal RK, Dadparvar S, Yu JQ, Babaria CJ, Cavanaugh T, Sherman M, Jacobstein J. Efficacy of Tc-99m depreotide scintigraphy in the evaluation of solitary pulmonary nodules.Cancer J. 2002; 8(5),400-4.

Hagn C, Schimd KW et al. Chromogranin A, B, and C in human adrenal medulla and endocrine tissues.Lab.invest 1986; 55, 405-411.

Hamberg LM, Hunter GJ, Alpert NM, Choi NC, Babich JW, Fischman AJ. The dose uptake ratio as an index of glucose metabolism: useful parameter or oversimplification? J Nucl Med 1994; 35(8), 1308-12

Hanahan D, Folkman J. Patterns and emerging mechanisms of the angiogenic switch during tumorigenesis. Cell 199; 86, 353-364.

Hanson MW. Scintigraphic Evaluation of Neuroendocrine Tumors. Appl Radiol, 2001; 30(6): 11-17.

Heitz, PH, Roth UJ, Chr.Zuber et al. Markers for neural and endocrine cells in pathology. In markers of neural and endocrine cells 1991. M Gratzl and Langley, Eds 203-216.

Helena R Balon, Stanley J Goldsmith, Barry A Siegel, Edward B Silberstein, Eric P Krenning, Otto Lang, and Kevin J Donohoe. Procedure Guideline for Somatostatin Receptor Scintigraphy with ^{111}In-Pentetreotide J Nucl Med 2001; 42, 1134-1138.

Heppeler A, Behe M, Froidevaux S, Hennig M, Jermann E, and Maecke HR. Metal coordination chemical aspects and tumour targeting of a promising somatostatin analogue. J Nucl Med 1998. 39 Suppl, 63P.

Herzog H, Rosch F, Stocklin G, Lueders C, Quaim SM, and Feinendegen LE. Measurement of pharmacokinetics of yttrium-86 radiopharmaceuticals with PET and radiation dose calculation of analogous yttrium-90 radiotherapeutics. J Nucl Med 1993; 34, 2222-2226.

Hoefnagel CA. Metaiodobenzylguanidine and somatostatin in oncology: role in the management of neural crest tumours. Eur J Nucl Med 1994; 21 561-581.

Hoefnagel CA. MIBG and radiolabelled octreotide in neuroendocrine tumors.
Q J Nucl Med 1995; 39(Suppl 1–4), 137–139.

Hofland LJ, van Hagen PM, Lamberts SW. Functional role of somatostatin receptors in neuroendocrine and immune cells. Ann Med 1999; 31 (Suppl. 2), 23-7.

Hoyer D, Luebbert H, Bruns C. Molecular pharmacology of somatostatin receptors. Naunyn-Schmiedeberg's Archives of Pharmacology 1994; 350, 441–453.

Hnatowich DJ, Layne WW, Childs RL, Lanteigne D, Davis MA, Griffin TV and Doherty PW. Radioactive labeling of antibody: A simple and efficient method. Science 1983; 220, 613-615.

Humm JL. Dosimetric aspects of radiolabeled antibodies for tumour therapy. J Nucl Med 1986; 27, 1490-1497.

Hunter GJ, Hamberg LM, Alpert NM, Choi NC, Fischman AJ. Simplified measurement of deoxyglucose utilization rate. J Nucl Med 1996; 37(6):950-5.

Jensen RT. Role of Somatostatin receptors in gasteropancreatic tumours. In Lamberts SWJ and Dogliotti L eds. The expanding role of octreotide I.Bioscientifica Ltd.Bristol UK 2002; P45-72.

Jenson ET, Holmberg L, Stridsberg M, Eriksson B, Theodorsson E, Wilander E and Oberg K. Carcinoid tumors. Analysis of prognostic factors and survival in 301 patients from a referral center. Annals of Oncology 1997; 8, 685–690.

Kaltsas GA, Mukherjee JJ, Plowman PN, Grossman AB. The role of chemotherapy in the nonsurgical management of malignant neuroendocrine tumours. Clin Endocrinol (Oxf) 2001 ₁; 55(5), 575-87.

Kaltsas GA, Korbonits M, Heintz E, Mukherjee JJ, Jenkins PJ, Chew SL, Reznek R, Monson JP, Besser GM, Foley R, Britton KE and Grossman AB. Comparison of Somatostatin Analog and Meta-Iodobenzylguanidine Radionuclides in the Diagnosis and Localization of Advanced Neuroendocrine Tumors. J Clin Endocrinol Metab 2001 ₂; 86(2), 895-902.

Kaltsas GA, Mukherjee JJ, Isidori A, Kola B, Plowman PN, Monson JP, Grossman AB, Besser GM. Treatment of advanced neuroendocrine tumours using combination chemotherapy with lomustine and-fluorouracil. Clin Endocrinol. 2002; 57,169-8.

Kaplan LM. Endocrine tumours of the gastrointestinal tract and pancreas. In: Wilson JD, Braunwald E, Isselbacher KJ, et al (eds). Harrison's principles and practices of Internal Medicine. New York: McGovern Inc, 1991; 1386–93.

Keire DA, Jang YH, Li L, Dasgupta S, Goddard WA III, and Shively JE. Chelators for radioimmunotherapy: I. NMR and ab initio calculation studies on 1,4,7,10-tetra(carboxyethyl)-1,4,7,10-tetraazacyclododecane (DO4Pr) and 1,4,7-tris(carboxymethyl)-10-(carboxyethyl)-1,4,10-tetraazacyclododecane (DO3A1Pr). Inorg Chem 2001; 40, 4310-4318.

Kimura M, Tominaga T. Outstanding problems with response evaluation criteria in solid tumors (RECIST) in breast cancer. Breast Cancer 2002; 9, 153.

Klöppel G, Veld PI. Neural and endocrine markers as diagnostic tools in pancreatic and gastrointestinal endocrine tumors. Acta Histochem 1990; 38 (suppl):93–98.

Klöppel G, Heitz P. Classification of normal and neoplastic neuroendocrine cells. Ann NY Acad Sci1994; 733:18–23.

Klöppel G, Heitz, PU, Capella C, Solcia E. Pathology and Nomenclature of Human Gastrointestinal Neuroendocrine (Carcinoid) Tumors and Related Lesion World J. Surg 1996; 20, 132–141.

Krasny RM, Lu DSK. Helical Computed Tomography for Abdominal Imaging World J Surg 1996; 20, 248–252.

Krejcarek GE and Tucker KL. Covalent attachment of chelating groups to macromolecules. Biochem Biophys. Res. Commun 1977; 2, 581-585.

Krenning EP, Bakker WH, Breeman WAP, et al: Localisation of endocrine-related tumours with radioiodinated analogue of somatostatin. Lancet 1989; 1:242-244.

Krenning EP, Kwekkeboom DJ, Bakker WH, et al: Somatostatin receptor scintigraphy with [111In-DTPA-D-Phe1] - and [123I-Tyr3] octreotide: The Rotterdam experience with more than 1000 patients. Eur J Nucl Med 1993; 20:716-731.

Krenning EP, Kooij PP, Bakker WH, et al. Radiotherapy with a radiolabeled somatostatin analogue [^{111}In-DTPA-D-Phe^1]-octreotide: a case history. Ann NY Acad Sci. 1994 $_1$; 733, 496–506.

Krenning EP, Kwekkeboom DJ, Oei HY, de Jong RJ, Dop FJ, de Herder WW, Reubi JC, Lamberts SW. Somatostatin receptor scintigraphy in carcinoids, gastrinomas and Cushing's syndrome. Digestion 1994 $_2$; 55 Suppl 3, 54-9.

Krenning, EP, Kwekkeboom, DJ, Pauwels, EK, Kvols, LK, Reubi, JC. Somatostatin receptor scintigraphy. In: Nuclear Medicine Annual. New York: Raven Press, 1995, 1 50.

Krenning EP, Kooij PP, Pauwels S, Breeman WA, Postema PT, De Herder WW, Valkema R, Kwekkeboom DJ Somatostatin receptor: scintigraphy and radionuclide therapy. Digestion 1996; 57 Suppl 1, 57-61.

Krenning EP, Valkema R, Kooij PP, Breeman WA et al. Scintigraphy and radionuclide therapy with (indium-111-labelled-diethyl triamine penta-acetic acid-DPhe1)-octreotide.Ital J Gastroenterol Hepatol 1999 ; 31 Suppl 2, S219-23.

Krois D, Riedel C, Angelberger P, Kalchhauser H, Virgolini I, and Lehner H. Synthesis of N--(6-hydrazinonicotinoyl)-octreotide: a precursor of a [99m.Tc] complex. Liebigs Ann 1996; 1463-1469.

Kuvshinoff BW, Ota DM. Radiofrequency ablation of liver tumors: influence of technique and tumour size. Surgery 2002; 132(4): 605-11; Discussion 611-2.

Kvols LK, Moertel CG, O'connell MJ, Schutt AJ, Rubin J, Hahn RG. Treatment of the malignant carcinoid syndrome. Evaluation of a long-acting somatostatin analogue. N Engl J Med 1986; 315, 663 6.

Kvols LK, Brown ML, O'Connor MK, et al. Evaluation of a radiolabeled somatostatin analog (I-123 octreotide) in the detection and localization of carcinoid and islet cell tumours. Radiology1993; 187, 129-133.

Kvols LK. Meatstatic carcinoid tumours and the malignant carcinoid syndrome. Ann N Y Acad Sci. 1994; 15; 733, 464-470.

Kwekkeboom D, Krenning EP, de Jong M. Peptide receptor imaging and therapy .J Nucl Med 2000; 41(10),1704-13.

Kwekkeboom DJ, Kam BL, Bakker WH, et al. Treatment with Lu-177-DOTA-Tyr3-octreotate in patients with somatostatin receptor positive tumors: preliminary results Eur J Nucl Med 2001; 28(suppl): 1027P.

Kwekkeboom DJ, Krenning EP. Somatostatin receptor imaging. Semin Nucl Med 2002; 32(2), 84-91.

Lamberts SWJ. The role of somatostatin in the regulation of anterior pituitary hormone secretion and the use of its analogues in the treatment of human pituitary tumors. Endocr Rev 1988; 9, 417-436.

Lamberts SWJ, Bakker WH, Reubi JC, et al: Somatostatin-receptor imaging in the localization of endocrine tumors. N Engl J Med 1990; 323, 1246-1249.
Lamberts SWJ, Krenning EP, Reubi JC. The role of somatostatin and its analogs in the diagnosis and treatment of tumours. Endocrinol Rev 1991; 12, 450-482.

Lamberts SW, Van der Lely A-J, De Herder WW, Hofland LJ. Octreotide. N Engl J Med 1996; 334, 246–254.

Lamberts SWJ, van der Lely A J and Hofland L J. New somatostatin analogs: will they fulfill old promises? Eur J Endocrinol 2002 $_1$; 146(5), 701-05.

Lamberts SW, de Herder WW, Hofland LJ. Somatostatin analogs in the diagnosis and treatment of cancer. Trends Endocrinol Metab 2002 $_2$; 13(10), 451-7.

Lang H, Oldhafer KJ, Weimann A, Schlitt HJ, Scheumann GF, Flemming P, Ringe B, Liver transplantation for metastatic neuroendocrine tumors. Pichlmayr R. Ann Surg 1997; 225(4): 347-54.

Langley K. The neuroendocrine concept today. Ann NY Acad Sci 1994; 733, 1–17.

Larsson C, Shogseid B, Öberg K, et al: MEN-1 gene maps to chromosome 11 and is lost in insulinoma. Nature 1988; 332:85–87.

Larsson C, Friedman E. Localization and identification of the multiple endocrine neoplasia type 1 disease gene. Endocrinol Metab Clin North Am. 1994; 23(1), 67-79.

Lau WY, Leung TWT, Ho S et al. Adjuvant intra-arterial iodine-131 labelled lipiodol for resectable hepatocellular carcinoma. Lancet 1999; 353,797-801.

Leah M, Williams EDA. Critical evaluation of methods for preparing pentavalent 99Tcm-DMSA, Nucl Med Commun 1999; 20(8) 769-73.

Lehy T, Mignon M, Cadiot G et al. Gastric endocrine cell behaviour in Zollinger-Ellison patients on long term potent anti-secretory treatment. Gastroenterology 1989; 96, 1029–1040.

Lewis I, Bauer W, Albert R, Chandramouli N, Pless J, Weckbecker G, Bruns C. A novel somatostatin mimic with broad somatotropin release inhibitory factor receptor binding and superior therapeutic potential. J Med Chem. 2003; 46(12):2334-44.

Lewis JS, Lewis MR, Cutler PD, Srinivasan A, Schmidt MA, Schwarz SW, Morris MM, Miller JP and Anderson CJ. Radiotherapy and dosimetry of 64Cu-TETA-Tyr3-octreotate in a somatostatin receptor-positive, tumor-bearing rat model. Clin Cancer Res 1999; 5, 3608-3616.

Lightdale CJ, Botet JF, Woodruff JM, Brennan MF. Localization of endocrine tumors of the pancreas with endoscopic ultrasonography. Cancer 1991; 68(8), 1815-20.

Liu S, Edwards DS and Barrett JA. ^{99m}Tc labeling of highly potent small peptides. Bioconjugate Chem 1997; 8, 621-636.

Liu S, Edwards DS, and Harris AR. A novel ternary ligand system for ^{99m}Tc-labeling of hydrazino nicotinamide-modified biologically active molecules using imine-N-containing heterocycles as coligands. Bioconjugate Chem 1998; 9, 583-595.

Loftus JP and van Heerden JA, Surgical management of gastrointestinal carcinoid tumors. Adv Surg1995; 28,317–336.

Lohmann DR, Fesseler B, Putz B et al. Infrequent mutation in the p53 gene in pulmonary carcinoid tumors. Cancer Research 1993; 53, 5797–5801.

London JF, Shawker TH, Doppman JL et al. Zollinger-Ellison syndrome: prospective assessment of abdominal US in the localization of gastrinomas.Radiology 1991; 178, 763–7.

London NJ & Giles GR. Liver transplantation for malignancy. Br.J.Cancer 1991; 64, 621-623.

Losa M, Ciccarelli E, Mortini P, Barzaghi R, Gaia D, Faccani G, Papotti M, Mangili F, Terreni MR, Camanni F, Giovanelli M. Effects of octreotide treatment on the proliferation and apoptotic index of GH-secreting pituitary adenomas. The Journal of Clinical Endocrinology and Metabolism 2001; 86, 11, 5194-5200.

Lucey MR. Endogenous somatostatin and the gut. Gut 1986; 27, 457-67.

Lunderquist A, Ericsson M, Nobin A, and Sanden G. Gelfoam power embolization of the hepatic artery in liver metastases of carcinoid tumors. Radiologe 1982; 22, 65.

Lundin L, LandeliusJ. Echocardiography for carcinoid heart diseaseAnn N Y Acad Sci. 1994; 733:437-45.

Marlink RG, Lokich JJ, Robins JR, and Clouse ME. Hepatic arterial emobolization for metastatic hormone-secreting tumors: Technique, effectiveness, and complications. Cancer1990; 65:22-27.

McCarthy KE, Woltering EA, Espenan GD, Cronin M, Maloney TJ, Anthony LB. In situ radiotherapy with ^{111}In-pentetreotide: initial observations and future directions. Cancer J Sci Am 1998; 4:84–102.

McMurry TJ, Brechbiel M, Kumar K and Gansow OA. Convenient synthesis of bifunctional tetraaza macrocycles. Bioconjugate Chem 1992; 3, 108-117.

McMurry TJ, Pippin CG, Wu C, Deal KA, Brechbiel MW, Mirzadeh S, and Gansow OA. Physical parameters and biological stability of yttrium (III) diethylene-triaminepentaacetic acid derivative conjugates. J Med Chem 1998; 41, 3546-3549.

McStay MK, Caplin ME. Carcinoid tumour.Minerva Med 2002; 93(5): 389-401.

Meares CF. Chelating agents for the biding of metals to antibodies. Nucl Med Biol 1986; 13, 311-318.

Melmon KL, Sjoerdsma A, Oates JA and Laster L. Treatment of malabsorption and diarrhoea of the carcinoid syndrome with methysergide. Gastoenterology 1965; 48, 18–24.

Memon MA, Nelson H. Gastrointestinal carcinoid tumours. Dis Colon Rectum 1997; 40(9), 1101-18.

Micheletti G, Poli M, Borsotti P, Martinelli M, Imberti B, Taraboletti G, Giavazzi R.Vascular-targeting activity of ZD6126, a novel tubulin-binding agent. Cancer Res. 2003; 63(7):1534-7.

Miller AB, Hoogstraten B, Staquet M et al. Reporting results of cancer treatment. Cancer 1981; 47, 207–214.

Moertel CG, Dockerty MB and ES Judd, Carcinoid tumours of the vermiform appendix. Cancer 1968; 21, 270–275.

Moertel CG. An odyssey in the land of small tumors. J Clin Oncol 1987; 5, 1503–1522.

Moertel CG, Kvols LK and Rubin J. A study of cyproheptadine in the treatment of meatstatic carcinoid tumour and the malignant carcinoid syndrome. Cancer 1991; 67, 33–36.

Moertel CG. Gastrointestinal carcinoid tumours and malignant carcinoid syndrome.In: Kelley WN (Ed). Textbook of Internal Medicine. Philadelphia: Lippincott Co, 1992: 1166–72.

Moyana TN, Xiang J, Senthilselvan A and Kulaga, A the spectrum of neuroendocrine differentiation among gastrointestinal carcinoids: importance of histologic grading, MIB-1, p53, and bcl-2 immunoreactivity. Archives of Pathology and Laboratory Medicine 2000; 124, 570–576.

Murphy WA, Lance VA, Moreau S, Moreau J & Coy DH. Inhibition of rat prostate tumor growth by an octapeptide analog of somatostatin Life Sciences 1987; 40, 2515–2522.

Neary PC, Redmond PH, HoughtonT, Watson GR, Bouchier-Hayes D. Carcinoid disease. Dis Colon Rectum 1997; 40, 349-62.

Nessi R, Basso Ricci P, Basso Ricci S, Bosco M, Blanc M, Uslenghi C. Bronchial carcinoid tumors: radiologic observations in 49 cases.J Thorac Imaging 1991; 6(2), 47-53

Newton JN, Swerdlow AJ, dos Santos Silva IM et al. The epidemiology of carcinoid tumours in England and Scotland. British Journal of Cancer 1994; 70, 5, 939–942.

Norheim I, Norheim-Theodorsson E, Brodin E and Oberg K, Tachykinins in carcinoid tumours: their use as a tumour marker and possible role in the carcinoid flush. J Clin Endocrinol Metab 1986; 64, 605–612.

Norton J, Levin B, Jensen R: Cancer of the endocrine system, in DeVita VT, Hellman S, Rosenberg SA (Eds): Cancer: Principles and Practice of Oncology 1993; 1371–1435. Philadelphia, JB Lippincott.

Norton JA. Surgical management of carcinoid tumors: role of debulking and surgery for patients with advanced disease. Digestion 1994; 55, 98–103.

Novartis Pharmaceuticals Corporation East Hanover, New Jersey 07936 Drug catalogue REV: May 1999 Printed in USA 89003002.

O'Donoghue JA, Bardies M, Wheldon TE. Relationships between tumor size and curability for uniformly targeted therapy with beta-emitting radionuclides. J Nucl Med 1995; 36, 1902–1909.

O'Dowd G, Gosney JR. Absence of overexpression of p53 protein by intestinal carcinoid tumours. Pathol 1995; 175(4):403-4.

Oberg K, Funa K & Alm G.Effects of leukocyte interferon upon clinical symptoms and hormone levels in patients with mid-gut carcinoid tumours and carcinoid syndrome N Engl J Med 1983; 309, 129-133.

Oberg K and Eriksson B. The role of interferons in the management of carcinoid tumours. Acta Oncol 1991; 30, 519-522.

Oberg K. The use of chemotherapy in the management of neuroendocrine tumours. Endocrinol Metab Clin North Am 1993; 22, 941–952

Oberg K. Advances in chemotherapy and biotherapy of endocrine tumors. Curr Opin Oncol 1998 ₁; 10(1), 58-65.

Oberg K. Carcinoid Tumors: Current Concepts in Diagnosis and Treatment. Oncologist 1998 ₂; 3(5), 339-345.

Öberg K. Neuroendocrine gastrointestinal tumours–a condensed overview of diagnosis and treatment. Annals of Oncology 1999; 10 (Suppl.2), S3-S8.

Oberg K. Chemotherapy and biotherapy in the treatment of neuroendocrine tumours. Ann Oncol 2001; 12 Suppl 2:S111-4.

Oberndorfer S. Uaber die "kleinen dunndarm carcinome". Verhandlungen der Deutschen gesellschaft fuer Pathologie 1907; 11, 113–116.

OctreoScan® scintigraphy for gastro-entero-pancreatic neuroendocrine tumours Medicare Services Advisory Committee (MSAC application 1003) Final assessment report August 1999.

Orlefors H, Sundin A, Ahlstrom H, Bjurling P, Bergstrom M, Lilja A, Langstrom B, Oberg K, Eriksson B. Positron emission tomography with 5-hydroxytryprophan in neuroendocrine tumors. J Clin Oncol 1998; 16, 2534-41.

Otte A, Jermann E, Behe M, Goetze M, Bucher HC, Roser HW, Heppeler A, Mueller-Brand J and Maecke HR. DOTATOC: a powerful new tool for receptor mediated radionuclide therapy. Eur J Nucl Med 1997; 24, 792-795.

Otte A, Mueller-Brand J, Dellas S, Nitzsche EU, Herrmann R, and Maecke HR. Yttrium-90-labeled somatostatin-analogue for cancer treatment. Lancet 1998; 351, 417-418.

Padhani AR, Ollivier L. The RECIST (Response Evaluation Criteria in Solid Tumors) criteria: implications for diagnostic radiologists. Br J Radiol 2001; 74, 983-6.

Paganelli G, Zoboli S, Cremonesi M, et al. Receptor-mediated radiotherapy with ^{90}Y-DOTA-D-Phe1-Tyr3-octreotide. Eur J Nucl Med 2001; 28, 426–434.

Palazzo L, Roseau G, Salmeron M. Endoscopic ultrasonography in the preoperative localization of pancreatic endocrine tumors. Endoscopy1992; 24 Suppl 1:350-3.

Papotti M, Macri L, Bussolati G, Reubi JC. Correlative study on neuro-endocrine differentiation and presence of somatostatin receptors in breast carcinomas. Int J Cancer 1989; 43, 365-9.

Pasieka JL, McKinnon JG, Kinnear S, et al. Carcinoid syndrome symposium on treatment modalities for gastrointestinal carcinoid tumours: Symposium summary. Can J Surg 2001; 44(1), 25–32.

Patel YC, Greenwood MT, Panetta R, et al. The somatostatin receptor family. Life Sci. 1995; 57:1249–1265.

Patel YC. Molecular pharmacology of somatostatin receptor subtypes. J Endocrinol Invest 1997; 20, 348 67.

Patel YC. Somatostatin and its receptor family. Front Neuroendocrinol 1999; 20, 157-198.

Pearse AGE. Islet development and the APUD concept. In pancreatic Pathology. G.Koppel and P.U.Heitz, 1995 Eds: Churchill Livingston 125-132.

Pearson AS, Izzo F, Fleming RY et al. Intraoperative radiofrequency ablation or cryoablation for hepatic malignancies. Am J Surg 1999; 178-6, 592–599.

Platt AJ, Heddle RM, Rake MO and Smedley H, Ondansetron in carcinoid syndrome Lancet 1992; 339, 1416.

Polak JM and Bloom SR. The diffuse neuroendocrine system. J Histochem Cytochem 1979; 27, 1398-1400.

Polak JM Ed. Diagnostic histopathology of neuroendocrine tumours. Churchill Livingstone, Edinburgh, London, Madrid, Melbourne, New York and Tokyo 1993; 71(8):2624-30.

Que FG, Nagorney DM, Batts KP, Linz LJ, Knols LK. Hepatic resection for metastatic neuroendocrine carcinomas. Am J Surg 1995; 169:36-43.

Rauly I, Saint-Laurent N, Delesque N, Buscail L, Esteve JP and Vaysse N et al. Induction of a negative autocrine loop by expression of sst2 somatostatin receptor in NIH 3T3 cells. J Clin Invest 1996; 97, 1874-83.

Reinig JW, Dwyer AJ, Miller DL, White M, Frank JA, Sugarbaker PH, Chang AE, Doppman JL. Liver metastasis detection: comparative sensitivities of MR imaging and CT scanning. Radiology 1987; 162, 43–7.

Reubi JC, Ha"cki WH, Lamberts SWJ. Hormone-producing gastrointestinal tumours contain a high density of somatostatin receptors. J Clin Endocrinol Metab 1987; 65, 11-27.

Reubi JC, Lamberts SW, Maurer R. Somatostatin receptors in normal and tumoral tissue. Horm Res 1988; 29, 65 -9.

Reubi JC, Kvols LK, Waser B, et al: Detection of somatostatin receptors in surgical and percutaneous needle biopsy samples of carcinoids and islet cell carcinomas. Cancer Res 1990; 50, 5969–5977.

Reubi JC, Waser B, Hornesberger U et al. Identification of somatostatin and gastrin receptors on endochromaffin-lke cells from mastomys gastric tumours Endocrinol 1992; 131, 166-172.

Reubi JC, Horisberger U, Studer UE, Waser B, Laissue JA. Human kidney as target for somatostatin: high affinity receptors in tubules and vasa recta. J Clin Endocrinol Metab 1993; 77, 1323–1328.

Reubi JC, Laissue J, Waser B, et al: Expression of somatostatin receptors in normal, inflamed and neoplastic human gastrointestinal tissues. Ann NY Acad Sci 1994; 733,122–137.

Reubi JC, Schar JC, Waser B, et al. Affinity profiles for human somatostatin receptor subtypes SST1-SST5 of somatostatin radiotracers selected for scintigraphic and radiotherapeutic use Eur J Nucl Med 2000; 27, 273–282.

Rickes S, Unkrodt K, Ocran K, Neye H, Wermke W.Differentiation of neuroendocrine tumors from other pancreatic lesions by echo-enhanced power Doppler sonography and somatostatin receptor scintigraphy. Pancreas 2003; 26(1), 76-81.

Rindi G, Luineti O, Cornaggia M et al., Three subtypes of gastric argyrophil carcinoid and the gastric neuroendocrine carcinoma: a clinopathologic study. Gastroenterology 1993, 105, 1264–1266.

Rochaix P, Delesque N, Esteve JP, Saint-Laurent N, Voight JJ, Vaysse N et al. Gene therapy for pancreatic carcinoma: local and distant antitumor effects after somatostatin receptor sst2 gene transfer. Hum Gene Ther 1999; 10, 995-1008.

Rolleman EJ, Valkema R, De Jong M, Kooij PP, Krenning EPSafe and effective inhibition of renal uptake of radiolabelled octreotide by a combination of lysine and arginine. Eur J Nucl Med Mol Imaging 2003; 30(1):9-15.

Ronnblom L, Alm GV and Oberg K. Autoimmunity after alpha-and gamma interferon therapy for malignant carcinoid tumours. Ann Intern Med 1991; 115, 178-183.

Rosch F, Herzog H, Stolz B, et al. Uptake kinetics of the somatostatin receptor ligand [^{86}Y]DOTA-DPhe1-Tyr3-octreotide ([^{86}Y] SMT487) using positron emission tomography in non human primates and calculation of radiation doses of the ^{90}Y-labelled analogue. Eur J Nucl Med 1999; 26, 358–366.

Rosch T, Lightdale CJ, Botet JF et al. Localization of pancreatic endoscopic ultrasonography. N Engl J Med 1992; 326, 1721-1726.

Rothmund M, Kisker O. Surgical treatment of carcinoid tumours of the small bowel appendix, colon and rectum. Digestion 1994; 55, 86–91, 104: 994–1006.

Rougier P, Mitry E. Chemotherapy in the treatment of neuroendocrine malignant tumors. Digestion 2000; 62 Suppl 1, 73-8.

Roul JL, Guyander D, Bretagne JF, et al. Prospective randomized trial of chemoembolisation versu intra-arterial iodine-131 Lipiodol in inoperable hepatocellular carcinoma. Hepatol 1997; 26, 1156-1161.

Ruoslahti E. Targeting tumor vasculature with homing peptides from phage display. Semin Cancer Biol 2000; 10, 435-442.

Sagara M, Sugiyama F, Horiguchi H et al., Activation of the nuclear oncogenes N-myc and c-jun in carcinoid tumors of transgenic mice carrying the human genome adenovirus type 12 E1 region gene. DNA Cell Biology 1995; 14, 95–101.

Sakamoto H, Nakai Y, Ohashi Y, Matsuda M, Sakashita T, Nasako Y, Kitayama H, Kawabe J, Okamura T, Ochi H. Monitoring of response to radiotherapy with fluorine-18 deoxyglucose PET of head and neck squamous cell carcinomas. Acta Otolaryngol Suppl 1998; 538, 254-60.

Sattelberger AP and Atcher RW. Nuclear medicine finds the right chemistry. Nat. Biotechnol 1999; 17, 849-850.

Schally AV. Oncological applications of somatostatin analogues. Cancer Res 1988; 48, 6977-85.

Schell SR, Camp ER, Caridi JG, Hawkins IF Jr. Hepatic artery embolization for control of symptoms, octreotide requirements, and tumor progression in metastatic carcinoid tumors. J Gastrointest Surg 2002; 6, 664-70.

Scherubl H, Hescheler J, Riecken EO: Molecular mechanisms of somatostatin's inhibition of hormone release: Participation of voltage-gated calcium channels and G-proteins. Horm Metab Res 1993; 27(suppl), 1–4.

Schwartz DA, Abrams MJ, Hauser MM, Gaul FE, Larsen SK, Rauh D, and Zubieta J A. Preparation of hydrazino-modified proteins and their use for the synthesis of 99mTc-protein conjugates. Bioconjugate Chem 1991; 2, 333-336.

Shapiro B. Ten years of experience with MIBG applications and the potential of new radiolabeled peptides: a personal overview and concluding remarks. Q J Nucl Med1995; 39(Suppl 1–4), 150–155.

Shi W, Johnston CF, Buchanan KD, Ferguson WR, Laird JD, Crothers JG, McIlrath EM.Localization of neuroendocrine tumours with [111In] DTPA-octreotide scintigraphy (Octreoscan): a comparative study with CT and MR imaging. QJM 1998; 91(4), 295-301.

Shojamanesh H et al., Prospective study of the antitumor efficacy of long-term octreotide treatment in patients with progressive metastatic gastrinoma. Cancer 2002; 94, 331–343.

Shen S, DeNardo GL, DeNardo SJ.Quantitative bremsstrahlung imaging of yttrium-90 using a Wiener filter. Med Phys 1994; 21(9), 1409-17.

Shen S, DeNardo GL, Yuan A, DeNardo DA, DeNardo SJ ,Planar gamma camera imaging and quantitation of yttrium-90 bremsstrahlung. J Nucl Med 1994; 35(8), 1381-9.

Skuladottir H, Hirsch FR, Hansen HH, Olsen JH, Pulmonary neuroendocrine tumors: incidence and prognosis of histological subtypes. A population-based study in Denmark.Lung Cancer 2002; 37(2), 127-35.

Siegal JA, Handy DM, Kopher KA, Zeiger LS et al,therapeutic beta irradiating isotopes in bone metastasis: a technique for brehmsstrahlung imaging and quantitation.AntibImmununoconjug Radiopharm 1992; 5;237-248.

Signore A. Receptor ligands. Q. J. Nucl. Med 1995; 39, 83-85.

Sisson JC, Wieland DM: Radiolabeled metaiodobenzylguanidine: Pharmacology and clinical studies. Am J Physiol Imaging 1986; 1, 96-103.

Sjoblom SM, Clinical presentation and prognosis of gastrointestinal carcinoid tumours. Scand J Gastroenterol 1988; 23, 779–787.

Slooter GD, Breeman WA, Marquet RL, Krenning EP, van Eijck CH. Anti-proliferative effect of radiolabelled octreotide in a metastases model in rat liver.Int J Cancer 1999; 81, 767-71.

Slooter GD, Mearadji A, Breeman WAP, Marquet RL, De Jong M. et al. Somatostatin receptor imaging, therapy and new strategies in patients with neuroendocrine tumours British Journal of Surgery 2001; 88(1) 31-40.

Smith MC, Liu J, Chen T, Schran H, Yeh CM, Jamar F, Valkema R, Bakker W, Kvols L, Krenning E, Pauwels S.OctreoTher: ongoing early clinical development of a somatostatin-receptor-targeted radionuclide antineoplastic therapy. Digestion 2000; 62 Suppl 1, 69-72.

Smith T, Crawley JC, Shawe DJ, Gumpel JM. SPECT using Bremsstrahlung to quantify 90Y uptake in Baker's cysts: its application in radiation synovectomy of the knee. Eur J Nucl Med 1988; 14 (9-10), 498-503.

Smith-Jones PM, Bischof C, Leimer D, Gludovacz D, Angelberger P, Pangerl T, Peck-Radosavljevic M, Hamilton, G, Kaserer K, Steiner G, Schlagbauer-Wadl H,

Maecke H, and Virgolini I. "Mauritius", a novel somatostatin analogue for tumour diagnosis and therapy. J Nucl Med 1998; 39 Suppl, 223P.

Smith-Jones PM, Bischof C, Leimer M, Gludovacz D, Angelberger P, Pangerl T, Peck-Radosavljevic M, Hamilton G, Kaserer K, Kofler A, Schlangbauer-Wadl H, Traub T, Virgolini I. DOTA-lanreotide: a novel somatostatin analog for tumor diagnosis and therapy.Endocrinology 1999; 140(11), 5136-48.

Soga J and Tazawa K, Pathologic analysis of carcinoids. Cancer 1971; 28, 990–998.

Sohaib SA, Turner B, Hanson JA, Farquharson M, Oliver RT, Reznek RH.CT assessment of tumour response to treatment: comparison of linear, cross-sectional and Volumetric measures of tumour size. Br J Radiol 2000; 73(875), 1178-84.

Solicia E, Capella C, Buffa R, et al. Endocrine cells of the digestive system.In: Johnson LR (Ed). Physiology of the gastrointestinal tract. New York: Raven Press, 1981; 39–58.

Solcia E, Capella C, Fiocca R et al. The gastroenteropancreatic endocrine system and related tumors. Gastroenterol Clin North Am 1989; 18, 671-693.

St Croix B., Rago C., Velculescu V., Traverso G., Romans K. E., Montgomery E., Lal A., Riggins G. J., Lengauer C., Vogelstein B., Kinzler K. W. Genes expressed in human tumor endothelium. Science 2000; 289, 1197-1202.

Stabin MG, Tagesson M, Thomas SR, Ljungberg M, Strand SE. Radiation dosimetry in nuclear medicine. Appl Radiat Isot 1999; 50(1), 73-87.

Steiner E, Stark DD, Hahn PF, Saini S, Simeone JF, Mueller PR, Wittenberg J, Ferrucci JT. Imaging of pancreatic neoplasms: comparision of MR and CT. Am J Roentgenol 1989; 152,487–91.

Stinner B, Kisker O, Ziekle A, Rothmund M. Surgical management for carcinoid tumours of small bowel,appendix, colon and rectum. World J Surg 1996; 20,183-8.

Stolz B, Weckbecker G, Smith-Jones P, Albert R, Raulf F and Bruns C. The somatostatin receptor tageted radiotherapeutic [^{90}Y-DOTA-D-Phe^1, Tyr^3] octreotide (^{90}Y-SMT 487) eradicates experimental rat pancreatic CA20948 tumours. Eur J Nucl. Med 1998; 7, 668-674.

Stridsberg M, Oberg K, Li Q, Engstrom U and Lundqvist G. Measurements of chromagranin A, chromagranin B (secretogranin I), chromagranin C (secretogranin II) and pancreastatin in plasma and urine from patients with carcinoid tumours and endocrine pancreatic tumours. Journal of Endocrinology 1995; 114, 49.

Sundin A, Eriksson B, Bergstrom M, Bjurling P, Lindner KJ, Oberg K and Langstrom B. Demonstration of [^{11}C] 5-hydroxy--tryptophan uptake and decarboxylation in carcinoid tumors by specific positioning labeling in positron emission tomography. Nuclear Medicine and Biology 2000; 27, 33–41.

Sweeney JFand Rosemurgy AS. Carcinoid tumors of the gut. Cancer Control 1997; 41, 18–24.

Thakur ML. Radiolabeled peptides: Now and the future. Nucl Med Commun 1995; 16, 724-732.

Thakur ML, Kolan H, Li J, Wiaderkiewicz R, Pallela VR, Duggaraju R, and Schally AV. Radiolabeled somatostatin analogues in prostate cancer. Nucl Med Biol 1997; 24, 105-113.

Therasse P, Arbuck SG, Eisenhauer EA et al., New guidelines to evaluate the response to treatment in solid tumors. J Natl Cancer Inst 2000; 92, 205–216.

Therasse P. Measuring the clinical response. What does it mean? Eur J Cancer 2002; 38, 1817-23.

Thierens HM, Monsieurs MA, Brans B, Van Driessche T, Christiaens I, Dierckx RA. Dosimetry from organ to cellular dimensions. Comput Med Imaging Graph 2001; 25(2), 187-93

Tsuchida Y, Therasse P. Response evaluation criteria in solid tumors (RECIST): new guidelines. Med Pediatr Oncol 2001; 37, 1-3

Valdes Olmos RA, Hoefnagel CA, Bais E, Boot H, Taal B, de Kraker J, Vote PA.Therapeutic advances of nuclear medicine in oncology Rev Esp Med Nucl 2001 Dec; 20(7), 547-57.

Valkema R, Steens J, Cleton FJ, Pauwels EK. The diagnostic utility of somatostatin receptor scintigraphy in oncology. J Cancer Res Clin Oncol 1996; 122, 513- 32.

Valkema R, Jamar F, Bakker WH, et al. Safety and efficacy of [Y-90-DOTA, Tyr(3)]octreotide (Y-90-SMT487; OCTREOTHER™) peptide receptor radionuclide therapy (PRRT): preliminary results of a phase-1 study Eur J Nucl Med 2001; 28(suppl): 1025P.

Vinik AI, Moattari AR. Treatment of endocrine tumours of the pancreas. Endocrinol Metab Clin North Am 1989; 18, 483-518.

Virgolini, I., Szilvasi, I., Kurtaran, A., Angelberger, P., Raderer, M., Havlik, E., Vorbeck, F., Bischof, C., Leimer, M., Dorner, G., Kletter, K., Niederle, B., Scheithauer, W., and Smith-Jones, P. Indium-111-Dota-lanreotide: biodistribution, safety and radiation absorbed dose in tumour patients. J Nucl Med 1998; 39, 1928-1936.

Virgolini I, Traub T, Leimer M, Novotny C, Pangerl T, Ofluoglu S, Halvadjieva E, Smith-Jones P, Flores J, Li SR, Angelberger P, Havlik E, Andreae F, Raderer M, Kurtaran A, Niederle B, Dudczak New radiopharmaceuticals for receptor scintigraphy and radionuclide therapy. Q J Nucl Med 2000; 44, 50-8

Virgolini I, Traub T, Novotny C, et al. New trends in peptide receptor radioligands. Q J Nucl Med 2001; 45: 153–159.

Virgolini I, Britton K, Buscombe J, Moncayo R, Paganelli G, Riva P. In- and Y-DOTA-lanreotide: results and implications of the MAURITIUS trial. Semin Nucl Med 2002; 32(2), 148-55.

Vucina J, Han R. Use of radionuclides in therapy.Med Pregl 2001; 54(5-6), 245-50. Waldherr C, Pless M, Maecke HR, Haldemann A, MuellerB. The clinical value of [90Y-DOTA]-D-Phe1-Tyr3-octreotide (90Y-DOTATOC) in the treatment of neuroendocrine tumours: a clinical phase II study J Ann Oncol 2001; 12, 941-5.

Waldherr C, Pless M, Maecke HR, et al. Tumor response and clinical benefit in neuroendocrine tumors after 7.4 GBq ^{90}Y-DOTATOC. J Nucl Med 2002; 43, 610–616.

Wallace S, Ajani JA, Charnsangavej C, DuBrow R. Yang DJ, Chuang V P , Carrasco CH, Dodd G D Jr, Carcinoid Tumors. Imaging Procedures and Interventional Radiology, World J Surg 1996; 20, 147–156.

Walrand S, Jamar F, Mathieu I, De Camps J, Lonneux M, Sibomana M, Labar D, Michel C, Pauwels S. Quantitation in PET using isotopes emitting prompt single gammas: application to yttrium-86.Eur J Nucl Med Mol Imaging. 2003 Mar; 30(3), 354-61.

Wang DG. Apoptosis in neuroendocrine tumours. Clinical Endocrinology 1999; 51, 1-9.

Wang DG, Johnston CF, Anderson N, Sloan JM and Buchanan KD. Overexpression of the tumor suppressor gene p53 is not implicated in neuroendocrine tumor carcinogenesis. Journal of Pathology 1995; 175, 397–402.

Wangberg B, Geterud K, Nilsson O et al. Embolisation therapy in the midgut carcinoid syndrome: Just tumour ischaemia? Acta Oncol 1993; 32, 251.

Wank SA, Doppman JL, Miller DL, Collen MJ, Maton PN, Vinayek R, Slaff JI, Norton JA, Gardner JD, Jensen RT. Prospective study of the ability of computed tomography to localize gastrinomas in patients with Zollinger-Eliison syndrome. Gastroenterology 1987; 92, 905–12.

Warburton R and Keevil B. Urinary 5-hydroxyindole-acetic acid by high-performance liquid chromatography with electrochemical detection. Ann Clin Biochem 1997; 34, 424–426.

Weckbecker G, Raulf F, Stolz B, Bruns C. Somatostatin analogs for diagnosis and treatment of cancer. Pharmacol Ther 1993; 60(2), 245-64.

Weidenmann B, Khun C et al. Synaptohysin identified in metastases of neuroendocrine tumours by immunocytochemistry andimmunoblotting. Am J Clin Pathl 1988; 87, 560-569.

Weidenmann B and Huttner W. Synaptophysin and chromogranins/secreto-grannins-widespread constituents of distinct types of neuroendocrine vesicles and new tools in tumour diagnosis. Virchows Archiv B Cell Pathol 1989; 58, 95-121.
Weiner RE, Thakur ML. Radiolabeled peptides in diagnosis and therapy. Semin Nucl Med 2001; 31(4), 296-311.

Wermer P. Genetic aspects of adenomatosis of endocrine glands. Am J Med 1954; 116,363–371.

Werner-Wasik M, Xiao Y, Pequignot E, Curran WJ, Hauck W.Assessment of lung cancer response after nonoperative therapy: tumor diameter, bidimensional product, and volume. A serial CT scan-based study.Int J Radiat Oncol Biol Phys. 2001; 51(1), 56-61.

Wessels BW, Meares CF. Physical and chemical properties of radionuclide therapy. Semin Radiat Oncol. 2000; 10(2), 115-22.

Wessels FJ, Schell SR. Radiofrequency ablation treatment of refractory carcinoid hepatic metastases. J Surg Res 2001; 95(1), 8-12.

Wester HJ, Brockmann J, Rosch F, Wutz W, Herzog H, Smith Jones P, Stolz B, Bruns C, and Stocklin G. PET-pharmacokinetics of 18F-octreotide: a comparison with 67Ga-DFO- and 86Y-DTPA-octreotide Nucl Med Biol 1997; 24, 275-286.

Wiedenmann B, Huttner W. Synaptophysin and chromogranins/ secretograninsd: Widespread constituents of distinct types of neuroendocrine vesicles and new tools in tumor diagnosis. Virchows Arch B Cell Pathol 1989; 58, 95–121.

Wiedenmann B, Ahnert-Hilger G, Kvols KL, and Riecken EO. New molecular aspects for the diagnosis and treatment of neuroendocrine gastroenteropancreatic tumors. Annals of New York Academy of Sciences 1994; 733 515–522.

Wilander E, Lundqvist M, Öberg K. Gastrointestinal carcinoid tumours. Prog Histochem Cytochem 1989; 19, 1-85.

Williams ED and Sandler M, The classification of carcinoid tumors. Lancet 1963; 1, 238–239.
Walrand S, Jamar F, Mathieu I, De Camps J, Lonneux M, Sibomana M, Labar D, Michel C, Pauwels S. Quantitation in PET using isotopes emitting prompt single gammas: application to yttrium-86.Eur J Nucl Med Mol Imaging 2003; 30(3), 354-61.

Yamada M, Komoto E, Naito Y, Tsukamoto Y, Mitake M. Endoscopic ultrasonography in the diagnosis of pancreatic islet cell tumors, J Ultrasound Med 1991; 10(5), 271-6

Zamora PO, Guhlke S, Bender H, Diekmann D, Rhodes BA, Biersack H, and Knapp FF, Jr. Experimental radiotherapy of receptor-positive human prostate adenocarcinoma with [188]Re-RC-160, a directly radiolabeled somatostatin analogue. Int. J. Cancer 1996; 65, 214-220.

Zeiger MA, Swartz SE, MacGillivray DC, Linnoila I and M. Shakir.Thymic carcinoid in association with MEN syndromes. American Surgeon 1992; 58, 430–434.

Zimmer T, Ziegler K, Bader M, Fett U, Hamm B, Riecken EO, Wiedenmann B.Localisation of neuroendocrine tumours of the upper gastrointestinal tract. Gut 1994 [1]; 35(4), 471-5.

Zimmer T, Ziegler K, Liehr RM, Stolzel U, Riecken EO, Wiedenmann B. Endosonography of neuroendocrine tumors of the stomach, duodenum, and pancreas Ann N Y Acad Sci 1994 [2]; 15, 733:425-36.

Glossary (Nuclear Medicine)

Nuclear Medicine: That branch of medicine which uses unsealed sources of radioisotopes for either diagnosis or therapy.

Radiopharmaceutical: A particular chemical with a pharmacological action containing a radioactive atom.

Radioisotope: Radioactive atoms which decay releasing energy as ionising radiation which have the same chemical property but different molecular weight. All radioisotopes of an element will have the same number of protons but a different number of neutrons.

Radionuclide: A specific radioisotope with particular characteristics. For example both ^{99m}Technetium and ^{99}Technetium are both the same radioisotope but the metastable form is denoted by an m superscript is a different radionuclide than the more stable form.

Activity: Measure of radioactivity given to a patient measured as the number of radioactive disintegrations per second (Becquerel-Bq).

Half life: Time taken for a radionuclide to decay to half of its initial activity.

γ (gamma) ray: Non particulate form of ionising radiation coming from the nucleus of a radionuclide.

β (beta) ray: a high-speed electron or positron emitted by a nucleus during radioactive decay or nuclear fission

X-rays: A type of radiation of higher frequency (or energy) that visible light but lower that gamma rays. Usually produced by fast electrons going through matter or by the de-excitation of excited atom.

Gamma camera: Instrument used to detect gamma rays and produce an image.

Scintigraphy: The process of producing an image with a gamma camera from a patient injected with radiopharmaceutical.

Photo-peak: Each radionuclide emits radiation of characteristic energy (energies). When detected by a detecting system this photo-peak is measured in kilo electron volts (keV).

Scintigraphy: The process of producing an image with a gamma camera from a patient injected with a radiopharmaceutical.

Absorbed radiation dose: Estimate of how much energy has been given to an irradiated tissue measured in joules per kilogram of tissue (Sieverts Sv).

Brehmsstrahlung: X-rays produced when fast electrons pass through matter. The brehmsstrahlung (German for "slowing-down radiation") energy varies from 0 to the energy of the electron.

Becquerel: SI unit of activity or nuclear transition rate equal to one per second (Bq).

Bifunctional chelate: Complexing agent with two sites for complexation.

Bioconjugate: An agent (usually a chelate used to conjugate radionuclide to an antibody

Chelation: In molecular or complex ion structure, the formation or presence of bonds (or other attractive forces) from two or more separate binding sites within the same ligand to a single central atom. C.

Dose: A general term denoting the quantity of radiation (energy) absorbed. For special purposes, it must be appropriately qualified, c. q. absorbed, maximum permissible, mean lethal.

Absorbed dose: The energy imparted to matter by ionizing radiation in a suitable small element of volume divided by the mass of that element of volume.

Effective dose equivalent: The absorbed dose multiplied by the quality factor and the product of all other modifying factors N, aimed at expressing on a common scale, for different types of radiations and distributions of absorbed dose, the biological effects associated with an exposure.

Ligand: A substance or part of a substance that binds to a specific receptor

Isotopes: Nuclides having the same atomic number but different mass numbers.

Conversion electron: An alternate process to x-ray emission during the de-excitation of an excited atom.

Adminstration of Radioactive Substances Advisory Committee (ARSAC):
A subcommittee within the department of health responsible for regulation of the medical use of radionuclides.

Skewness
Skewness is a measure of symmetry, or more precisely, the lack of symmetry. A distribution, or data set, is symmetric if it looks the same to the left and right of the center point.

Kurtosis
Kurtosis is a measure of whether the data are peaked or flat relative to a normal distribution. That is, data sets with high kurtosis tend to have a distinct peak near the mean, decline rather rapidly, and have heavy tails. Data sets with low kurtosis tend to have a flat top near the mean rather than a sharp peak. A uniform distribution would be the extreme case.

BIBLIOGRAPHY

---

1. ANNALS OF THE NEW YORK ACADEMY OF SCIENCES, VOLUME 733, Sept 15, 1994 Molecular and cell biological aspects of gastroenteropancraetic neuroendocrine tumour disease.Betram Weidman, Larry K Kvols, Rudlf Arnold, Ernst-Otto Riecken.

PUBLICATIONS

JOURNAL ARTICLES

1.Gnanasegaran G, Buscombe JR, Neuroendocrine Tumours - Part One: The role of Nuclear Medicine in Imaging Neuroendocrine Tumours, World J Nucl Med 2003; 2; 3; 232-240.

2.Gnanasegaran G, Buscombe J R, Neuroendocrine Tumours - Part Two: The role of Nuclear Medicine in the treatment of neuroendocrine tumours, World J Nucl Med 2003; 2; 4: 314-323.

3) G.Gopinath, A. Ahmed, J.R.Buscombe, M.E.Caplin, J.C.Dickson, A.J.W.Hilson Prediction of clinical outcome in treated neuroendocrine tumours of carcinoid type using functional volumes on ^{111}In-pentetreotide SPECT Imaging Nuclear medicine communications; 2004, 25; 299-303

PUBLISHED ABSTRACTS

1.G.Gopinath, J.R.Buscombe, M.E.Caplin, A.J.W.Hilson, Use of [111] In-octreotide SPECT in the assessment of tumour response in patients treated with chemotherapy and chemoembolization for foregut neuroendocrine tumours , European Journal of Nuclear Medicine 2003; 30; 2; p190 (S282)

2.Gopinath G, Buscombe J R, Caplin M E, Hilson A J W, Functional volume assessment of neuroendocrine tumours on SPECT imaging and correlation with CT scan and clinical outcome, Journal of Nuclear Medicine, 2003; 44; 5; 413p (1474)

3. G.Gopinath[1]J.R.Buscombe[1], M.E.Caplin[2], M.Aldrige[1], A.J.W.Hilson[1], Prediction of bone marrow toxicity in patients with neuroendocrine tumours after targeted therapy with Y-90 lanreotide, Nuclear medicine communications 2003, 24; 4; 449

4. G.Gopinath, A. Ahmed, M.E.Caplin, J.C.Dickson, J.R.Buscombe, A.J.W.Hilson, Can functional volumes on octreotide SPECT imaging predict clinical outcome in treated neuroendocrine tumours, European Journal of Nuclear Medicine 2002; 29; 1; S118.

5.G.Gopinath, J.R.Buscombe, J.C.Dickson, A.J.W.Hilson, Difference in biodistribution of various radiolabeled somatostatin analogues, European Journal of Nuclear Medicine 2002; 29; 1; S231

6.G.Gopinath, J.R.Buscombe, M.E.Caplin and A.J.W.Hilson, Does the Biodistribution of In-111 octreotide predict the Biodistribution of therapeutic Y-90 lanreotide? , Journal of Nuclear Medicine, 2002; 43; 5; 315p.

7. G.Gopinath, J.R.Buscombe, J.C.Dickson, G. Heath, and A.J.W.Hilson, Radiolabeled Somatostatin analogues Biodistribution- Much to explore, Cancer Biotherapy and Radiopharmaceuticals, 2002, 17; 3; p355

8.G.Gopinath, J.R.Buscombe, G. Heath, A.J.W.Hilson,Biodistribution of Y-90 lanreotide and In-111 octreotide- Are they different?, Nuclear Medicine Communications 2002, 23; 4; 382

UCL Graduate School Poster Competition

1.G.Gopinath[1]J.R.Buscombe[1], M.E.Caplin[2], M.Aldrige[1], A.J.W.Hilson[1],Assessment of tumour response in patients with neuroendocrine tumours using [111]Indium-pentetreotide imaging (p),UCL Graduate School Poster Competition 12 March 2003 UCL, London, UK

Royal Free Hospital and Medical School Annual Research Day Poster Competition
1. Radiolabeled Somatostatin analogues Biodistribution- Much to explore (p) Royal Free Hospital and Medical School Annual Research Day April 2002, U.K

<div style="border:1px solid">

NET PATIENT PROFORMA

NAME AND D.O.B:
DATE:

<u>Please could you complete this questionnaire prior to seeing the doctor.</u>

Please score the following on a scale of 1-10 by
ticking the relevant box.
1= very bad   10=excellent

	1	2	3	4	5	6	7	8	9	10
Flushing										
Wheezing										
Shortness of Breath										
Palpitations										
Abdominal Pain										
Itching										
Other pain										

- How many episodes of flushing do you have per day and how often does each one last?

- How often are your bowels open?

- Is your bowel movement:
Normal   Loose   Constipated   Variable
(Please circle one)

- Have you lost weight in the last 4 weeks?

- Is your appetite:
Normal   Reduced   Increased
(Please circle one)

- Since you last saw the doctor do you feel?
Same   Better   Worse
(Please circle one)

- Please list your medications below:

</div>

NET Patient Clinical Evaluation proforma
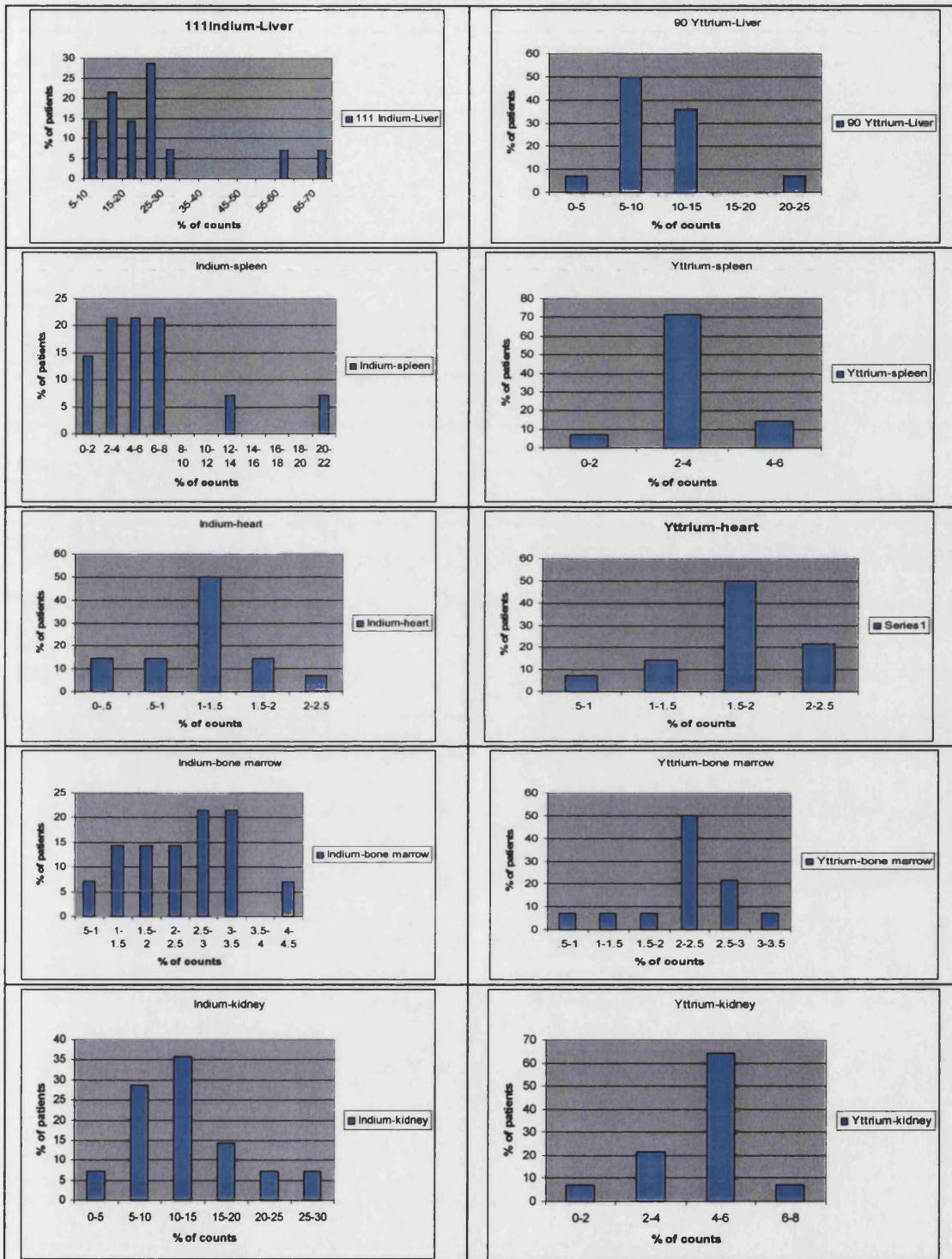
Test for Normality before application of Student t test (SPSS) ^{111}In-pentetreotide and ^{90}Y-lanreotide **[The Student t test is generally bell shaped, but with smaller samples sizes shows increased variability (flatter)in other words, the distribution is less peaked than normal distribution and with thicker tails].**

Observation	Skewness	Kurtosis	Test Statistic	Conclusion
In-liver	1.591114	4.6313025	0.29391	Strong evidence against normality
Y-liver	1.2571589	4.2989276	0.2137615	Suggestive evidence against normality
In-spleen	1.7261676	5.4204644	0.2124664	Little evidence against normality
Y-spleen	-0.4553929	3.510768	0.1409426	No evidences against normality
In-Heart	0.2708324	2.3343857	0.1071845	No evidences against normality
Y-Heart	0.9772382	5.6201183	0.2518883	Strong evidence against normality
In-Bone marrow	0.3275483	2.4689782	0.1241806	No evidences against normality
Y- Bone marrow	-0.8625415	3.5015999	0.1770936	No evidences against normality
In-kidney	0.745485	2.6339566	0.1866957	No evidences against normality
Y-kidney	-1.0079207	4.5845268	0.1790653	No evidences against normality

Lilliefors Test for Normality before application of Student t test (SPSS) [^{111}In-pentetreotide and ^{90}Y-lanreotide]
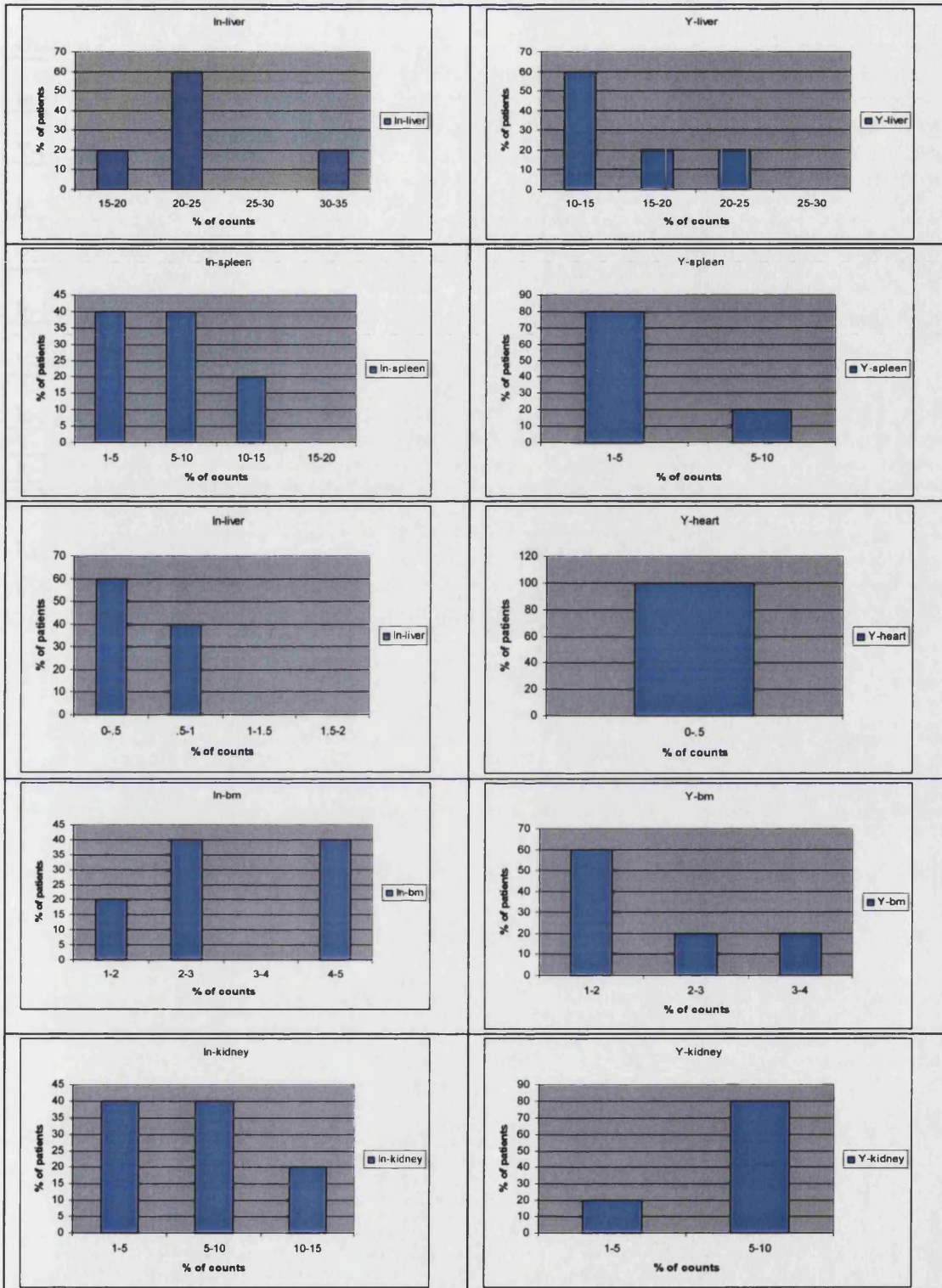
Test for Normality before application of Student t test (SPSS) ^{111}In-pentetreotide and ^{90}Y-SMT

Observation	Skewness	Kurtosis	Test Statistic	Conclusion
In-liver	0.9507712	2.531286	0.2591974	No evidences against normality
Y-liver	0.4163053	1.6351435	0.2505063	No evidences against normality
In-spleen	0.0971516	0.140382	1.854492	No evidences against normality
Y-spleen	1.2029858	2.8598532	0.3251061	Suggestive evidence against normality
In-Heart	0.5929271	1.5625	0.3854022	Strong evidence against normality
Y-Heart	0.8675276	2.7291667	0.3808717	Sufficient evidence against normality
In-Bone marrow	0.0335974	1.2710808	0.2603394	No evidences against normality
Y- Bone marrow	0.5705038	1.5668252	0.3442591	Sufficient evidence against normality
In-kidney	0.9374335	2.625262	0.2639243	No evidences against normality
Y-kidney	2.3737382	2.3737382	0.2049504	No evidences against normality

Lilliefors Test for Normality before application of Student t test (SPSS) ^{111}In-pentetreotide and ^{90}Y-SMT

Wilcoxon Signed Ranks Test

^{111}In-pentetreotide and ^{90}Y-lanreotide

Ranks

		N	Mean Rank	Sum of Ranks
Y_LIVER - I_LIVER	Negative Ranks	13(a)	7.85	102.00
	Positive Ranks	1(b)	3.00	3.00
	Ties	0(c)		
	Total	14		
Y_SPLEEN - I_SPLEEN	Negative Ranks	10(d)	7.50	75.00
	Positive Ranks	3(e)	5.33	16.00
	Ties	0(f)		
	Total	13		
Y_HEART - I_MARROW	Negative Ranks	10(g)	8.80	88.00
	Positive Ranks	4(h)	4.25	17.00
	Ties	0(i)		
	Total	14		
Y_MARROW - I_MARROW	Negative Ranks	9(j)	7.28	65.50
	Positive Ranks	5(k)	7.90	39.50
	Ties	0(l)		
	Total	14		
Y_L_KID - I_L_KID	Negative Ranks	14(m)	7.50	105.00
	Positive Ranks	0(n)	.00	.00
	Ties	0(o)		
	Total	14		

a Y_LIVER < I_LIVER
b Y_LIVER > I_LIVER
c Y_LIVER = I_LIVER
d Y_SPLEEN < I_SPLEEN
e Y_SPLEEN > I_SPLEEN
f Y_SPLEEN = I_SPLEEN
g Y_HEART < I_MARROW
h Y_HEART > I_MARROW
i Y_HEART = I_MARROW
j Y_MARROW < I_MARROW
k Y_MARROW > I_MARROW
l Y_MARROW = I_MARROW
m Y_L_KID < I_L_KID
n Y_L_KID > I_L_KID
o Y_L_KID = I_L_KID

Test Statistics (b)

	Y_LIVER - I_LIVER	Y_SPLEEN - I_SPLEEN	Y_HEART - I_MARROW	Y_MARROW - I_MARROW	Y_L_KID - I_L_KID
Z	-3.107(a)	-2.062(a)	-2.235(a)	-.816(a)	-3.296(a)
Asymp. Sig. (2-tailed)	.002	.039	.025	.414	.001

a Based on positive ranks.
b Wilcoxon Signed Ranks Test

Wilcoxon Signed Ranks Test

^{111}In-pentetreotide and ^{90}Y-SMT

Ranks

		N	Mean Rank	Sum of Ranks
S_LIVER - I_LIVER	Negative Ranks	5(a)	3.00	15.00
	Positive Ranks	0(b)	.00	.00
	Ties	0(c)		
	Total	5		
S_SPLEEN - I_SPLEEN	Negative Ranks	4(d)	3.25	13.00
	Positive Ranks	1(e)	2.00	2.00
	Ties	0(f)		
	Total	5		
S_HEART - I_HEART	Negative Ranks	0(g)	.00	.00
	Positive Ranks	5(h)	3.00	15.00
	Ties	0(i)		
	Total	5		
S_MARROW - I_MARROW	Negative Ranks	1(j)	5.00	5.00
	Positive Ranks	4(k)	2.50	10.00
	Ties	0(l)		
	Total	5		
S_L_KI - I_L_KI	Negative Ranks	5(m)	3.00	15.00
	Positive Ranks	0(n)	.00	.00
	Ties	0(o)		
	Total	5		

a S_LIVER < I_LIVER
b S_LIVER > I_LIVER
c S_LIVER = I_LIVER
d S_SPLEEN < I_SPLEEN
e S_SPLEEN > I_SPLEEN
f S_SPLEEN = I_SPLEEN
g S_HEART < I_HEART
h S_HEART > I_HEART
i S_HEART = I_HEART
j S_MARROW < I_MARROW
k S_MARROW > I_MARROW
l S_MARROW = I_MARROW
m S_L_KI < I_L_KI
n S_L_KI > I_L_KI
o S_L_KI = I_L_KI

Test Statistics(c)

	S_LIVER - I_LIVER	S_SPLEEN - I_SPLEEN	S_HEART - I_HEART	S_MARROW - I_MARROW	S_L_KI - I_L_KI
Z	-2.023(a)	-1.483(a)	-2.023(b)	-.677(b)	-2.032(a)
Asymp. Sig. (2-tailed)	.043	.138	.043	.498	.042

a Based on positive ranks.
b Based on negative ranks.
c Wilcoxon Signed Ranks Test

In-liver	-0.2255579	1.5020962	0.1779793	No evidences against normality
Y-liver	0.5845481	2.5334362	0.1663974	No evidences against normality
In-spleen	1.5018276	4.5768807	0.2289256	Little evidence against normality
Y-spleen	-0.1842244	3.3296606	0.1723132	No evidences against normality
In-Heart	0.491136	2.7605617	0.1132239	No evidences against normality
Y-Heart	0.2622459	5.1931709	0.8323853	Sufficient evidence against normality
In-Bone marrow	0.1008937	2.7527583	0.1197642	No evidences against normality
Y- Bone marrow	-1.1685178	3.6392757	0.2238698	Suggestive evidence against normality
In-kidney	0.6112421	2.3540075	0.1775989	No evidences against normality
Y-kidney	-0.8121505	3.9834008	0.1429417	No evidences against normality

Test for Normality before application of Student t test (SPSS) ^{111}In-pentetreotide and ^{90}Y-lanreotide (excluding patients 10 and 12)